STATUS OF THESIS

Title of thesis | LITHOFACIES MODELING OF CRETACEOUS RESERVOIR IN DOBA BASIN, SOUTHERN CHAD

I MOUHAMADALHADI HISSIEN RAMAD

hereby allow my thesis to be placed at the Information Resource Center (IRC) of Universiti Teknologi PETRONAS (UTP) with the following conditions:

1. The thesis becomes the property of UTP
2. The IRC of UTP may make copies of the thesis for academic purposes only.
3. This thesis is classified as

[×] Confidential

[ ] Non-confidential

If this thesis is confidential, please state the reason:
Subject to PETRONAS, approval for releasing the data (confidential)

The contents of the thesis will remain confidential for _____ years.

Remarks on disclosure:

Endorsed by

Signature of Author

Signature of Supervisor

Permanent address: Caree - 7,
Quartee: Klemat
2èm Arrondissement
N`DJamena, Chad

Name of Supervisor
Assoc. Prof. Wan Ismail Wan Yusoff

Date : _____

Date : _____

UNIVERSITI TEKNOLOGI PETRONAS

LITHOFACIES MODELING OF CRETACEOUS RESERVOIR IN DOBA BASIN, SOUTHERN CHAD

by

MOUHAMADALHADI HISSIEN

The undersigned certify that they have read, and recommend to the Postgraduate Studies Programme for acceptance this thesis for the fulfillment of the requirements for the degree stated.

Signature: _____

Main Supervisor: Assoc. Prof. Wan Ismail Wan Yusoff

Signature: _____

Co-Supervisor: _____

Signature: _____

Head of Department: Assoc. Prof. Dr. Abdul Hadi Abd Rahman

Date: _____

LITHOFACIES MODELING OF CRETACEOUS RESERVOIR IN DOBA BASIN, SOUTHERN CHAD

by

MOUHAMADALHADI HISSIEN

A Thesis

Submitted to the Postgraduate Studies Programme

as a Requirement for the Degree of

MASTER OF SCIENCE

PETROLEUM GEOSCIENCE

UNIVERSITI TEKNOLOGI PETRONAS

BANDAR SERI ISKANDAR,

PERAK

MARCH 2013

DECLARATION OF THESIS

Title of thesis | LITHOFACIES MODELING OF CRETACEOUS RESERVOIR IN DOBA BASIN, SOUTHERN CHAD

I MOUHAMADALHADI HISSIEN RAMAD

hereby declare that the thesis is based on my original work except for quotations and citations which have been duly acknowledged. I also declare that it has not been previously or concurrently submitted for any other degree at UTP or other institutions.

Witnessed by

Signature of Author	Signature of Supervisor
Permanent address: Caree - 7, Quartee: Klemat 2èm Arrondissement N`DJamena, Chad	Name of Supervisor Assoc. Prof. Wan Ismail Wan Yusoff
Date :	Date :

DEDICATION

I dedicate this thesis to my Parents, my Wife and my children Hissien, Intissar and Habo

بعد الحمد والشكر لله على نعمه التي لاتعد ولاتحصى

أهدى هذه الرسالة

إلى الوالدين الكريمين، زوجتى وأولادى حسين، انتصار وحبو

ACKNOWLEDGEMENTS

The writing of this thesis has been of the most significant academic challenges that I have ever faced in my life. It would not be possible to achieve what have been done in this work without ALLAH`s consent and then my patience, the support and guidance from some people herein mentioned. Therefore, my gratitude addressed to them:

The PETRONAS Sdn Bhd. Malaysia and Universiti Teknologi PETRONAS for the assistance as well as special thanks extended to the PETRONAS Chad office for releasing the research data.

My Supervisor Associate Professor Wan Ismail Wan Yusoff, for his effort, advices and continuous encouragement for me to the completion of this study.

My field supervisor M Kamal. B Embong, for his supervision on the technical aspect of the study, especially concerning software application on modelling.

My deepest gratitude goes to my parents, my wife and my children (Hissien, Intisar and Habo) for their patience, support and being a constant source of inspiration during this period.

I am especially indebted to all my friends, and colleagues who have been advising and encouraging me during preparation of this thesis.

Thank you.

.

ABSTRACT

The application of reservoir lithofacies static modeling to illustrate facies lateral and vertical distribution of the reservoir has been modeled for the K-oil field in the Doba Basin, southern Chad. The basin is a part of the West and Central African Rift System (WCARS), and the basin sediments are non-marine

The study area is located in an anticline structure oriented in the NE - SW trend in the southeastern part of the basin and is intersected by NW-SE normal faults. The sediment deposition system is sequences of braided deltas formed by progradation of a fluvial system into a standing body of water.

The studies include data collection, preparation, quality controlling and importing to the modeling software (Petrel Version 2008), conceptual model, setting project unit, faults modeling, horizons modeling, facies prediction, 3D gridding, well correlation, environmental facies interpretation, lithofacies prediction, wells blocking, data analysis and facies modeling documentation as well as results and conclusions. The data used for this study are from well logs, cores, depth map, and report.

A 3D reservoir lithofacies model of a Cretaceous braided delta system of the Doba basin was generated by using modeling software. The results are from three realizations in Pixel-based and Object-based techniques, where three models were analyzed and compared. The optimal model was determined from the object-based method.

The finding illustrated that the selected model was consistent with the conceptual analog of the braided delta system as the reservoir is continuous from southwest to northeast within the channel built and show environmental changed laterally and vertically in the wells position, with coarse sandy bar dominant in the southwest and lacustrine in northeast. The risk of sand distribution within the channel belt is low and

the model shows consistency with the analog of a braided system for the non-marine sediment interval of Cretaceous strata.

Reservoir porosity and permeability are expected to be good within the extent of the coarse sand bar in the southwest part of the area. The train estimation method used to predict lithofacies and object-based techniques with realizations are effective tools in generating a braided reservoir model. The pixel-based methods failed to produce consistent models with the braided analog except in the case of expanding the variogram ranges. The result demonstrates that stochastic object-based method is appropriate to model subsurface reservoir facies distribution for the braided delta environment. The techniques, facies fraction and variogram range affect the result.

In future studies, the lithofacies produced may be integrated with seismic attribute data to improve the estimation of facies quality and distribution, reprocessing of seismic data to produce seismic impedance that can be integrated within the facies model. In addition, if any additional core data is available it can be included in the study, as well as the reservoir model with input from lithofacies model can be used to update the dynamic reservoir model for future management of the reservoir performance and assessment.

ABSTRAK

Ponggunaan pemodelan lithofasies statik untuk menggambarkan pengagihan fasies takungan sisi dan menegak telah dimodelkan untuk medan minyak K pada lembangan Doba, Selatan Chad.Sedimen lembangan adalah bukanlaut dan ia-nya sebahagian daripada Barat dan Tengah Sistem Rekah Afrika (WCARS).

Kawasan kajian terletak dalam struktur antiklin berorientasikan trend NE-SW di bahagian tenggara lembangan dan disilangi dengan sesar biasa NW - SE. Sistem sedimen deposit adalah jujukan delta braided yang dibentuk oleh progradasi sistem berhubung dengan sungai ke dalam takungan air. Kajian termasuk pengumpulan data, penyediaan, mengawal kualiti dan mengimport ke perisian pemodelan, menetapkan unit projek, pemodelan kerosakan, pemodelan ufuk, ramalan fasies, pengridan 3D.Pemblokkan telaga, analisis data dan pemodelan fasies serta men dokumen casikeputusan dan kesimpulan. Data yang digunakan untuk kajian ini adalah Datalog, data teras, pitakedalamanDanlaporan.

Sebuah lithofacies takungan 3D model delta sistem bersirat berusia Kapor di lembah Doba telah dijana dengan menggunakan perisian pemodelan. Keputusan daripada tiga realisasi SIS, TGS dan teknik berasaskan Objek, tiga model telah dianalisis, dan model optimum telah ditentukan daripada kaedah berasaskan Objek. Model terhasil menggambarkan bahawa takungan melnjurus dalam saluran yang terbina di kawasan timur laut dimana fasies bar kasar berpasir adalan dominan. Risiko Taburan pasir dalam saluran adalah rendah dan model adalab selaras dengan analog sistem bersirat untuk sedimen marin bukan laut sela strata kapor. Hasilnya menunjukkan bahawa kaedah stokastik berasaskan objek adalah sesuai untuk model takungan fasies pengedaran subpermukaan untuk persekitaron bersirat persekitaran.

TABLE OF CONTENT

LIST OF FIGURES

LIST OF TABLES

LIST OF ABBREVIATION

AAPG	American Association of Petroleum Geology
AZIM	Azimuth
CALI	Caliper
CARS	Central Africa Rift System
Coord	Coordinates
DX	Difference between the X value of the point and the well's x-coord
DY	Difference between Y value of the point and the well's y-coord
FT	Feet
GR	Gamma Ray
H_5_a	Top of the zone five (reservoir)
H_5_b	Bottom of the zone five (reservoir)
INCL	Inclination
KB	Kelly Bushing
KM	Kilometer
M	Meter
MD	Measure Depth
MD	Measure Depth
NE	North East
NNW	Neural Net Work
NPHE	Neutron porosity
QC	Quality Control
RESD	Deep Resistivity
RESS	Shallow Resistivity
RHOB	Density
SIS	Sequential Indicator Simulation
SW	South West
TEM	Train Estimation Model

TGS	Truncated Gaussian Simulation
TVDSS	Subsea Total Vertical Depth
UWI	Unique Well Identify
VPC	Vertical Proportion Curve
WCARS	West and Central Africa Rift System
AAPG	American Association of Petroleum Geology
AZIM	Azimuth
CALI	Caliper
Coord	Coordinates
DX	Difference between the X value of the point and the well's x-coord
DY	Difference between Y value of the point and the well's y-coord
FT	Feet
GR	Gamma Ray
INCL	Inclination
KB	Kelly Bushing
KM	Kilometer
M	Meter
MD	Measure Depth
NE	North East
NNW	Neural Net Work
NPHE	Neutron porosity
QC	Quality Control
RESD	Deep Resistivity
RESS	Shallow Resistivity
RHOB	Density
SIS	Sequential Indicator Simulation
SW	South West
TGS	Truncated Gaussian Simulation
TVDSS	Subsea Total Vertical Depth
MD	Measure Depth

UWI	Unique Well Identify
VPC	Vertical Proportion Curve
CARS	West and Central Africa Rift System

CHAPTER 1

INTRODUCTION

1.1 Research Background

This research describes a study undertaken to model lithofacies of braided delta reservoir of Cretaceous age in the Doba basin by using Sequential Indicator Simulation (SIS), Truncated Gaussian Simulation (TGS) and Object-based modeling techniques. The data used for this thesis are from well logs, cores and depth map as well as reports in addition to other available sources from the internet (papers, journals and books) and a petrel software manual. The work will focus on generating 3D reservoir lithofacies models for the braided system environment. One of the important advances in reservoir modeling in recent years is the use of stratigraphy and geological analogues to build a 3D conceptual reservoir model that helps in exploration and development [1].

The study will provide lithofacies distribution for five uncored wells and an optimum reservoir lithofacies model of a braided delta system of Cretaceous age in the study area in the Doba basin, Chad.

Reservoir lithofacies modeling is an integrated study of geology and geophysics data by distributing discrete facies throughout the model grid based on modeling algorithm on the appropriate reservoir to produce a 3D model and the consistency of a model depends on the amount, property and distribution as well as accuracy of the data [2]. The criteria that could involve the model are parameter set, variogram ranges that come from well correlation and depositional system as well as facies model in consideration of paleogeography.

Commonly braided systems are having heterogeneous reservoirs but rich in the sands with different thickness and sizes. The reservoir heterogeneities can be predicted at an early stage in the field development through facies analysis and analog studies. However, the reservoir continuity and extension can be realized with reservoir model.

In oil business the determination of uncertainties in reservoir facies distribution assists to obtain a consistent description between geological interpretation and reservoir properties for generating flow simulations which helps to minimize and decrease the cost.

This thesis demonstrates a methodology applied in facies modeling. The study focuses on the application of the pixel-based and object-based modeling methods on data obtained over the selected reservoir in an oil field in the Doba basin. The models produced illustrated lithofacies distribution laterally and vertically, and describe reservoir facies related to the heterogeneity of the reservoir.

The pixel-based (SIS and TGS) and object-based modeling techniques are usually used to construct a reservoir facies distribution model. The pixel based methods aspire to produce model realizations with more well data which are appropriate to fit a variogram in spatial correlation. Pixel-based methods present poor representation of the actual facies geometries. Absolutely not object-based method allows to reproducing hard geometries which are able to produce shapes of objects. SIS technique is suitable once the facies geometry is uncertain or the facies types are controlled by several trends (secondary data controlled probability of facies). TGS is useful in modeling environment within transition through a sequence of facies able to control the boulders between different facies, whilst the Object-based modeling technique is important to produce depositional morphology (channels).

1.2 Problem Statement

The use of reservoir modeling assists in assessing the geometric distribution, continuity, and extension of reservoir properties, which are the key factors for

predicting fluid flow [3]. Reservoir facies models in stochastic methods have been generated to identify lateral and vertical lithofacies distribution that controls fluid flow in order to optimize the potential of a field and to decrease the uncertainties of sand distribution. Hence the definition of the facies model represents one of the most important phases in the workflow of reservoir geological modeling.

In the study of the clastic reservoir static modeling, the facies distributions are important to illustrate and predict reservoir heterogeneity [4].

These problems provide motivation to study the process of 3D static model for the heterogeneous clastic reservoir in a selected reservoir in the Doba basin.

The geology of the area is complex and the field is still under evaluation. Therefore a 3D Static model for accurate understanding of facies distribution and its hydrocarbon potential is needed.

1.3 Title Study Area

The study area is an oil field in the Doba basin of Chad that was discovered in 1977. As the oil exploration in Chad started as early as in the 1970s, twenty-nine exploration wells have been drilled with 10 oil discoveries.

The Doba basin is located in the southern part of Chad in between the Yola and Benoue basins to the southwest and the Doseo and Salamat basins to the east. It is in the West and Central Africa Rift System (WCARS) as shown in Figure 1.1.

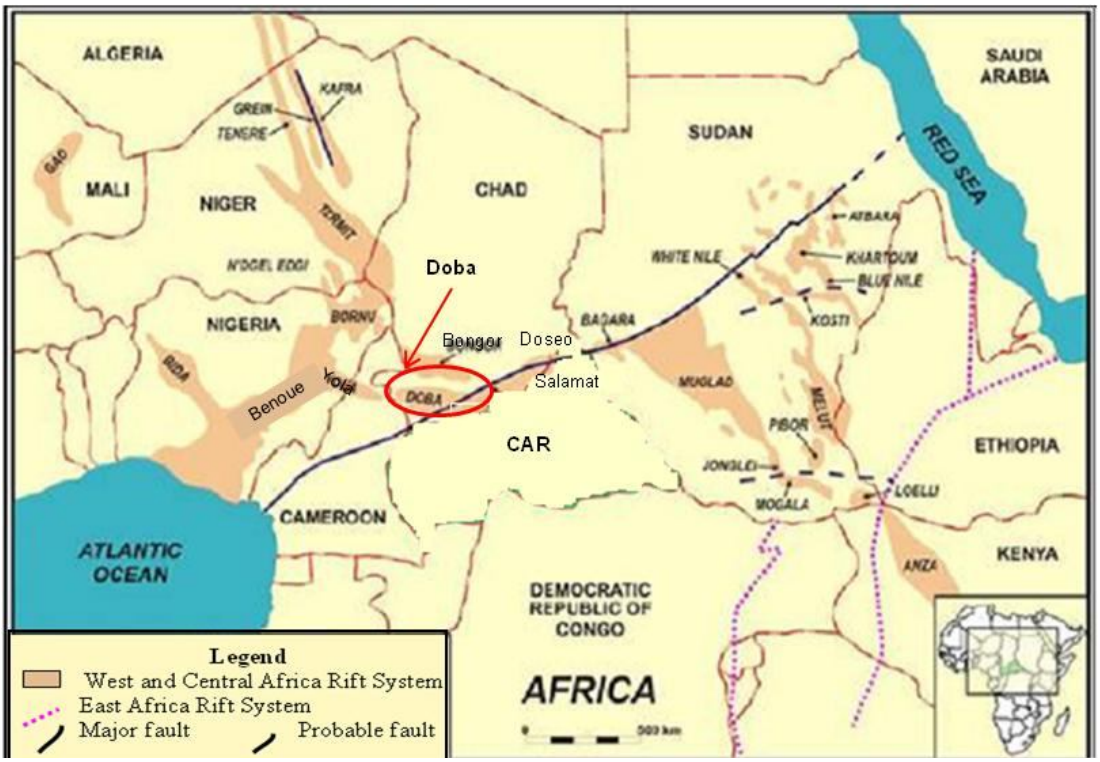

Figure 1.1: The tectonic features of the West and Central Africa Rift System (WCARS). The Doba basin is demonstrated by a red circle, modified after [5].

Development of the WCARS spans the Phanerozoic following the Pan-African crustal consolidation event in the Cambro-Ordovician. Most of the key tectonic and stratigraphic elements in WCARS, however, resulted from early Cretaceous rifting and subsidence of the African plate relating to the breakup of Gondwana as well as early Tertiary tectonic events [5].

The study area is the K-Oil Field, located about 440 km south of N'Djamena in Doba basin as shown in Figure 1.2

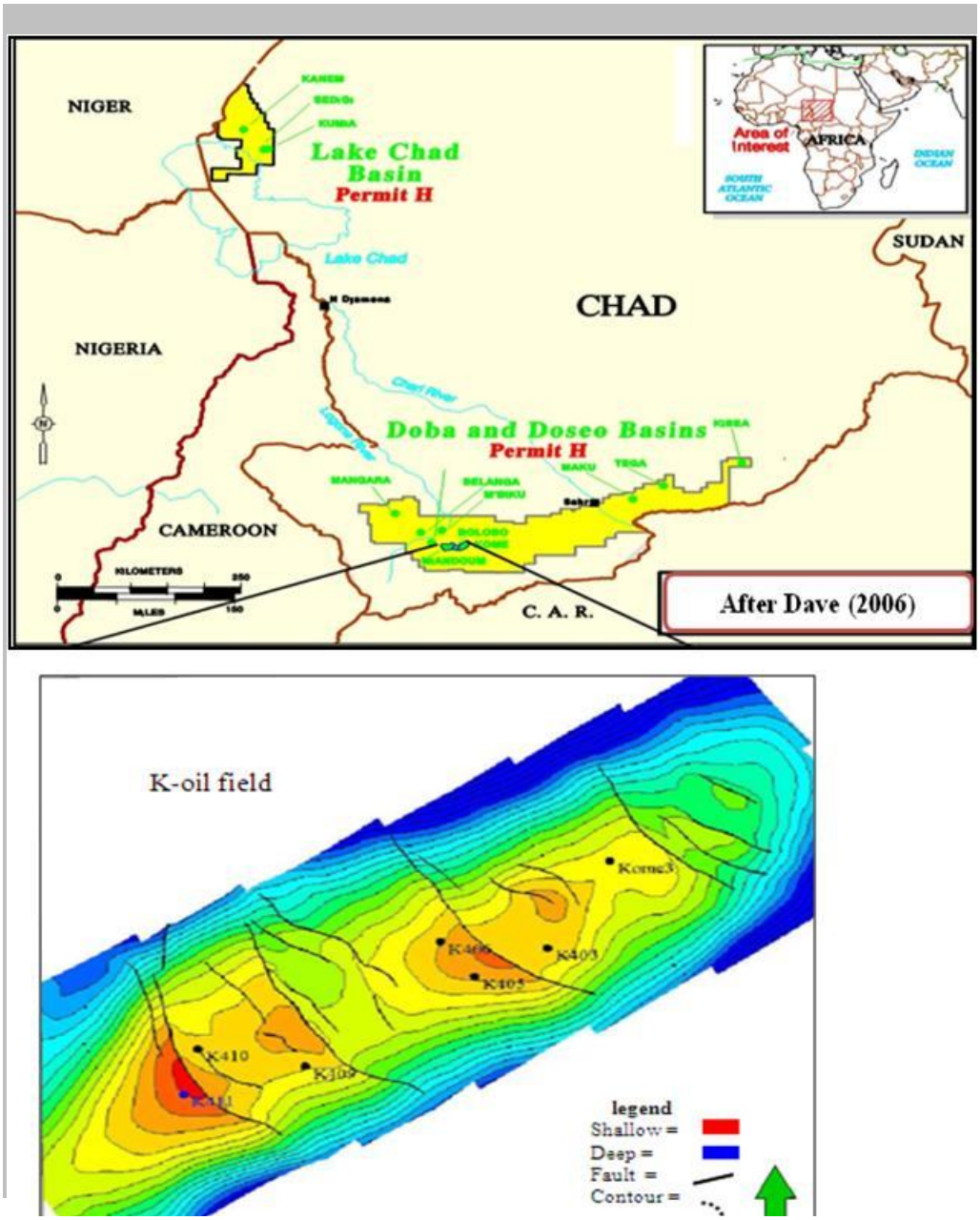

Figure 1.2: Map showing exploration basin in yellow color with the location of the K-Oil Field of Doba basin, modified after [9].

The area was discovered by a consortium in January 1977 with the drilling of well H1. Based on the data from six review wells and information from the 3D seismic acquired over the field, the most recent estimate of recoverable oil is 548 million barrels.

The petroleum industry of Chad has become an important sector of the economy of that country. It does not currently produce petroleum, but discoveries of oil

fieldssuggest the prospect of drilling of 300 shafts in the Doba region and the production of 150,000 barrels of crude per day [6].

In the Doba region, Exxon took charge of operations and exposed the field in 1989. Chad´s principal reserves are found in four sedimentary basins in the south of the country, and in a small basin to the north of Lake Chad.

Other exploration activities have continued separately from the Doba project. In 1999, three companies, Trinity Gas and Carlton Energy of the America as well as Nigerian Oriental Energy Resources, signed an accord with the government of Chad to explore the 430,000km^2. Block H (Exxon Mobil areas) as shown in Figure 1.3.

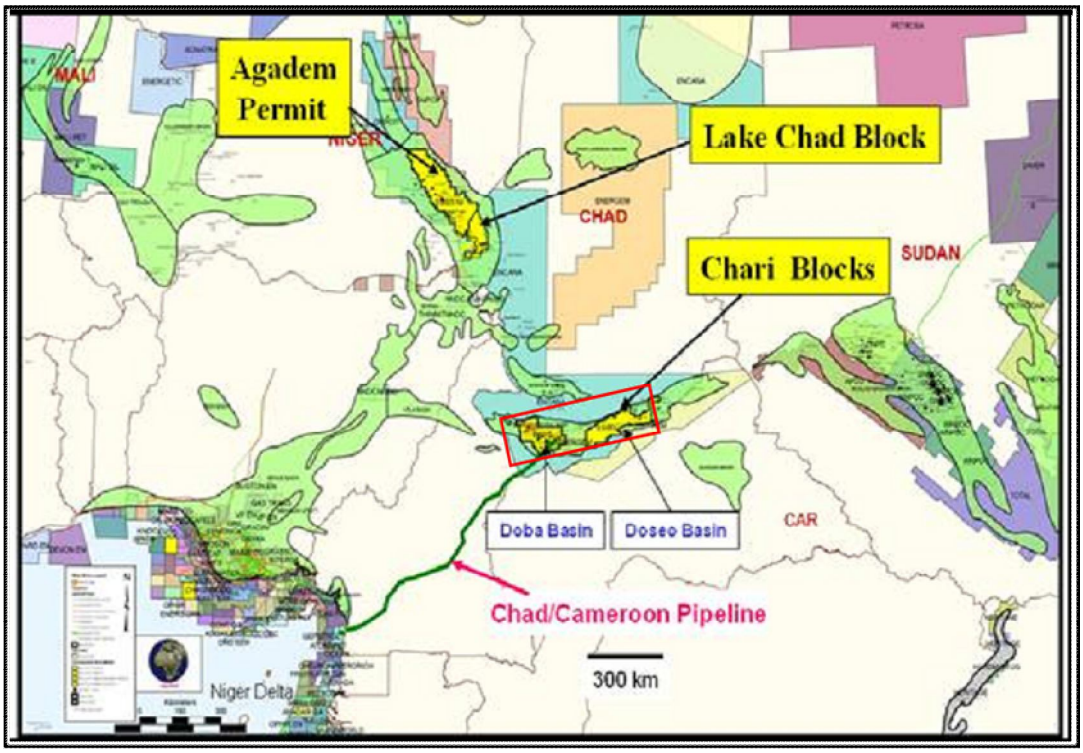

Figure 1.3: Exploration activities in block H around the study area after [5].

1.4 Objectives of Research

The objective of this research focuses on building an advance research on Cretaceous reservoir facies using 3D modeling methods in the K-Oil Field of the Doba Basin. In understanding the sand distribution, continuity, and extension of the

reservoir lithofacies, modeling is the principal aim of this research. The objectives of this study are:

1. To understand and predict the geometry and heterogeneity of the reservoir facies in 3D in order to mitigate uncertainties in well placement.

2. To describe reservoir facies using statistical information (geometry, variogram analysis and facies fraction).

3. To illustrate lithofacies distribution laterally and vertically.

4. To model reservoir facies distribution of the braided delta system using stochastic methods in several realizations, comparing among the models and determining the optimal model.

1.5 Scope of Research

The scopes of this study started with literature review on the conceptual deposition environment to proceed with modeling of reservoir lithofacies. Subsequently, it is followed up with importing and digitizing data in a software program, Petrel Version 2008. The data gathering prepared, verified, and imported to the software was initially quality checked.

Five core images of depth ranging 11357 ft (3461.5 m) to 11614 ft (3540 m) of a well, H5 were reinterpreted and calibrated with logs (after consideration of matching depth and depth shifting) for facies environmental interpretation and lithofacies prediction and generating facies maps of the reservoir were carried out to proceed with reservoir modeling.

Finally reservoir facies model realization in SIS, TGS and Object-based techniques were carried out after creating surface, zoning, layering, and well logs up-scaling as well as analysis of well parameter setting.

The output results from three realizations based on 3D modeling techniques were analyzed. The optimal model results of 3D reservoir lithofacies models of braided

delta in the study area were compared with an analogue. The model revealed the importance of the reservoir modeling for well placement and dynamic model input.

The limitation of this research includes the lack of secondary data to support and justify the interpretation of environmental facies classification and lithofacies prediction in between the wells. The observation from the available seismic data is also poor due to low continuity of seismic facies which define the sand facies and shale facies. From the six well logs used for environmental facies interpretation and lithofacies prediction, only a well contain the limited core image. It doesn't show sediment features properly, in some cases, and the core is limited and does not penetrate the whole interval.

Although the pixel-based methods failed to capture the environmental concept (variogram need more well data to fit properly) except in realization where expanding the variogram ranges. In lithofacies prediction the train estimation model result did not detect sand bar facies which are thin layers of about 2 feet in the reservoir zone.

1.6 Thesis Organization

This thesis consists of five chapters that include results of facies analysis and reservoir lithofacies modeling carried out to obtain the objectives described above.

The background of this research in Chapter 1 covers the development of the reservoir lithofacies modeling by using pixel-based and object-based modeling techniques. The explanations of the advantage of different modeling technique are also included.

The conceptual background of the environment of deposition of the area is explained in Chapter 2.

The methodology adopted for this research including giving details on the data available, data preparation and importing, setting project unit, faults modeling, horizons modeling, 3D gridding are described in Chapter 3. In addition, well correlation, environmental forces interpretation, focus prediction, well blocking, data

analysis and the methods used for reservoir facies modeling as well as the geostatistical analysis of the reservoir facies, are also explained in this Chapter.

The results from well correlation, environmental interpretation, and lithofacies prediction for non cored wells are discussed. In addition to the choosing of appropriate modeling techniques and parameter set of object- based and pixel-based as well as reservoir facies, model realizations were explained, discussed, and compared in Chapter 4.

In Chapter 5, the results of this study of the reservoir lithofacies models are summarized and the directions for the future work are recommended.

CHAPTER 2

LITERATURE REVIEW

This chapter described the Cretaceous reservoir lithofacies distribution of K-Oil Field in the Doba Basin, in order to understand the depositional environment and lateral and vertical distribution of the reservoir facies.

2.1 Geologic Setting

The Doba Basin is an elongated northwest-southeast trending basin. These genetically related structures constitute the Cretaceous-Tertiary rift basins of the West and Central Africa Rift System (WCARS) [7], [5].

Most of the key tectonic and stratigraphic elements in the WCARS resulted from the early Cretaceous through early Tertiary rifting and subsidence of the African Plate [1], [8].

In Central Africa, north-south extension occurred in the Neocomian Stage and northeast-southwest extension occurred in the Aptian stage. These two rift events were then followed by a sag event spanning the Albian through Turonian Stages, during which several thousand meters of subsidence and concomitant accumulation of continental and lacustrine sedimentation occurred. Inversion events occurred in the Late Cretaceous (Santonian) and in the Eocene resulting in erosion and subsequent accumulation of 1500 to 3000 meters of continental deposits.

The anticline structures of e basin are the product of this multiple phase of deformation. Finally, widespread uplift marked by an extensive unconformity occurred during the Oligocene and early Miocene.

In the Doba Basin, the two extensional events are expressed as onlap of Lower Cretaceous strata onto the rift Graben margins, whereas the sag phase is expressed as an Upper Cretaceous succession that extends beyond the central rift system margin, but thickens into the older rift basin axis. The Lower Cretaceous strata are interpreted as fluvial, deltaic, and lacustrine deposits. The Upper Cretaceous strata represent interbeded fluvial-lacustrine deposits [9].

2.1.1 Tectonic History

The basin contains up to 10 km of non-marine sediments. The tectonic and climatic evolution of the region is complex, started in the early Cretaceous. The basin was identified by using gravity data, but three decades of subsequent exploration activities have significantly increased the understanding of the basin`s evolution.

The basin development is believed to experience multiple extensional and inversion events producing the structures observed today. The evolution of the basin in terms of trap development was influenced by the non-marine and lacustrine depositional settings of rift structures and topography created by the Cretaceous extension. In order to understand the distribution of play elements within these basins, it is necessary to first unravel their evolution and identify those features which influence depositional environments during the time in question. The basins were sites of extension on a Pan African shear zone beginning in the Neocomian [10].

In the Doba basin the faults trend northeast-southwest and develop en-echelon within southeast dipping half-grabens. Accommodation and relay zones are present in the basin where these faults intersect the Neocomian faults.

A series of north-dipping normal faults were created along the southern margin of the basin, while faults along the northern margin amalgamated to form a long, complex fault zone. The paleogeographic map of an interval area was used to define the deposition of direction as in Figure 2.1

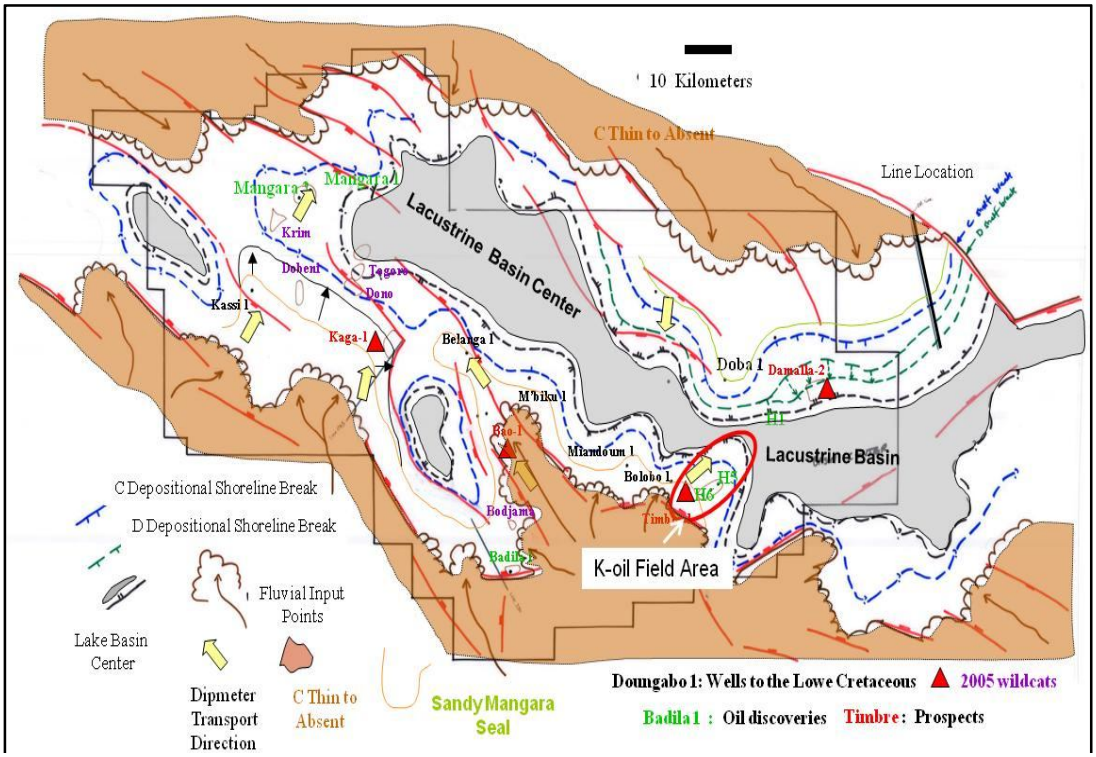

Figure 2.1: Paleogeographic map for the shallow interval of the study area, show lacustrine facies deposited, and diameter transport direction modified after [9].

The greatest inversion in these regions is in the order of 100 - 200 million years. Lesser inversion continued until about 40 million years when the African Plate was placed under large compression stresses once again, due to convergence of Africa and Europe during the Pyrenean Originy. The inversion of the Neocomian-age normal faults is common and several northeast to southwest-trending anticlines are present. In some places these earlier faults are reactivated, while in others, new reverse faults are formed.

The highest inversion is roughly 500 - 700 meters on these structures. The western portion of the basin was being uplifted in response to heating associated with the Cameroon volcanic belt.

The basin was next deformed by regional northeast extension beginning in the late Oligocene. This north-northwest trending fault system often reactivates pre-existing Aptian-aged faults, sometimes for only a segment of their length, before continuing on newly-formed fault strands. In other cases, the faults are detached in an Upper

Cretaceous shale interval. Regional uplift associated with the African super plume has created a widespread erosion surface with an age of about 10 million years that has beveled the entire section in the basins so that no surface expression of the most recent structures are observable. Table 2.1 shows a summary of the tectonic and stratigraphic of the Doba Basin.

Table 2.1: Tectonic and Stratigraphic of the basin.

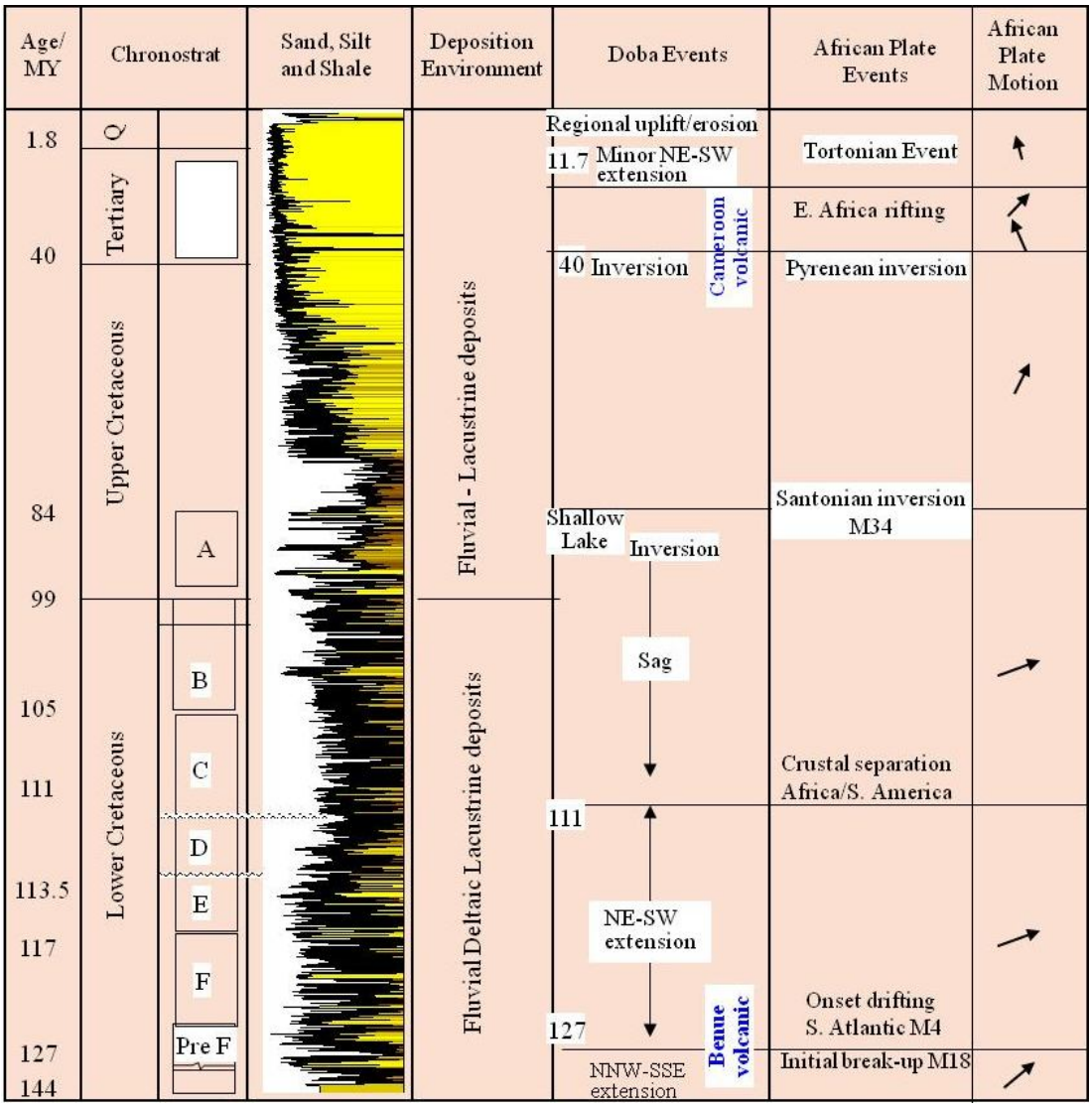

2.1.2 Environmental Deposition

The environmental depositional concept of the basin is defined as an alluvial fan deposited into a standing body of water. The fan deltas were formed by progradation of a braided fluvial system into the standing body of water (Figure 2.2). The fan deltas

contain no direct evidence for the presence of fan alluvial, and such systems are better classified as a braided delta which differentiated the environmental setting of true fan deltas from that of braided deltas [10].

The classification of the system may lead to the correct expected facies of sandstone geometry and reservoir quality. Vertical and lateral lithofacies associations and paleocurrent patterns must be used to identify the depositional systems correctly.

The importance of depositional facies is in controlling the reservoir properties and understanding of environmental types to preparing the necessary input data for modeling.

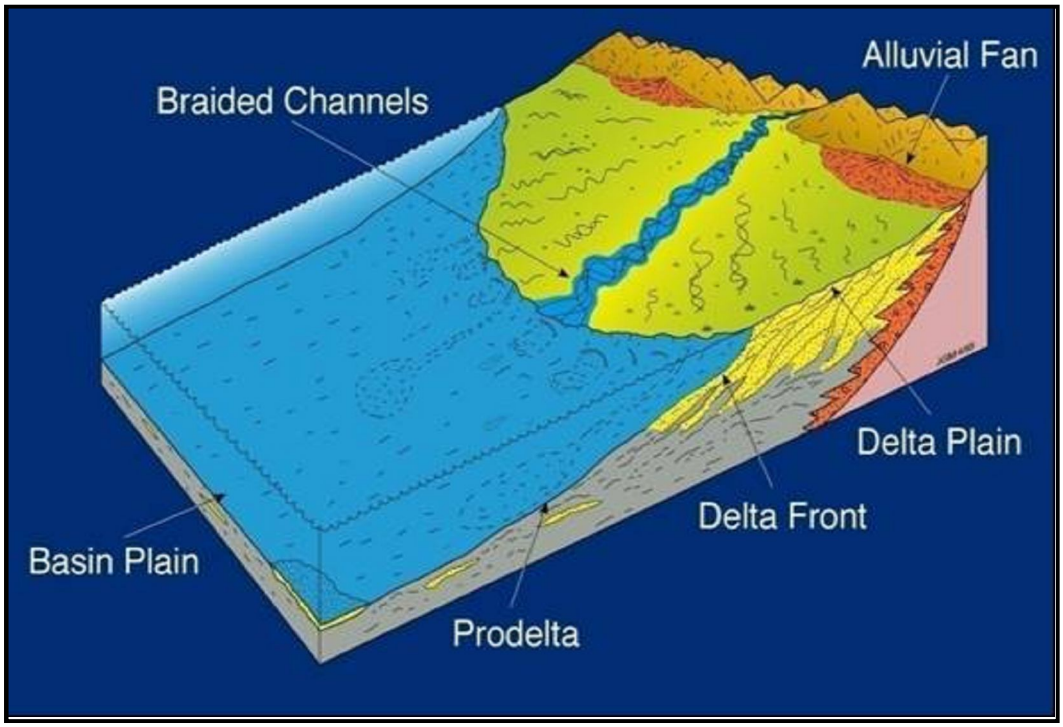

Figure 2.2: Block diagram of a Braided Delta depositional system, after [10].

2.1.2.1 Braided Sandstone

The character of the typical braided stream proposed is one of the bases in modeling reservoir lithofacies. Coarse sandy braided stream that consists of fining strata packages that are composed of coarse to very coarse-grained, trough cross-stratified sandstones, Pebbles and cross-bedded laminated fining system is dominant.

Fining sandstone packages are bound at their base by sharp scour surfaces that, in rare cases, are overlain by beds containing clay.

Fining sands are stacked to vertically form multistory sand block well-log. Based on the predominance of trough-cross stratification as well as scour surfaces and associated clay layers, these fining sandstone packages are interpreted to represent bars that formed in low-sinuosity braided channels. The lack of clay deposition within the braid-bar suggests that deposition occurred during relatively high discharge and that shallow deposits were not preserved. Coarse sandy deposits are found throughout the intervals.

Stream mouth bar facies association that consists of fine to medium-grained sandstone beds, are occasionally clay laminated. Mouth Bars are interpreted to be deposited subaqueous on the lacustrine margin of the lacustrine braided delta, down dip of braided feeder channels. They are typically semi-amalgamated, and interpreted to have high to medium lateral connectivity. Stream Mouth Bars have a blocky to thin gamma ray log pattern with a low to moderate gamma ray response. Figure 2.3 shows a GR motive for different sand body grain.

Cylindrical GR	Funnel GR	Bell GR
Coarsening blocky shape, sharp base & top 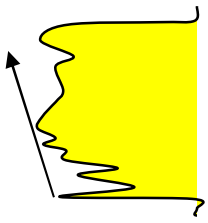	Coarsening sharp top 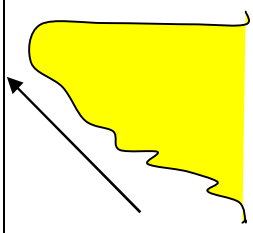	Fining sharp base 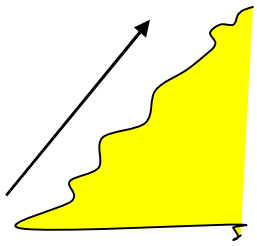
Coarsening	Coarsening prograding	Fining retrograding

Figure 2.3: Gamma ray response for different main sand body grain

2.1.2.2 Lacustrine Sandstone

The lower Cretaceous delta is classified as a braided delta and consists of delta front facies of fine grained parallel laminated sandstone. Thin wavy laminations present in the distal [11]. Delta front facies typically are capped by Stream Mouth Bar deposits Figure 2.4.

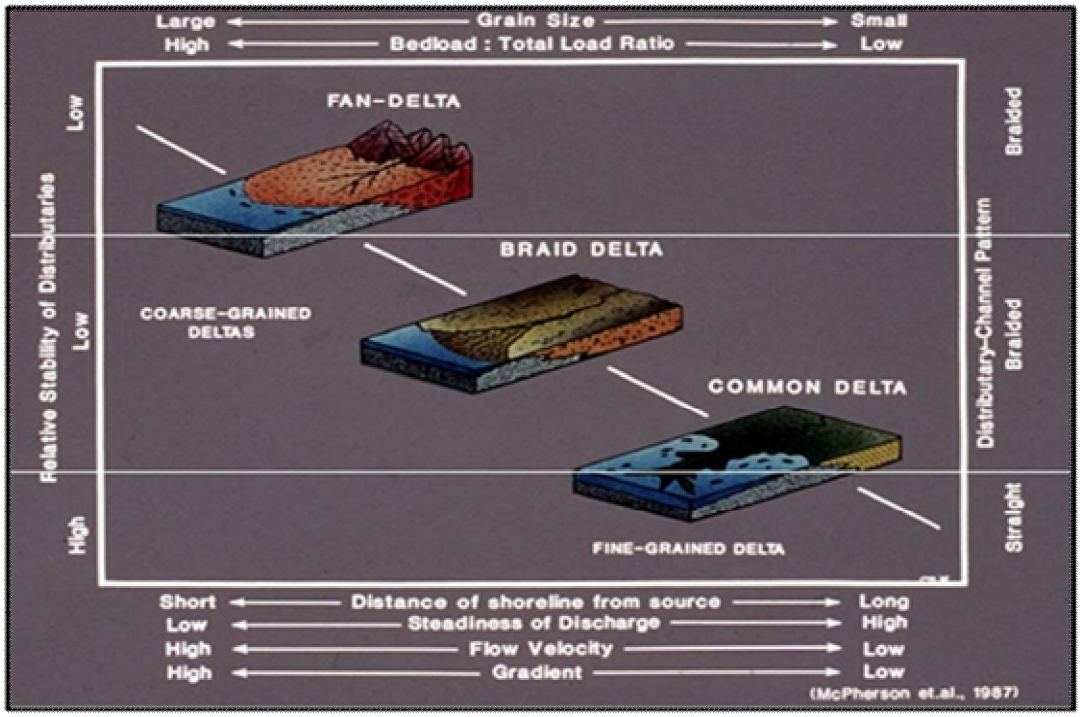

Figure 2.4: Classification for deltas based on grain size, distance from source, and other factors, after [11].

The delta front is subaqueous on the down dip margin of the Lacustrine Braided Delta. Sands are interpreted to be semi-amalgamated to amalgamated sheet like sands with good lateral and poor vertical connectivity. The gamma ray log pattern is thin, serrated, and coarsening upward, with a low to moderate gamma ray response [9].

2.1.2.3 Lake Margin Facies

This facies is composed of fine to very-fine grained sandstones, muddy sandstones; beside siltstones other features include occasional coarse floating grains, contorted bedding, wavy to rippled lamination, and root traces. Lake Margin facies

typically are non reservoirs, and may represent seal facies. The lake margin facies association is interpreted to have been deposited lateral to the braided complex at the lake margin or as deltaic facies rarely which were later exposed and bioturbated. The Gamma ray pattern is thin to serrate.

2.2 Reservoir Geometry

The available seismic data show typical drainage systems in the Doba Basin, with porous continuity in the reservoir sand as shown in Figure 2.5. However, there is a little visualization of the three dimensional distribution of reservoir sand possible from the available seismic data.

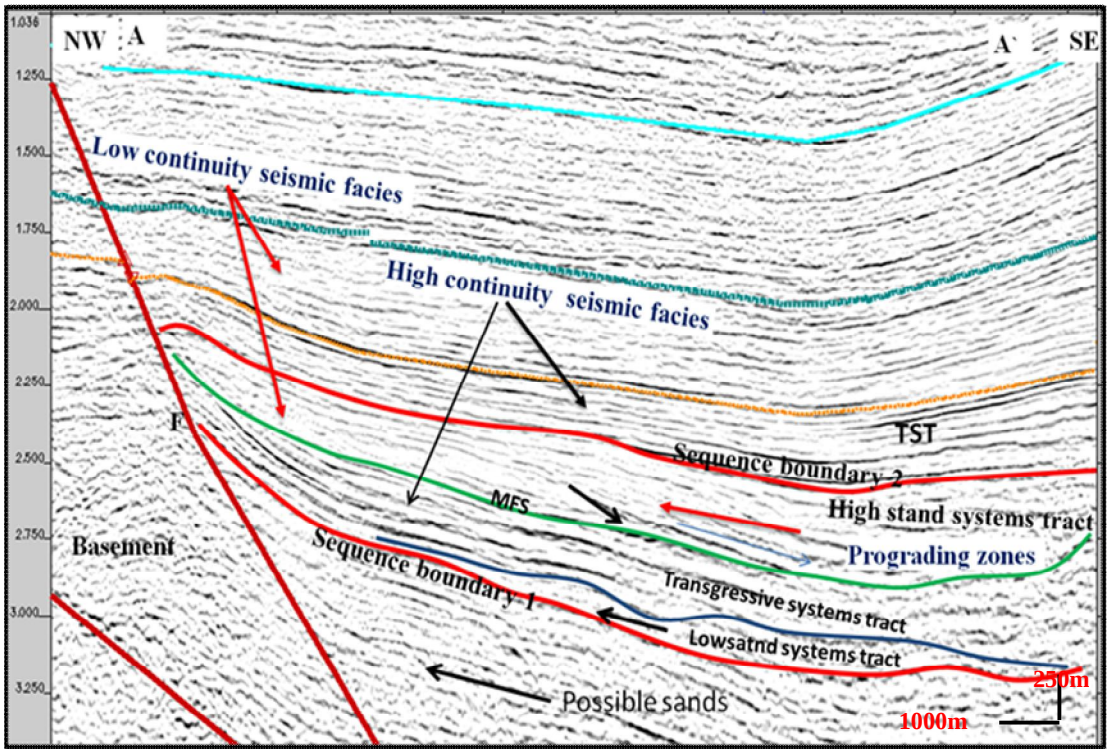

Figure 2.5: Typical seismic section showing the Doba Synrift drainage Systems are trending NE - SW direction, re-interpreted after [10].

In developing the reservoir model, it is critical to understand the existing reservoir architecture, thickness, size, distribution, and orientation of the reservoirs sandstone bodies. These parameters of sandstone bodies are different from one core to another

depending on their origin. The understanding of the sand bodies is important in order to predict the geometry and the orientation before commencing any reservoir study.

Complete system tracts are observed, with prominent prograding zone within the stand system tract. The top of the reservoir shown in Figure 2.6 are core facies with well log. Details of reservoir sand distributions may suggest a reasonable model based on available seismic data.

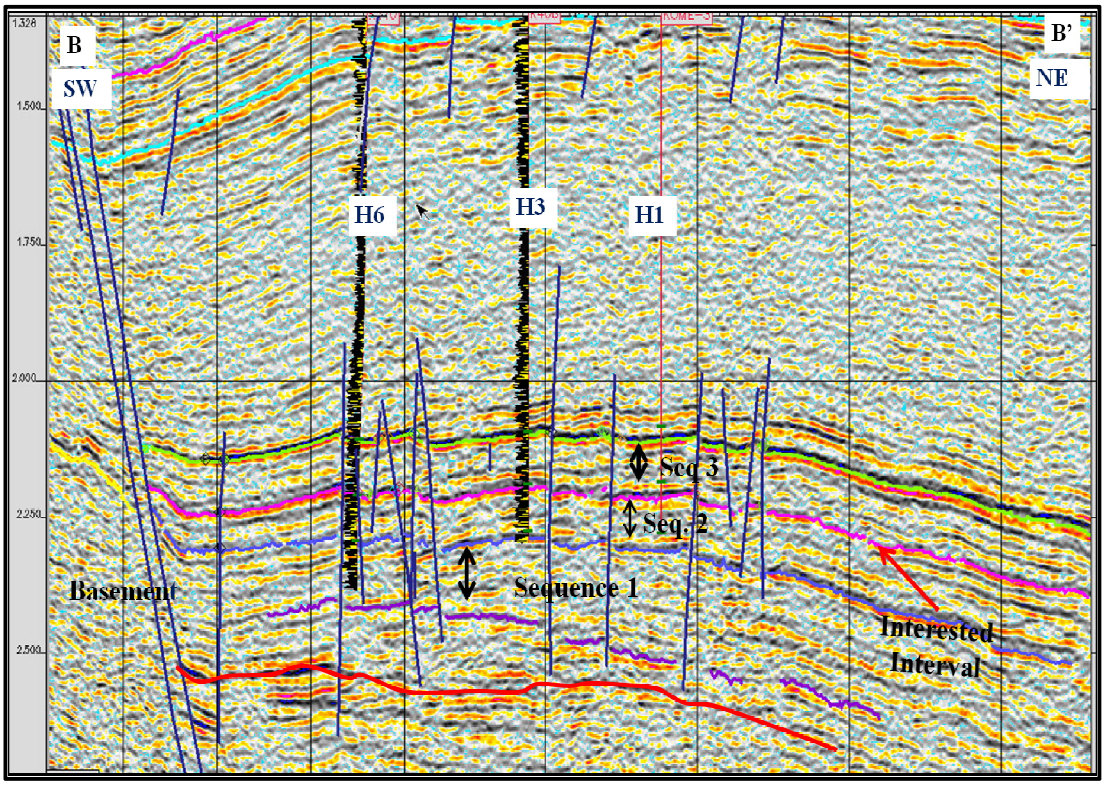

Figure 2.6: SW - NE Seismic section across the field showing the top of the reservoir in pink color for the horizon interval studies, modified after [10].

= normal faults dissected the interval

= Arrow shows top and bottom of sequences

2.3 Conceptual Reservoir Models

The braided delta depositional model has been proposed for field reservoir study based on the regional paleogeography study which shows the development of the

interval reservoir of a thick braided sandstone layer. A braided stream sandstone package is typically clean and exhibits a blocky to fining characteristics with some shale breaks. The fluvial sandstones of the Cretaceous are interspersed with deposits of overflow finer grain and lacustrine clays [12].

The Cretaceous reservoirs of the study interval are oil bearing fields.

To date there is no assessment of the reservoir in full to understand the rate of flow oil and gas from the discovery wells. As such, the distribution of sand is critical to get the optimal reservoir model.

CHAPTER 3

METHODOLOGY

3.1 Workflow

This chapter describes the methodology of facies modeling from data gathering, well correlation, and faults modeling to facies modeling. Figures 3.1 and 3.2. Shows the main steps and details workflow of the reservoir lithofacies modeling respectively.

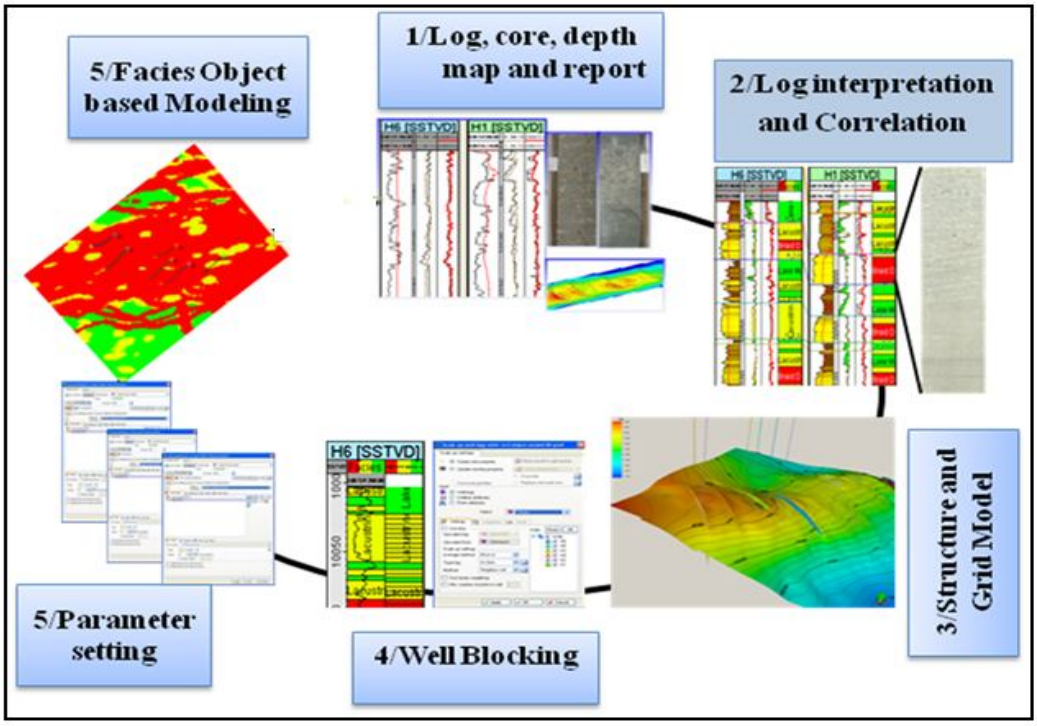

Figure 3.1: Methodology of building static 3D reservoir lithofacies modeling of braided delta complex.

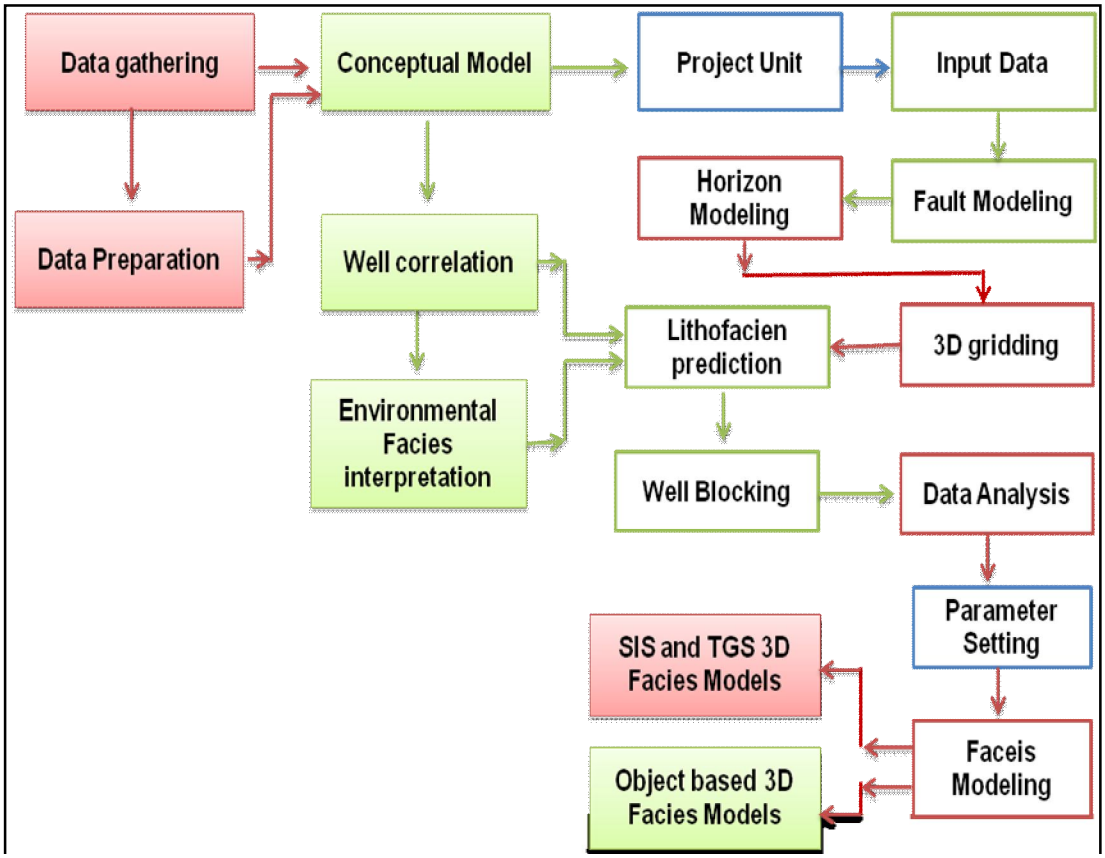

Figure 3.2: The research workflow of this study.

Data calibration steps are being utilized in this research along with details of the characteristics and measurement capabilities. It also includes the modeling techniques used in the Petrel software. For this study the Pixel-based and Object-based methods are operational in data analysis for modeling purposes. The pixel-based comprised Sequential Indicator Simulation (SIS) and Truncated Gaussian Simulation (TGS).

3.2 Braided Reservoir Concept

This study requires a strong background of model concept. The braided environment concept is the deposition created at the bottom of the mountains, where the gradient of the ground surface decreases over a relatively short distance and steeply inclined. The rivers flow at high energy and low sinuosity, on these situations the coarser grained sediment like the gravel move along the river floor by rolling and sliding, coarse sand move by jumping, finer sand and mud remain in suspension and

are carried downstream beyond the confines of the braided river system [13]. Figure 3.3 and Figure 3.4 are illustrated figurations of a braided river system and sediment movement respectively.

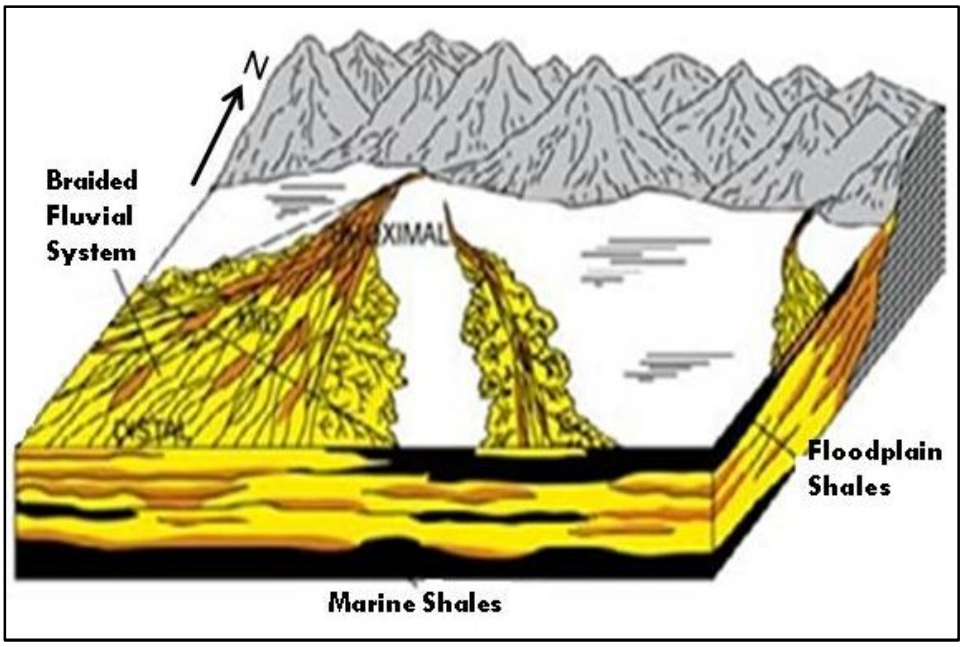

Figure 3.3: A braided river system environments, modified after [12].

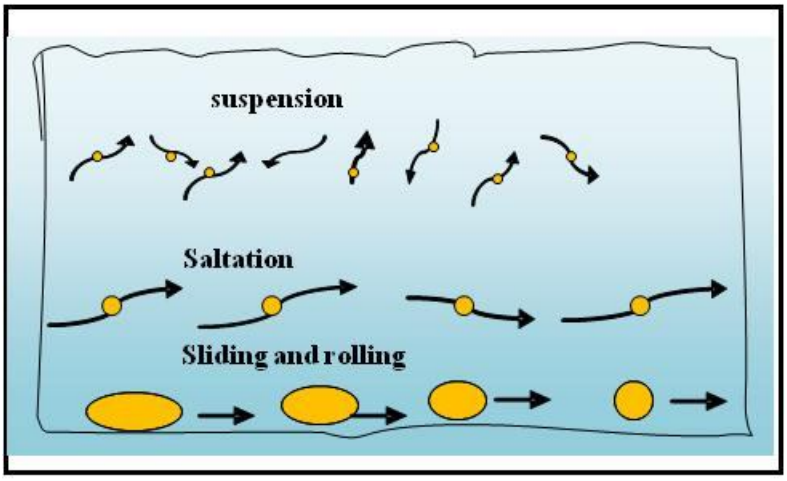

Figure 3.4: Example of movement and transportation of sediments within a braided river system modified after [12].

Heavy grains (gravel) move along the river by rolling and sliding while medium weight grains (sand) move by jumping (saltation). The sediments that are transported

by saltation and rolling or sliding are collectively termed bed load. Suspended load consists of the fine grains that remain in suspension during downstream transport. Friction between the river column and the river bed results in reduction of velocity near that interface. River-flow velocities are faster in the upper parts of the column. The typical deposit of a braided river is coarse sand with few mud and gravel and sand deposits typically are laterally continuously and vertically connected. Braided rivers often flow intermittently because of variations in rainfall in the adjacent mountains. With new flows, a river may change its course repeatedly, thereby giving rise to the braided pattern that is diagnostic of this type of deposit [14], (Figure 3.3).

A braided-river deposit is coarse grained and consists of gravel and sand, with little to no mud. Because of this the beds tend to be laterally continuous over much or all of the width of the braided plain, although the presence of some shale beds may disrupt the continuity locally.

The conceptual deposition of this environment as braided delta system form basis showing in operationalizing modeling the lithofacies for reservoir heterogeneity.

3.3 Available Data

The data required for this research are:

a) Well Logs

b) Core images

c) Depth map

d) Reports

The regional geology and exploration history are derived from reports, published papers, and document that are available from the internet and other sources.

The reports include a core description and facies analysis study done previously by [10]. Core images data of a cored interval of Cretaceous rock.

Based on the literature of lower Cretaceous and the evidences from log motives and images data available from the well H5 the environmental deposition and facies are classified into braided complex (blocky gamma ray shape and show fining upwards) and lacustrine complex (high to low gamma response and show coarsening) environment, while facies are classified into four units and used as guidance details are in Figures 3.5, 3.6, 3.7 and Figure 3.8.

Core Images	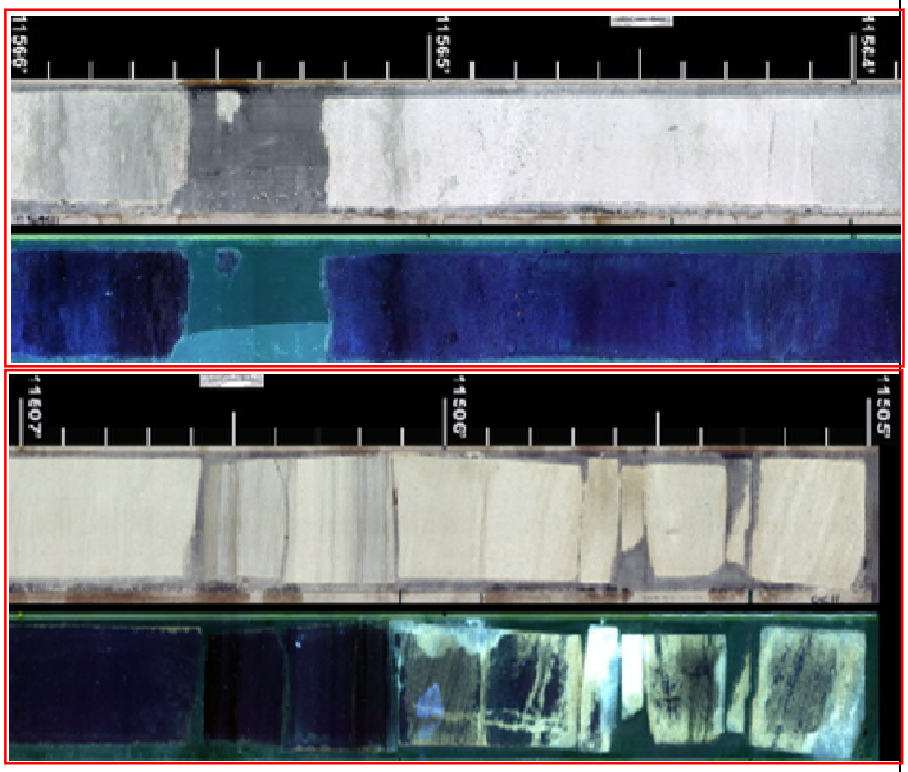
Description	Coarse to medium grained Sandstone, showing Cross bedding, and fining system in some case. It represents a reservoir
Environment	Braided delta complex
Facies	1 (Sandy bar facies)

Figure 3.5: Example of Core data used for this study. The core samples represent Sandbar facies of a braided delta complex environment.

Core Images	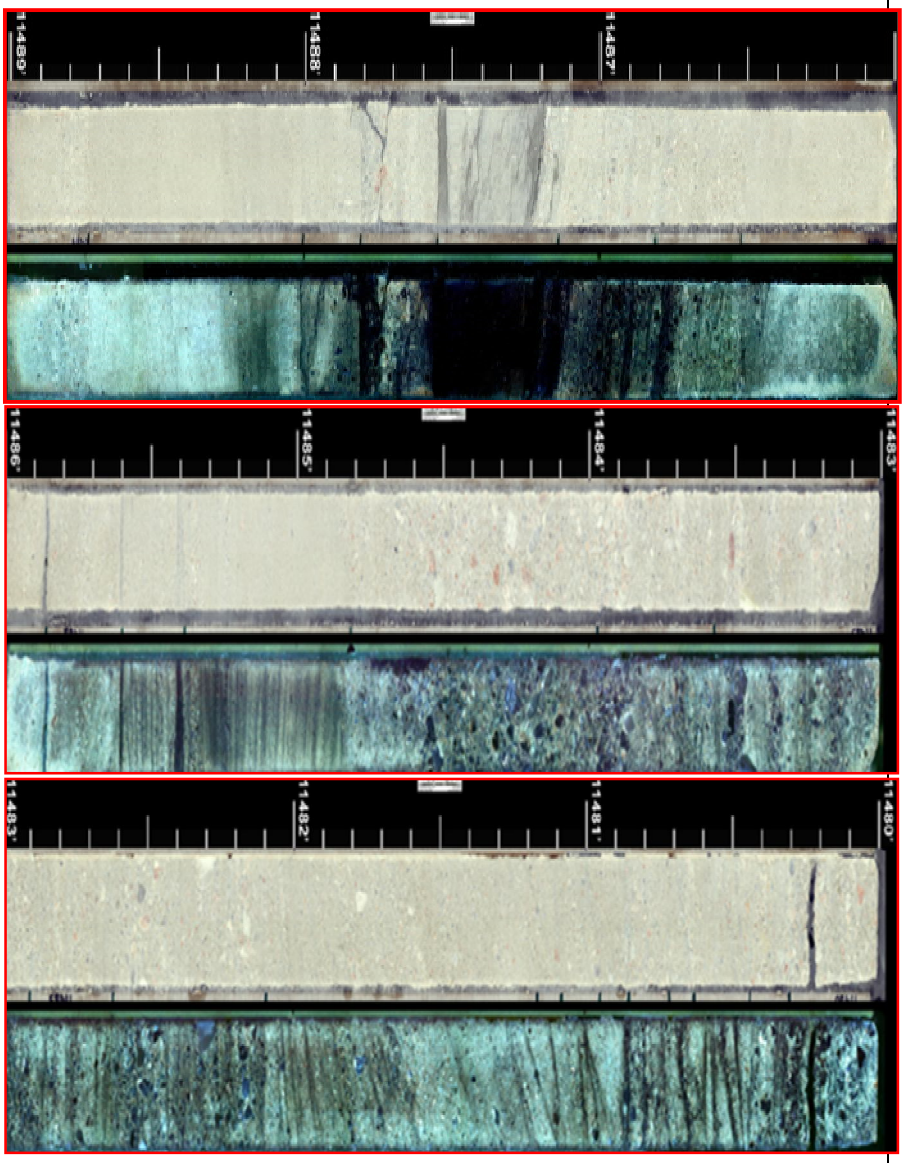
Description	Coarse to very coarse grained Sandstone, contain pebbles and showing cross bedding, fining system dominant and represent a good reservoir
Environment	Fluvial, Braided delta complex
Facies	0 (Coarse Sandy bar facies)

Figure 3.6: Example of Core data used for this study. The core samples represent coarse sandy bar facies of a braided delta complex environment.

Core Images	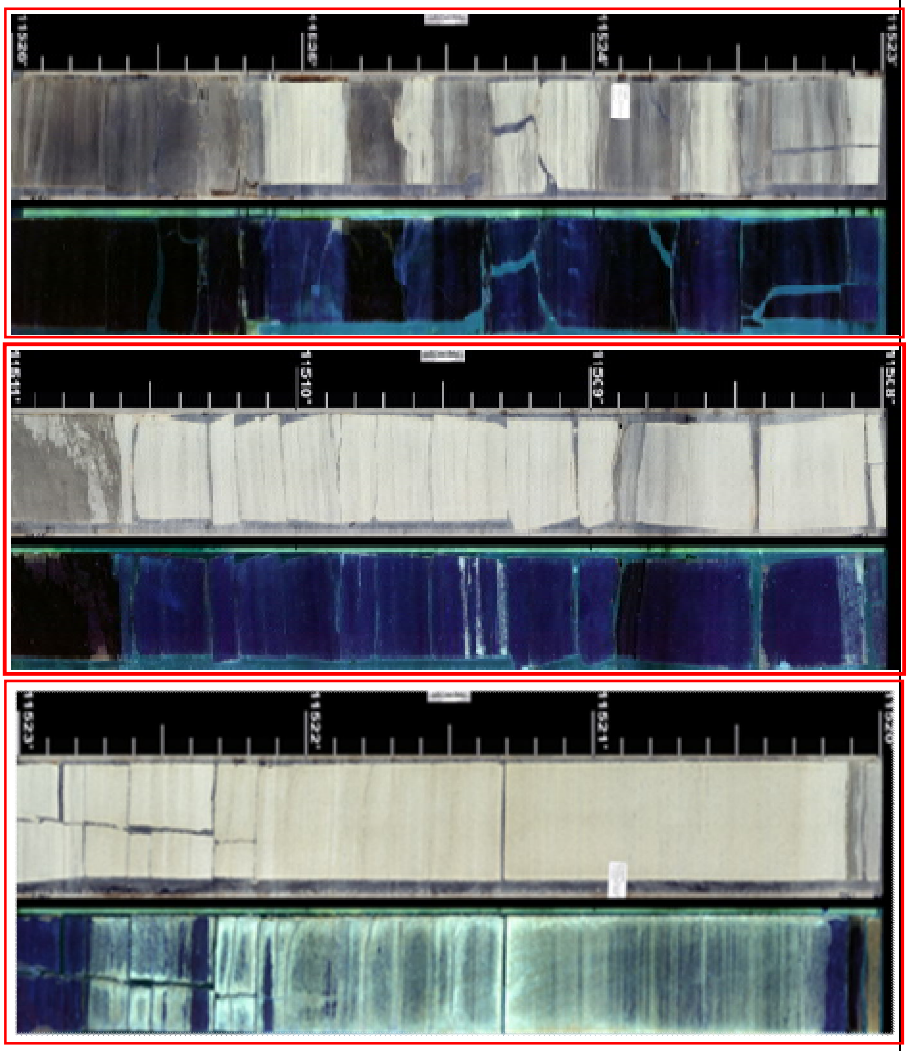
Description	Fine to very fine grained Sandstone. Showing lamination rich in mudstone and less porous facies due to the fine grained. It does not represent a reservoir
Environment	Lake, Lacustrine complex
Facies	2 (Lacustrine)

Figure 3.7: Example of Core data used for this study. The core samples represent Delta front facies of a lake margin, lacustrine complex environment.

Core Images	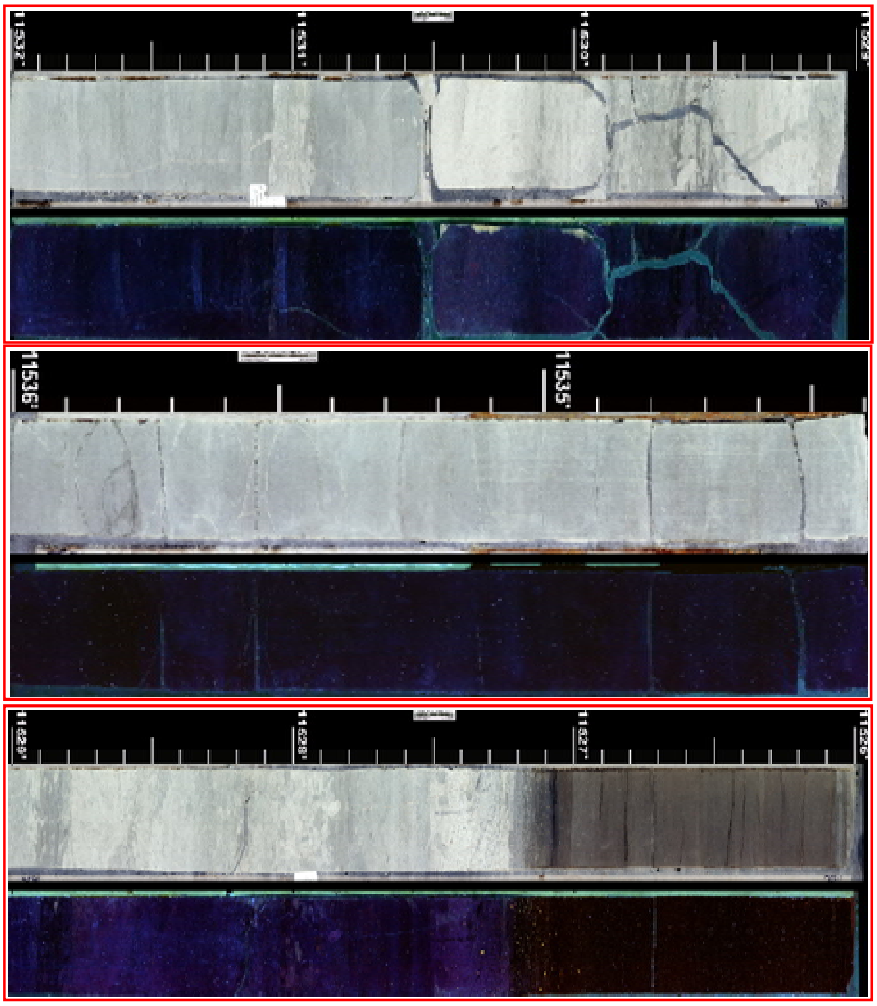
Description	Fine grained Sandstone (silty) with some thin laminations and thin Gamma ray pattern, serrated and show coarsening system. Does not represent a good reservoir.
Environment	Lake margin, lacustrine complex
Facies	3 (Delta front)

Figure 3.8: Example of core data used for this study. The core samples represent delta facies of lacustrine complex lake margin (delta complex) environment.

The other data available is a structural depth map of H_5_a (3514.3 m) which is digitized and imported into the model as surface for modeling purposes as shown in Figure 3.9. Six were line logs which are used as main input in correlation and

lithofacies modeling process. The top and base of the interval for this study were taken from the available maps.

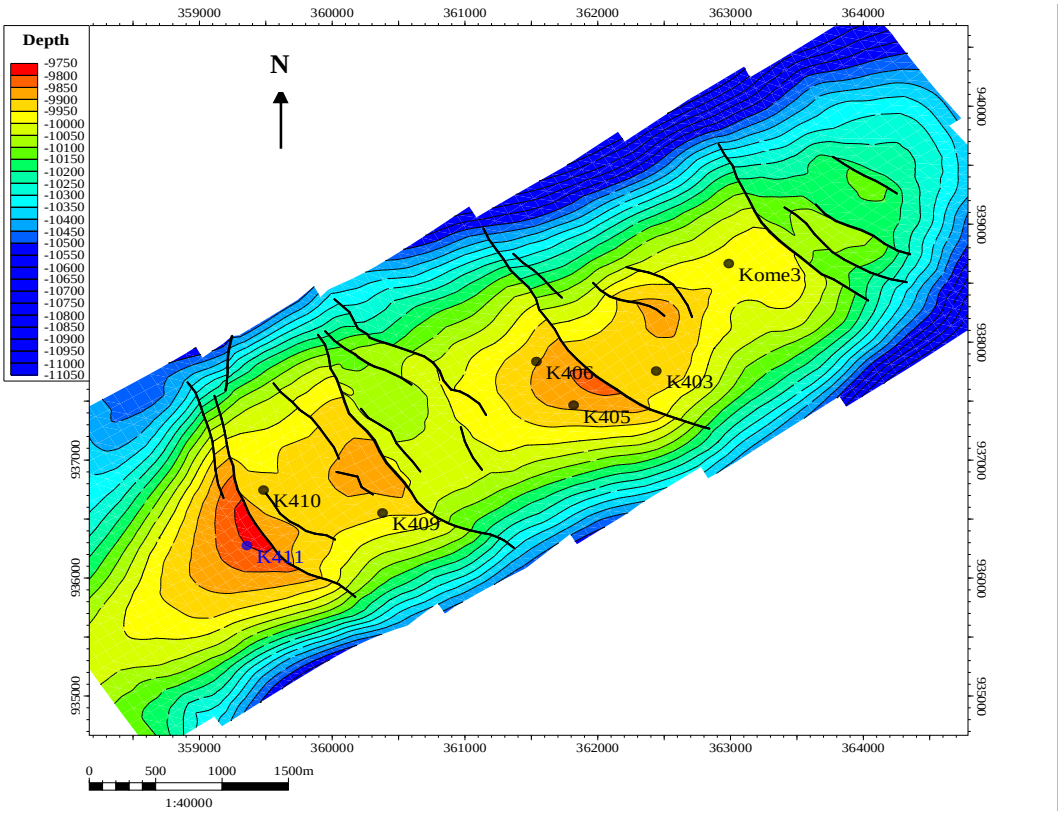

Figure 3.9: Depth map of K field having an elongated doubly plunging NE - SW anticline dissected by NW-SE normal faults. The top and bottom of the reservoir is taken based on the depth map.

3.4 Data Preparation and Setting Project Unit

The available data were compiled and selected in appropriate format "ASCII and LAS file". The formatted data are then imported into the software Petrel version 2008. The main input are well heads data, well deviation data, and finally the well logs data. The six development logs used for this study are from wells H1, H2, H3, H4, H5, and H6. Figure 3.10 shows the location of the well in the study area.

The data import started by importing depth map and well logs data into Petrel software and ended by quality control are included in Appendix A.

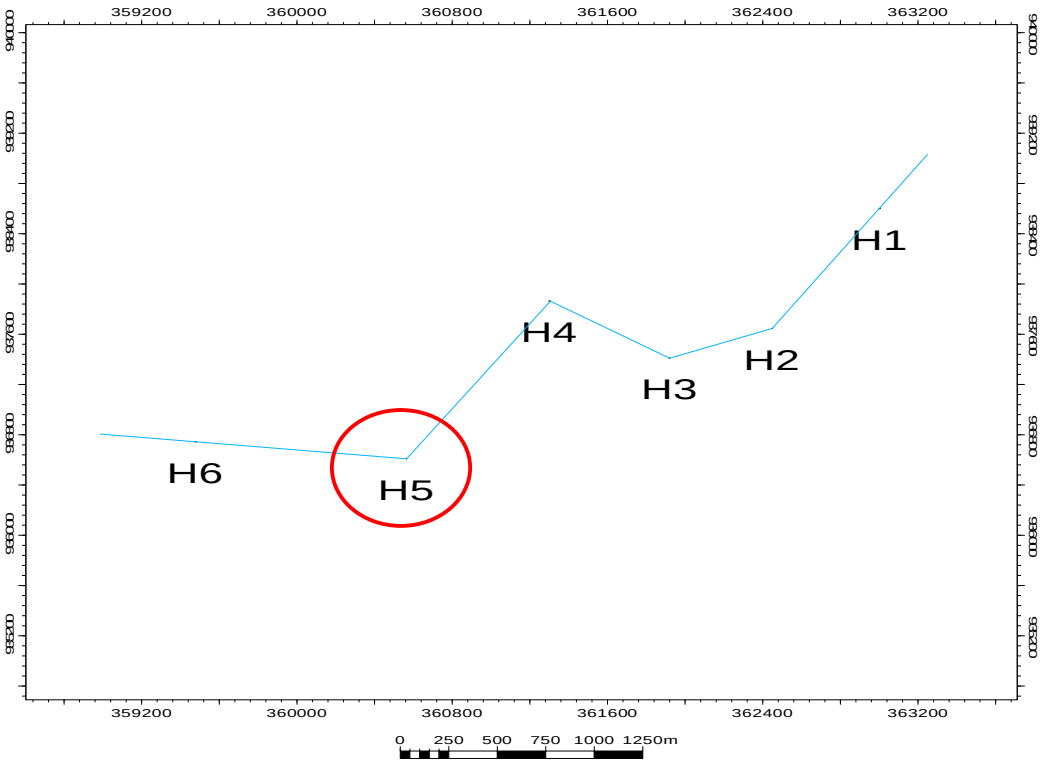

Figure 3.10: Map shows locations of study Wells on K oil field, the well H5 used as an index to other wells in this study.

The structural depth map of the top reservoir which is at 3514.3 meters at H_5_a is digitized and imported. The main curve that is imported for lithofacies modeling and well log correlations are the Gamma Ray, density, Neutron Porosity, Sonic, Resistivity Deep, and Shallow curves. Details of data imported are shown in Table 2 in Appendix A.

3.5 Well Log Analysis

Lithology and depositional facies are interpreted according to basic well log analysis [15]. The petrophysical principles methods were applied to identify the baseline on the Gama Ray (GR). The low GR is for sand and high for shale and baselines are taken as constant [16].

Facies log was generated based on five (5) core data of well H5 from top of the logging depth of 3466.9 meters - 3546 meters measured depth. The interval was

converted into the total vertical depth (TVDSS) of 3048.9 meters - 3158.6 meters. Four depositional facies were identified, they are: coarse sandy bar, sandy bar, delta front and lacustrine coded by 3, 2, 0 and 1 respectively. These sand facies are coded, analyzed, and used for modeling are from H_5_a zones.

3.6 Well Correlation

The six well logs for the study interval have been correlated based on the principal concept of sequence stratigraphy. Core data are also used in the interpretation including picking of geological markers. The aims of this correlation are to define the depositional unit, the lithology and stratigraphic packages and to determine the vertical distribution of the reservoir and non reservoir zones.

The development of geologic pattern display of structure and stratigraphy that are equivalent in time, age, or stratigraphic position through use of electric wire-line logs is generally referred to as log correlation [18]. The well correlation assists to interpret subsurface facies between the wells via treating sediments as packages generated through a time interval and linked to earth cycle processes. The reservoir correlation assists to observe facies distribution properly and understand the geometry of the reservoir that can facilitate modeling heterogeneity.

In correlation the concentration to the shale sections is important, after the identification of major sands with GR curve. Shale is deposited in low energy

Environments are easy to recognize and correlated. Sand is not a good marker due to its variation in thickness and characters and discontinuous from well to well. The resistivity curves in the same sand shape in two well logs may be different due to variations in fluid content that could make resistivity differences [17]. Therefore the correlation of the six wells is made based on shale pattern. Figure 4.4 in Chapter 4 shows the log correlation of the six wells.

Cores interpretation for an interval of 209 meters – 228 meters is used to verify the well logs correlation. The four facies are shown in Figures 3.5, 3.6, 3.7 and Figure 3.8 that has been matched to the logs.

The description of reservoir geometry and orientation will be discussed in Chapter 4 in result and discussion.

The maximum flooding surface top of the thick shale layer (thickness 6.1meters - 13.7 meters) was taken as a datum for this correlation (Figure 4.4 in Chapter 4). In each sequence, shale to shale was correlated and then followed by sand to sand correlation. The correlated sands which are deposited as sand bars are interpreted as braided complex. Most of the sands are well connected laterally and vertically, thick and blocky pattern with low GR and showing fining upward, the core show coarse to very coarse grains. The sands which were deposited at the delta front were interpreted for H_3a, H_4a and H_5a sands showing the three channels varying in thickness and orientation. Figure 4.5 in Chapter 4 shows zone H_5_a sands for the six wells.

The sand deposit orientation increase towards the northeast of H1, the thickness improves to the south and well H1 proved that. The correlations had shown both the existing stratigraphy and facies correlation.

The thickness of the channel is observed from the correlation and the width from analog and published papers of similar environment.

From the well logs and core data, the top and base of the target interval was checked and defined for the depositional unit and correlated with the lithology and stratigraphy packages.

3.7 Depositional Unit Identification

The shapes of the gamma ray curve in similar environmental and core images are used to determine horizon packages. Five core samples are used as references from well H5, and 16 horizons were identified based on the shape of GR curve and the core data.

The picking of horizon packages here is based on the logs curves motifs that look similar and also if they are in the same environment. Four lithofacies identified from the five core data (depth ranging 11357 ft (3461.5 meters) to 11614 ft (3540 meters)

of the well H5 and 15 zones as shown in Figure 4.4. They are correlated across the field. Approximately three channels reservoir zones were observed in the study interval and only one was selected and used for the facies modeling purpose, on the upper interval (the top shale layers of H_2_b at depth 3468.9 meters) the continuous and thickest shale layers was flattened and taken as datum to control the correlation.

3.8 Reservoir Facies Modeling

The main steps of reservoir facies modeling applied are based on the traditional concept of reservoir modeling workflow methods. They are: Setting project unit, faults modeling, horizons modeling, 3D gridding, facies prediction, wells blocking, data analysis and facies modeling. The steps were started with the preparation of the appropriate logs data, depth map and imported into the software. Details of the data are shown in Appendix A.

3.9 Facies Definition

The facies was defined as a body of rock unit that form under certain conditions of sedimentation, reflecting a particular process or environment [27]. In this study the facies have been established as the coarse sand bar, sandy bar and delta front as well as lacustrine. They are the fluvial deposits where sediments are believed to be transported and deposited by rivers in a continental environment. The fluvial deposits, consisting of alluvial fans, deltas fan, braided-river deposits, and incised-valley fill contain special properties that are easily distinguished from the others, such as grain size, sand-body geometry, and orientations. An understanding of the differences in their characters is important for a subsurface reservoir evaluation, because it affects fluid flow in the reservoir.

The braided river deposits is the deposit that was created at the bottom of the mountains, where the gradient of the ground surface is steeply inclined [13]. Based on the available data (well logs, cores and reports), the four facies association was selected for this reservoir facies modeling.

Details from the core analysis suggest a sandy bar, coarse sand bar is reservoir zone, and delta front, lacustrine are non reservoir zone. These facies are used as input for lithofacies reservoir static modeling purpose. The concepts of these four groups of facies were described previously in Chapter 2.

3.10 Facies Coding

Facies log was generated based on the depositions sub-environment classification in the previous section. The four depositional facies of the coarse sand bar, sandy bar and delta front as well as lacustrine were coded 0, 1, 2 and 3 respectively, are illustrated in Figure 3.11. The facies coding setting are used in the modeling process.

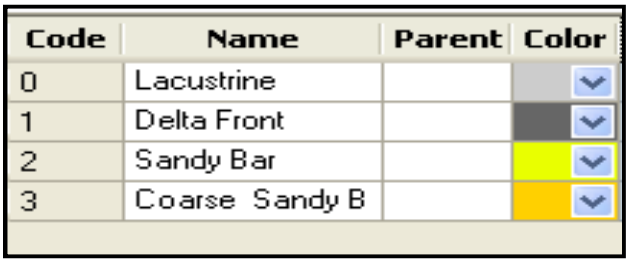

Figure 3.11: Setting window tabs for facies coding.

3.11 Facies Generation and Lithofacies Estimation

Based on interpretation of the top and base of the interval for the reservoir and also from the shapes of main log curves used, such as Gama ray, Resistivity and Density which also indicate clearly the different deposition environments [19].

In addition to core images justified the depositional environment interpretation. The depositional facies for the cored zone of H5 were inserted in the class A in Petrel by paint discrete later used as reference to generate lithofacies for non cored interval. In this case the two environments painted are braided complex and lacustrine complex in orange and green color respectively as in Figure 4.6 and Figure 4.7 in Chapter 4.

According to the previous review, possible feature and observation from cored wells and wire-line logs curves, two depositional environments like braided complex

(coarse - very coarse grained, pebbly sand and trough cross bedding with curved thick blocky gamma ray logs) and lacustrine complex (fine - very fine grained, laminated and low - high gamma ray logs) are present.

The depositional facies for wells H6, H4, H3, H2, and H1, were generated manually based on analysis of cored wells and Gamma Ray (GR), Density (RHOB), Neutron porosity (Nphi), Resistivity Deep, Shallow Resistivity Logs. Gama Ray was used to identify shale and sand in normal condition where high Gama ray is for shale while low Gama ray for sand. The RHOB and NPhi were gathered in one panel to identify and differentiate between sand zone and shale zone as well.

Deep and shallow resistivity were put together in one panel and used to identify between reservoir and non reservoir zones. The GR baseline is used to delineate the shale and sand zones where low GR represents sand zone and high for shale zone.

The baseline taken was the same for all wells. The sand zones are showing low GR, high resistivity (Res), low density (RHOB) and neutron porosity (NPHI) response while the shale zones are showing the inverse. The sand bodies are ranging from a thin layer to thick layers.

3.11.1 Lithofacies Prediction at Wells

Classification of lithofacies and their perfect demonstration in a three dimension model is important in reservoir static modeling. By obtaining a consistent description between geological interpretation and petrophysical properties (Phi, k, and SW) it is viable to generate flow simulations. Core samples of reservoir from wells are the best sources to provide lithofacies information [19]. In spite of this, cores are not usually in use due to the cost.

A technique for estimating lithofacies in non cored wells is necessary. In this case, lithofacies from cores are generated from wells with cores to train wells without core through the similarity of physical rock properties measured by the logs in the cored and non cored wells. Neural networks are used for facies determination from well logs

which cannot replace the geological interpretation, but could assist to increase efficiency [21].

3.11.2 Neural Network Theory

The neural network is a data handling tool to carry out mathematical modeling. The Artificial Neural Net Work (ANN) architecture is constructed by connection weight between the neurons activation function and training algorithm [22]. It comprises of elements of neurons. The neurons are arranged in layers and are interconnected by weights and biases between the layers. The first and last layers are known as input and output respectively. The layers located between the input and output layers are called hidden layers as illustrated in Figure 3.12.

The number of input neurons is dependent on the number of input variable in the Neural Net (NN) model while the output number neurons are dependent on the number desired on output from the model. There is no hard and fast rule to determine the number of neurons in the hidden layers. This depends on the complexity of the problem sought.

The stages considered in NN uses are training, validation, and test. In training and validation stage the input and target data are introduced to the neural network. While in testing stage a different set of data containing only input value is fed to the network. Since the input and target data are introduced to the network during training and validation, the stages are able to merge and take into account as one stage if long range of data is not available.

The NN is planned by connecting weights between the neurons, activations, and training algorithm [22]. Example of a schematic representation of a multi-layers NNW is illustrated as per Figure 3.12.

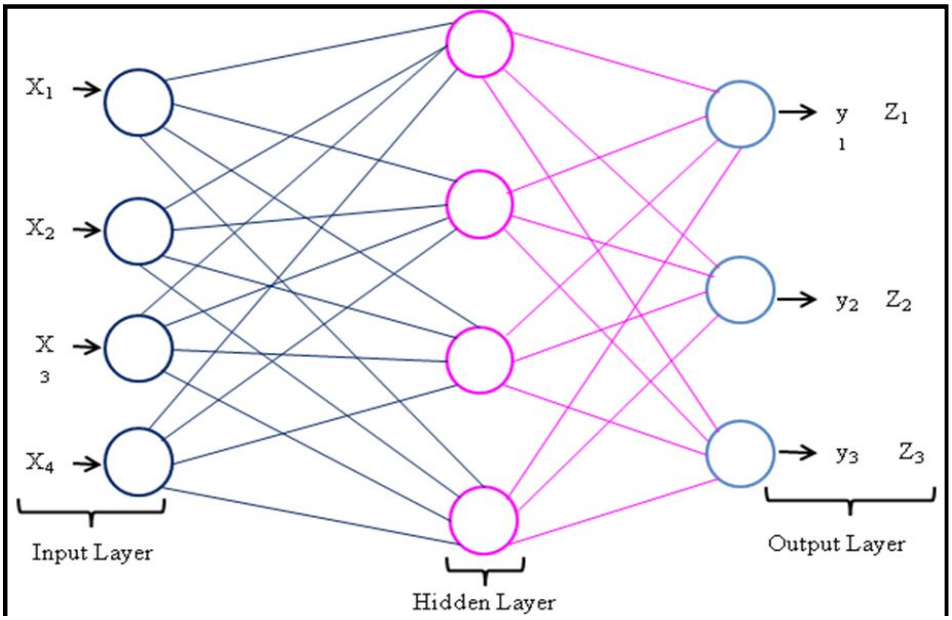

Figure 3.12: Showing graphical neural network structure, x and y are the input and output neurons respectively is the target provided during the training of the network [23] and [24].

3.11.3 Train Estimation Model

The Train Estimation Model (TEM) is a process giving access to the neural network methods [25]. Based on the input data in this case wire-line logs and core data, the process computes an estimation model that will respond in a similar way when presented with similar input data. The estimation model can be used in a variety of modeling processes such as classification and estimation models [25]. In this study the classification model is selected. The train estimation test was run four times to predict a lithofacies for none cored wells of the field by using the log data of the six wells and core lithofacies description of a well. The input data is subdivided into four distinct facies classes. Subsequently, a model was then computed from the probability of the input data to a level of a specific class [26]. The window setting for training data in the estimation of the model is shown in Figure 3.13.

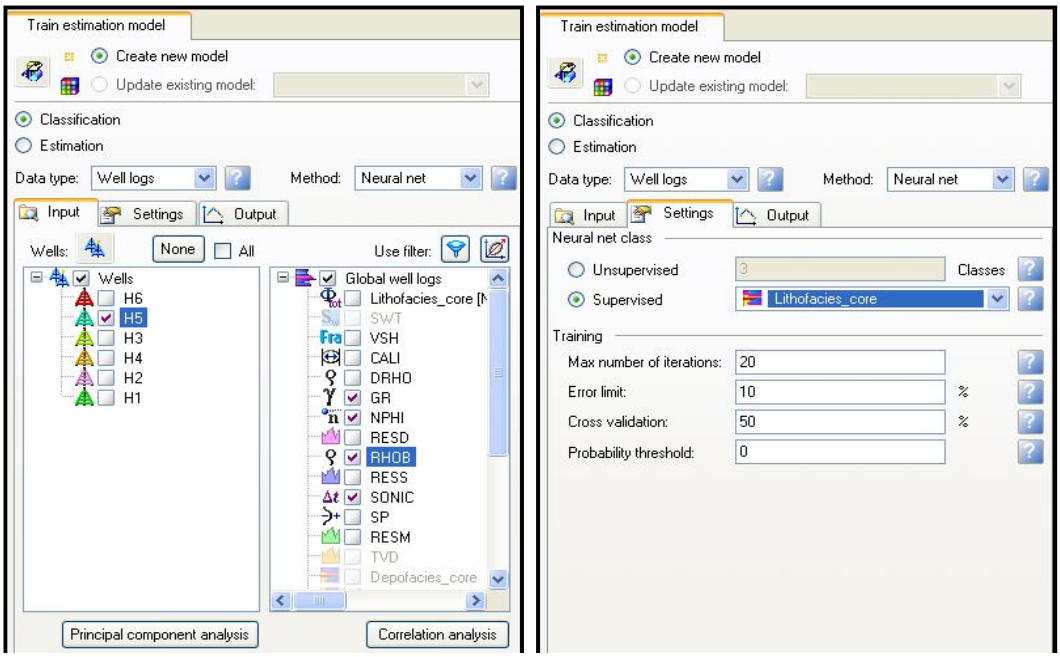

Figure 3.13: Setting windows for train estimation model, showing the input data, model type and training elements.

Subsequently the class with the highest probability assigned to the input data was used to calibrate the neural network. The uncertainties are constrained by log quality and facies interpretation. The results show a relationship in facies obtained by facies prediction between the wells and actual facies from well data.

The four train estimation tests were applied by running the following set of the log data:

1- GR

2- GR and RHOB

3- GR and NPHE

4- GR , ROHB, NPHE and SONIC

Based on the degree of high similarity for the predicted facies to the cored facies, the optimal result was selected (test-4) and used as input for the modeling. However, from the visual observation of the train on the reservoir zone of H5, the Sandy Bar facies are not appearing which suggests that although the probability of the

propagation is acceptable but may not necessarily be 100% true due to the inability to train the sand bar layer with a thickness of about 1meter [26].

Figure 4.12 in Chapter 4 show the log traces columns from left to right are: Measured Depth, Gama Ray, and Core facies, Neural Net one (NN1): (GR only), NN2 (GR and NPHI), NN3 (GR&RHOB), NN4 (GR, NPHI, RHOB and SONIC).

The selected test was applied to the other non cored wells, as part of quality control process. The lithofacies estimated by the trained neural network were calibrated to gamma ray and checked to ensure NN is working properly. In some case where NN is not working properly, the prediction is modified manually based on the Gamma ray reading.

This predicted lithofacies established was used later as input for the modelling purpose. The predicted lithofacies at the locations of the non cored wells are shown in Figure 4.13 in Chapter 4.

3.11.4 Faults Modeling

The primary stage of structural modeling is to build a 3D structural model. Fault modeling is the first step in the structure model of the 3D static reservoir facies modeling. Traditionally, faults modeling are important in view of sealing trap in exploration, production, and reservoir development as well as in the reservoir facies modeling since faults can improve well placement in addition to key in understanding compartments in hydrocarbon reservoirs.

Faults are significant suppliers to reservoir properties, since oil reservoirs with low medium permeability are productive largely due to transport of fluids to well bore via the fractures. [28].

Once a fault cuts a reservoir sequence it is desirable to predict the likely sealing behavior of the fault system [29].

Traditionally faults modeling are able to generate from the available data such as three dimensional seismic surfaces, two dimensional fault line and three dimensional fault plane as well as two dimensional seismic interpretations.

In the study area, a total of 18 normal faults trending northeast-southwest were digitized as lines and converted into polygons or fault boundaries at each surface are displayed in a 3D cube. The faults pillars are created by selecting the fault polygons from the upper surface. In this step the pillars represent the faults migration with depth which will be used to convert to fault planes. After the fault net is constructed, the fault surfaces and their corresponding fault lines were created using a fault modeling parameter in the Petrel application panel. Figure 3.14 shows a series of normal faults dissected the study interval of the K-Oil Field.

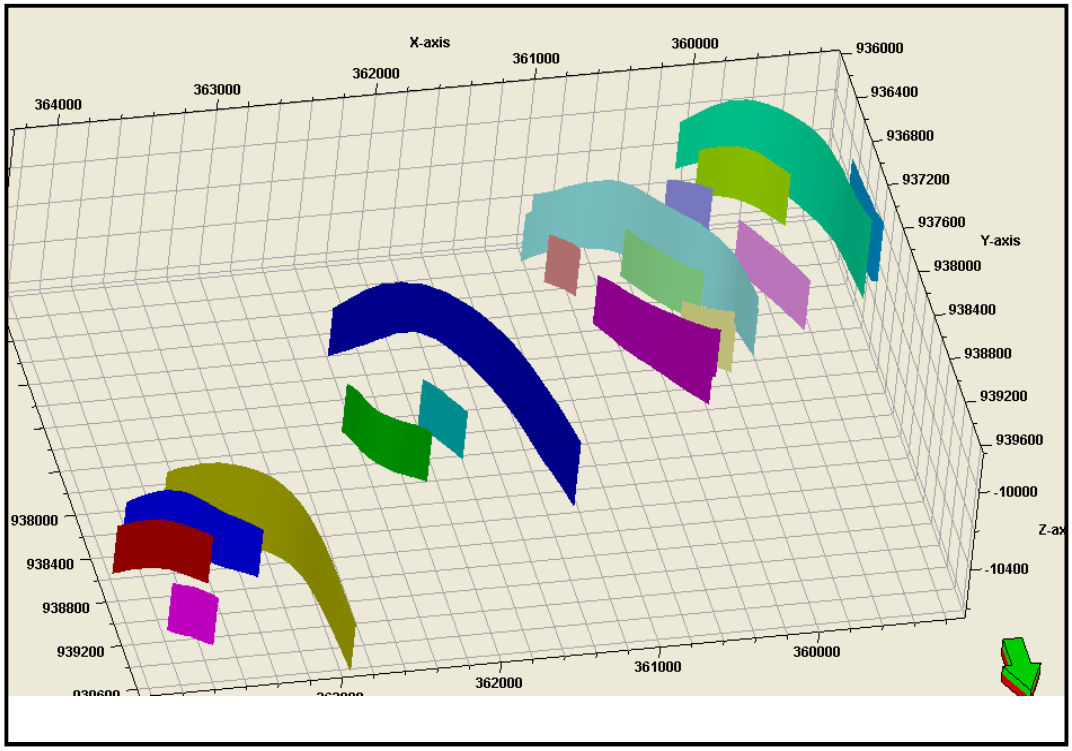

Figure 3.14: 3D Fault planes generated on the top horizon, showing NW-SE series of normal faults dissected the modeled zones (the colors refer to different faults).

3.12 Horizons Generation

The horizons generation is the step in defining the vertical layering of the 3D grid used in Petrel. It is the process of inserting depth surface into the 3D frameworks. The well picks for the top and bottom of each zone were imported into the horizons directory and placed in the appropriate depth locations for building the model. They have been matched to appropriate true depth of the top and bottom of the interval. The surfaces were regrided for well adjusted and matched with well markers. Figure 3.15 shows the window panels for area on top and bottom horizons, while the surface is H-5_a and H_5_b created is in Figure 3.16.

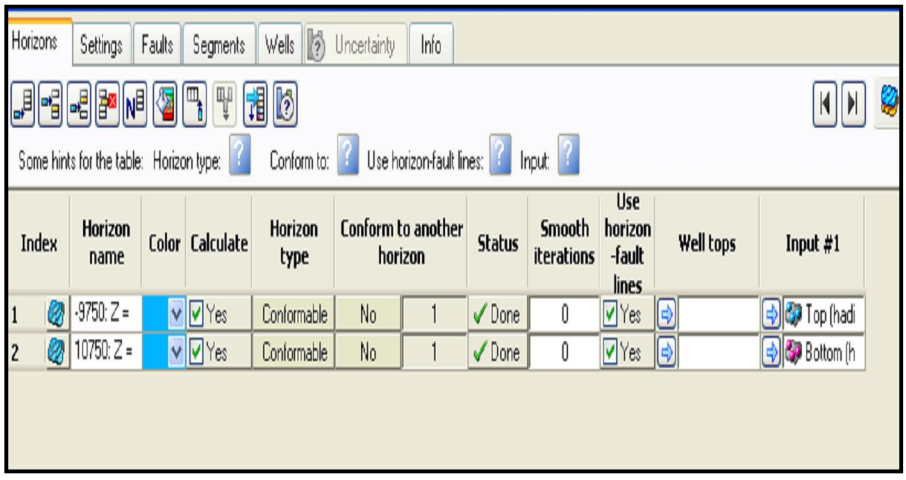

Figure 3.15: The window panel for creating top and bottom horizon.

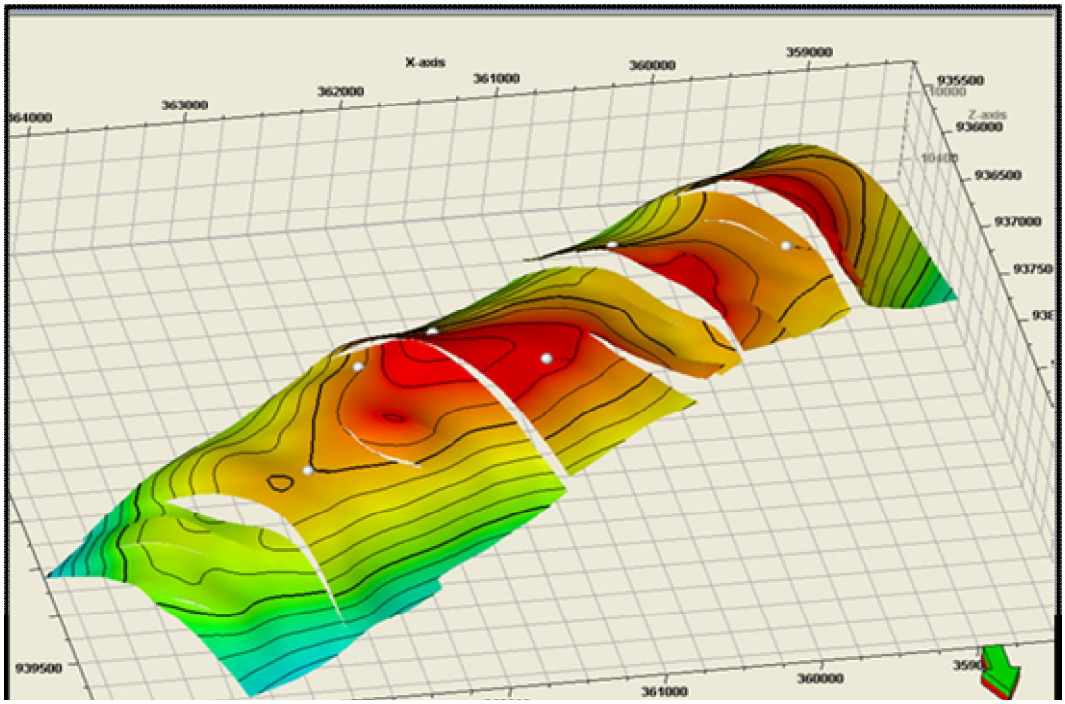

Figure 3.16: 3D views horizons generated adjusted to well markers represents the zone H_3_a reservoir (the red color represents shallow zones and the blue is the deep zones), showing intersected of normal faults oriented on NE SW.

3.13 Three Dimensional Grid Generation

The 3D grid generation is the second step in defining the vertical layering. It is a process of generating a container, containing faults and horizons in order to populate the reservoir properties such as facies in this case. It represents a last step in the structural modeling stage that combines the structural and the stratigraphic of the reservoir to create 3D grid cells of the reservoir. This process needs a good estimation of the lateral and vertical resolution of the grid in order to capture the necessary geological information about the channel in all dimensions.

Three stratigraphic zones were created based on the three thicknesses map of 50 m x 50 m lateral resolution and variable vertical resolution were generated for each zone depending on the vertical faces variation in order to capture the geology. The general grid window and information are shown in Figures 3.17 and 3.18 respectively.

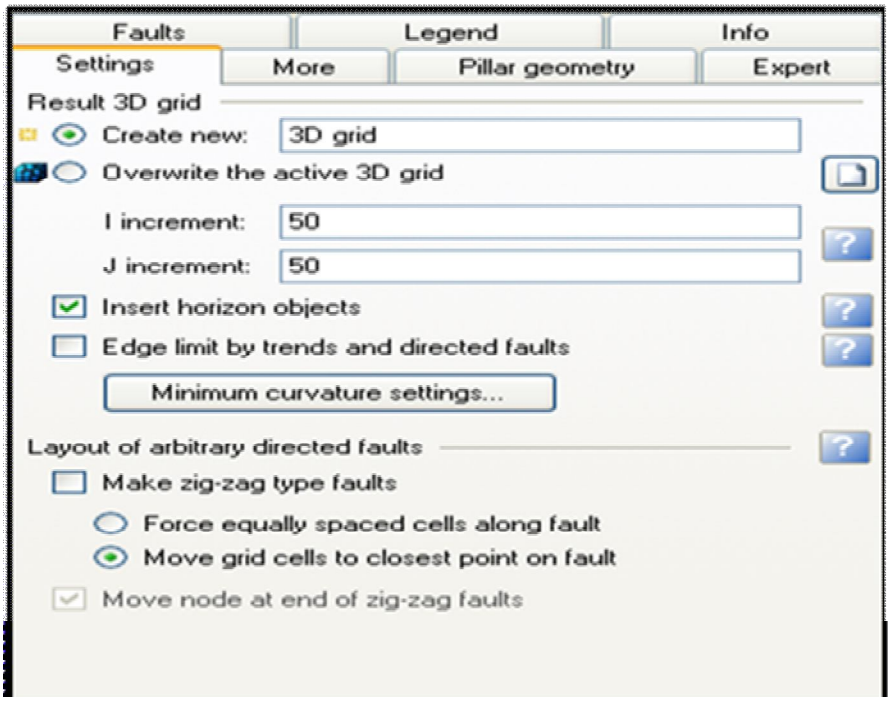

Figure 3.17: The window showing the grid tab for geometry specification input.

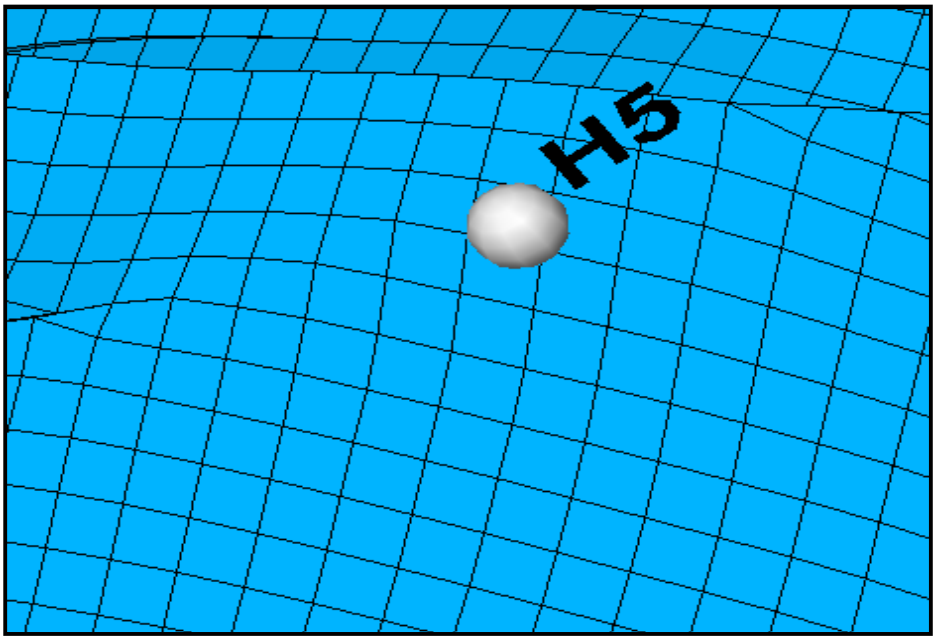

Figure 3.18: Grid of 50 m x 50 m tab input data created to capture the channel bodies.

3.14 Creating Zones

After the creation of horizons, the next step is to create zones that can reflect the reservoir. This depends on the well markers, which are unable to generate facies maps base on wells and grids.

The procedure of making zones is similar to the way of making horizons. The zones created are cross-checked with the well markers. Areas outside the well will follow the conformable thickness from the isochors grids. Isochors thickness between the top and base of each reservoir facies is used to define zones. Out of 14 zones created only seven zones are imported that covers the entire reservoir zones used for this modeling, and also including the reservoir zones. The layers build proportional based on the vertical distance between the upper and the lower horizon of the zones as in Figure 3.19 and Figure 3.20.

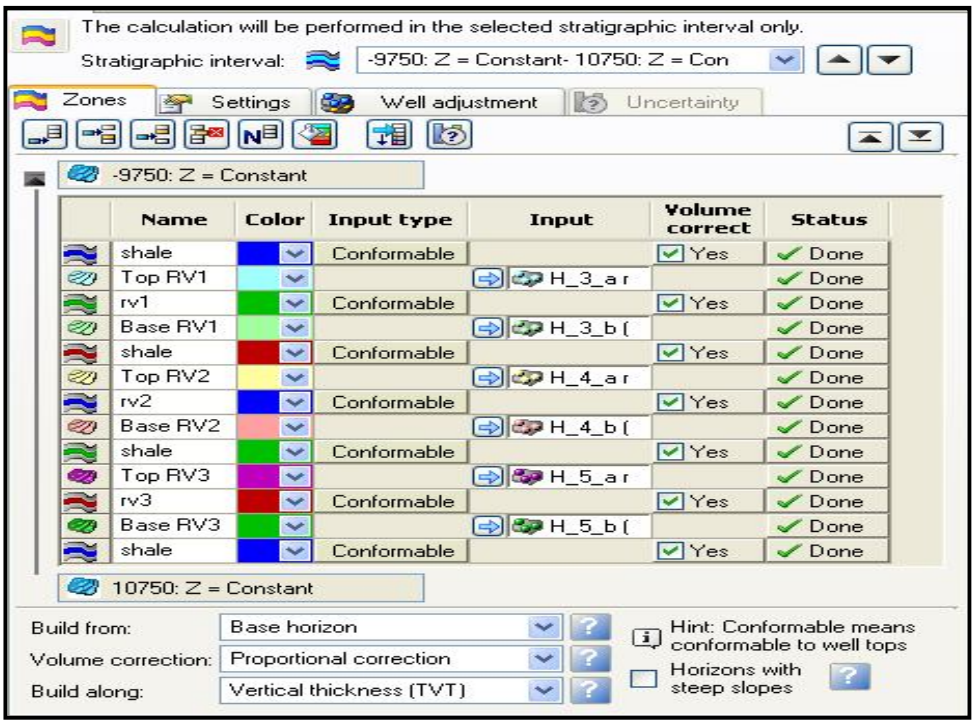

Figure 3.19: Window tap show creation of zones for the study interval zones.

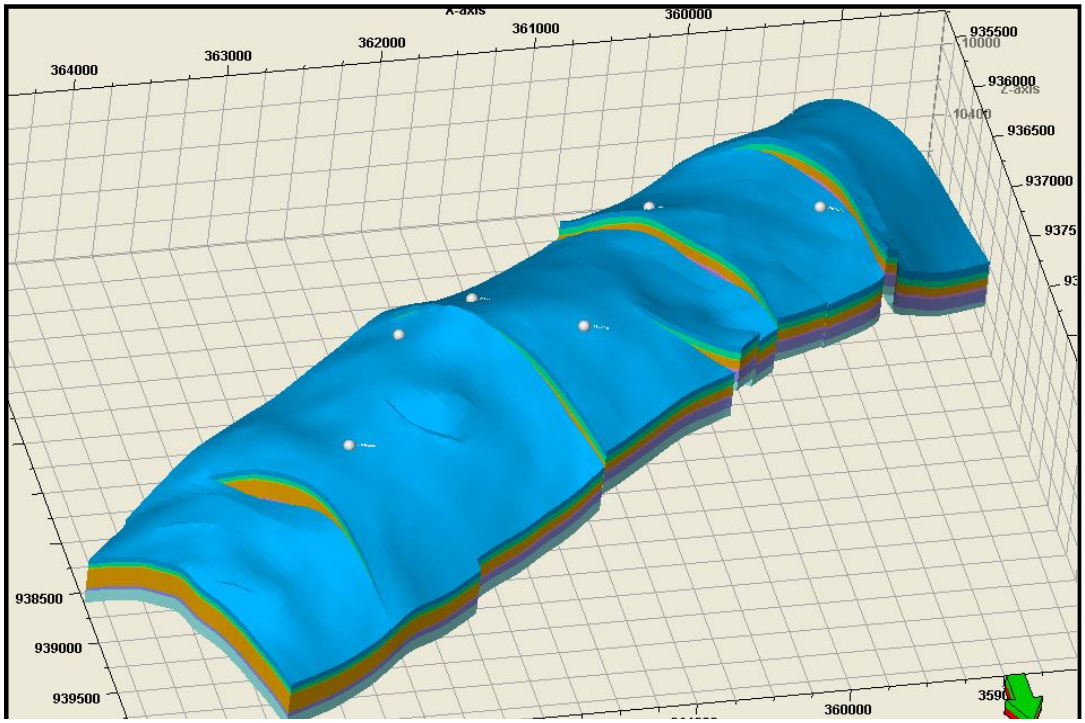

Figure 3.20: Zones were created by using the top structure map; seven internal horizons were generated honoring the well markers (the points in white colors).

3.15 Generating Thickness Maps

A generation of thickness maps is depending on parameters such as the horizon and 2D maps of the reservoir. The maps can be generated from the top and bottom structure maps based on interpretation of the seismic and well data.

Facies maps are created across the H_5_a reservoir to interpolate the sand thickness and its depositional direction. The geology and geomorphologic features are observed from the maps by looking to the different zones.

The facies maps created in reservoir lithofacies modeling are used to assess the distribution of the facies as shown in Figure 3.21 and Figure 3.22.

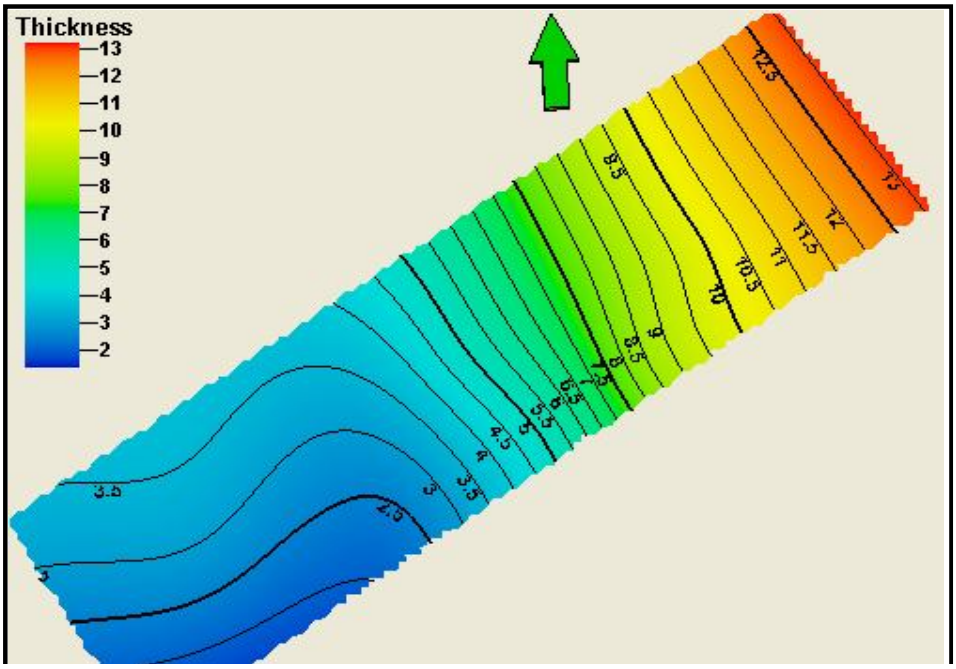

Figure 3.21: Litho-facies of lacustrine distribution (the red color represents the lacustrine facies) showing fine sand increasing in a NE direction.

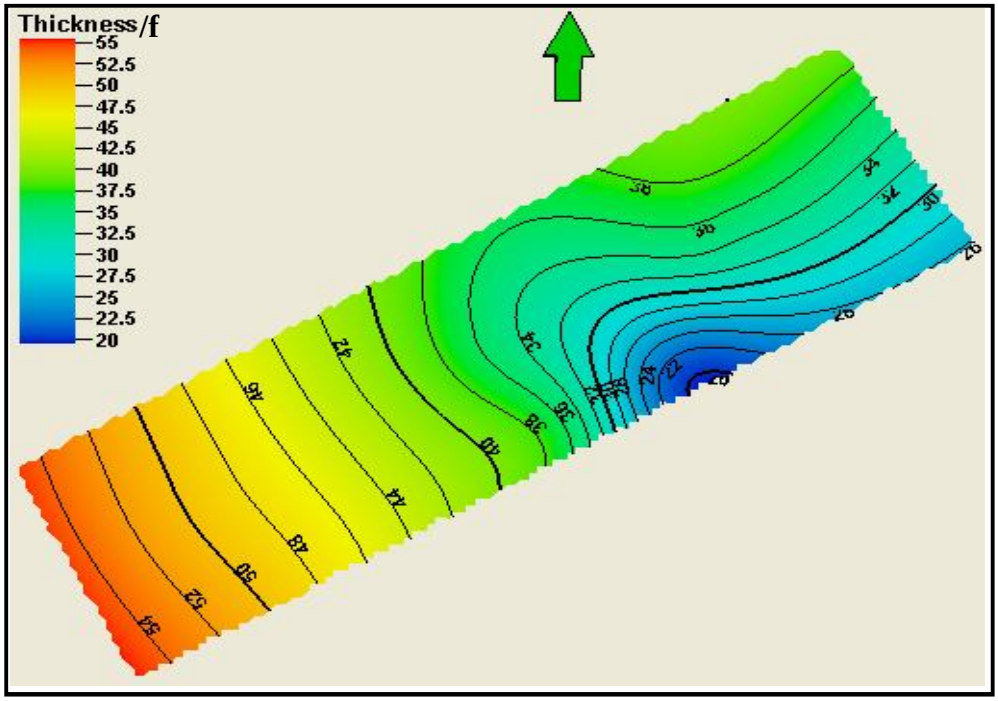

Figure 3.22: Maps showing Coarse sand bar facies increasing in SW direction (the red color represents high Coarse sand bar facies where the blue color mean less or zero Coarse sand).

The reservoir facies maps of the coarse sand bar and delta front were generated by making the surface of the differences between picks for the reservoir zone.

Facies map of coarse sand bars shows a thickness increase in the southwest while the delta front map shows increasing into the northeast. This could be related to the sediment direction prograding to the northeast.

The reservoir thickness is ranging between 9.14 meters - 19.20 meters at the wells location. The reservoir deposit shows an increase of the sand thickness in the southwest part and a decrease in the northeast of the study area. A table of reservoir thickness is illustrated in Appendix A.

3.16 Layering

In structural modeling the step comes after making horizon, 3D gridding and zoning is the layering. It is a process of subdividing zones into smaller layers vertically to replace the property variations at log scale.

Layers are assigned proportionally in the reservoir zone based on basic geological concept and considering a surface was eroded but not truncated from top or bottom.

According to the basic geostatistical technique of assigning layers proportionally, the sand thickness of a reservoir zone is considered and assigned a minimum thickness of almost one meter to capture the necessary facies in vertical resolution and to honor the typical channel deposition pattern. The layering parameters and the typical learning section are shown in Figure 3.23 and Figure 3.24 respectively.

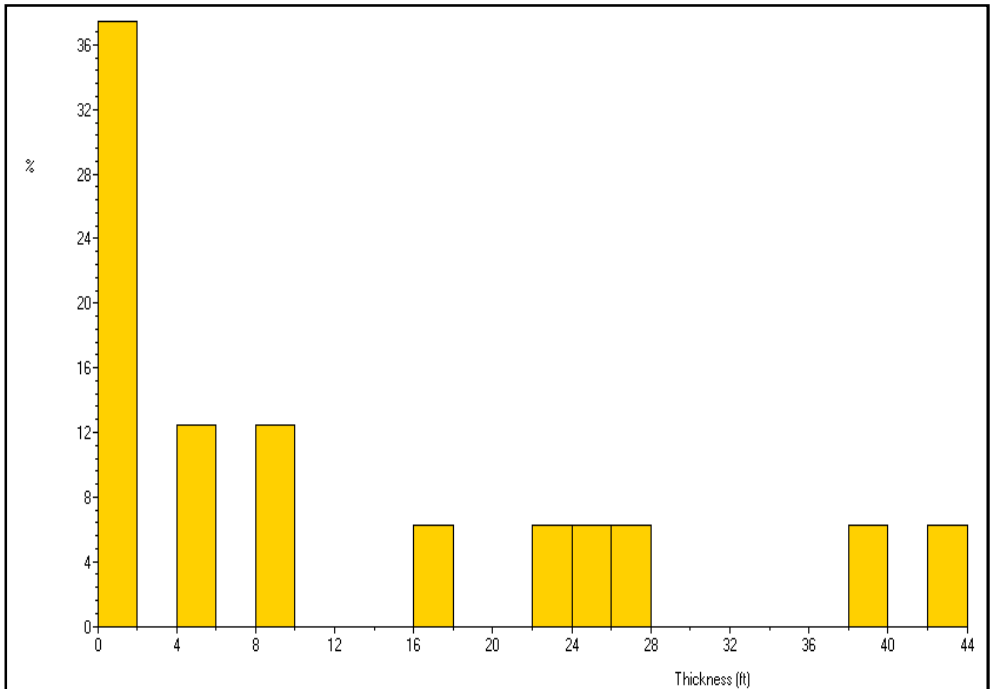

Figure 3.23: Vertical resolution histograms shows reservoir thickness percentage for the coarse sandstone (the axes x = thickness in feet and y = thickness percentage).

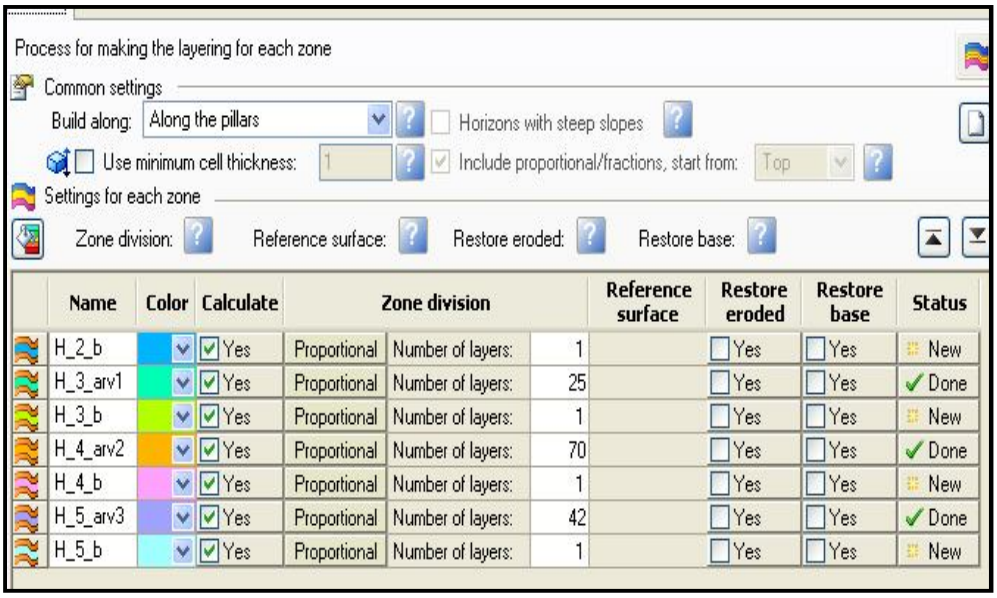

Name	Color	Calculate	Zone division			Reference surface	Restore eroded	Restore base	Status
H_2_b		Yes	Proportional	Number of layers:	1		Yes	Yes	New
H_3_arv1		Yes	Proportional	Number of layers:	25		Yes	Yes	Done
H_3_b		Yes	Proportional	Number of layers:	1		Yes	Yes	New
H_4_arv2		Yes	Proportional	Number of layers:	70		Yes	Yes	Done
H_4_b		Yes	Proportional	Number of layers:	1		Yes	Yes	New
H_5_arv3		Yes	Proportional	Number of layers:	42		Yes	Yes	Done
H_5_b		Yes	Proportional	Number of layers:	1		Yes	Yes	New

Figure 3.24: Zones subdivided cells to resolve the property variations vertically.

These will place for controlling log resolution in well blocking in the next step. Here all layers of less than one meter will not be appearing. Gross reservoir sands zones are considered as one layer for each zone to minimize time of model resolution

processing and concentrate on the reservoir zones. There were 141 layers in total and out of which 137 layers are reservoir zones and 4 layers are non reservoir as shown in Table 3.1.

Table 3.1: Modeled zones layering in reservoirs and non reservoirs zones

Model	Zones	Methods	Layer/1m	Remarks
1	H_2b	Proportional	1	Non reservoir
1	H_3a	Proportional	25	Reservoir
1	H_3b	Proportional	1	Non reservoir
1	H_4a	Proportional	70	Reservoir
1	H_4b	Proportional	1	Non- reservoir
1	H_5a	Proportional	42	Reservoir
1	H_5b	Proportional	1	Non reservoir
Total layers			141	

3.17 Well logs Blocking

This step is subsequent to assigning the layers into the different zones. Well blocking is a method of calibrating between the logs and the focus in a way to carry data into the grid resolutions created before to the grid cell sizes. This process is sometimes known as scale-up well logs. It helps to arrange information in several ways.

The well logs were recorded as a continuous data and sampling in each few centimeters, on the previous time at every 15 cm interval. This data will be averaged in order to assign single log property value of approximately one meter to capture the necessary geological information for the study interval penetrated by the wells.

Therefore, to relate this small scale data representation to geological grid, it is necessary to upscale the well data in order to have information in stratigraphic grid.

Although well logs of a fine layer resolution that is less than a meter will make the model very large and will take a long time to process, the method is taken into consideration during the layering process for each zone. The layers in reservoir zone

were assigned with a thickness of about one meter to optimize log resolution and run time, where none reservoir sands are not assigned interval layers but only assumed as one layer for each zone due to non reservoir character to minimize the run time and the logs resolution. The reservoir zones were given 42 layers, up-scaled along the wells and controlled by the up-scaled facies setting.

The input data for the scales-up are selected from the well logs and lithofacies for the six wells of the study interval. The average method used was selected from the icon showing “most of” as every cell will have facies value matching to the highest frequency facies value within each grid model cell, and the logs treated as lines as well as the method showing “neighbor cells” was selected too. The methodology for the scales-up facies from the six wells is illustrated as per Figure 3.25

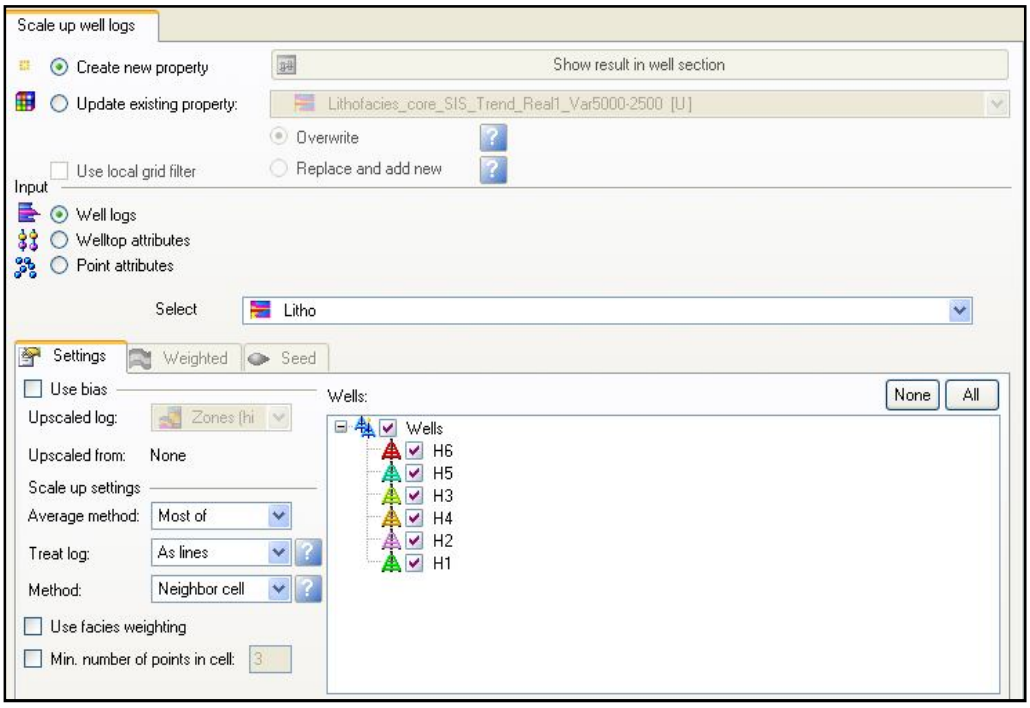

Figure 3.25: Setting for scale-up well logs, showing the input and methods.

The up-scaled logs results are used to cross check against the layering process to make sure that the vertical facies are properly captured. The result shows logical properly identified vertical resolution that captures the necessary information as illustrated per Figure 4.14 in Chapter 4.

The scaled-up well log facies analysis and quality controls of the reservoir zone of wells H6, H5 and H2 are shown in Figure 4.15, Figure 4.16 and Figure 4.17 in Chapter 4. In each figure, the columns from the left to the right are representing measured depth, Gama ray and the original lithofacies as well as the lithofacies blocked respectively. The facies in orange and yellow color represent the original and scaled-up reservoir facies, while the gray and black color is representing the non reservoir facies.

From the observation of the calibration, the panel is showing that blocked facies data are properly fitted with the original log facies data, which proved that the vertical grid resolution selected for the modeling purpose is normal since it captured the major geological information.

The up-scaled facies logs are in concord with the classified facies from logs. These will make sure that nearly all significant facies are being captured during facies modeling. From the observation of the reservoir zone in well H2, there are missing thin delta front facies layers, while in well H5 there is a little missing of the coarse sand bar. However the lithofacies are better captured in well H6.

3.18 Input Data Analysis for Modeling

In facies modeling, the quality control and input data preparation for facies and petrophysical modeling is an essential step in order to control the input and the possible occurrence of strange data values. The guidelines for the modeling process of this study were used for the modeling. The data analysis assists to obtain a better understanding of distribution, trend, and the relationships between the data as well as to understand the geostatistical distribution of the data in the wells.

The lithofacies log origin and scaled-up were verified by using proportion curves, histogram and controlled by variogram. The data analysis is divided into analysis process for facies proportion, thickness, as well as defining variograms and the analysis tools are the histogram, function windows to inspect the property distributions and the correlation between properties [25].

In pixel-based 3D lithofacies modeling, the variogram analysis is the key step. The variogram is a basic tool to analyze the spatial variability through the statistical algorithms to create facies in the 3D. Vertical variogram analysis was done in the beginning to define the nugget and the variogram type as these are common for all directions. An example of variogram for vertical direction is shown in Figure 3.26.

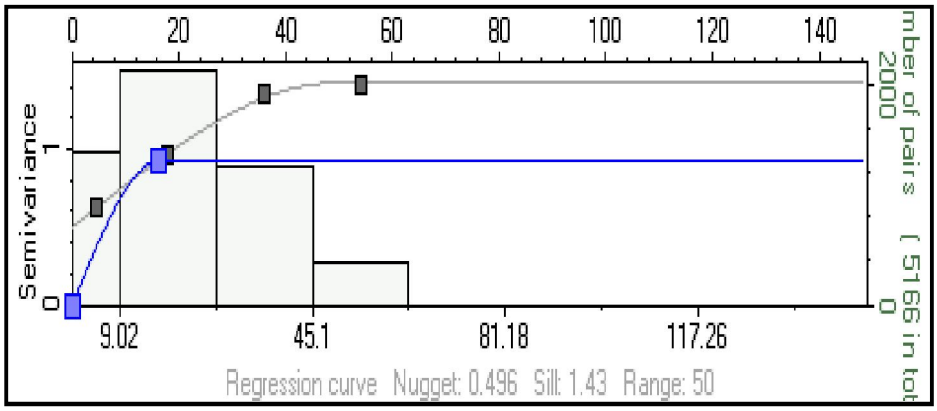

Figure 3.26: Example of variogram fitted within the vertical direction

The variogram analysis is done in three directions, two in the horizontal direction and one in the vertical direction. The parameters obtained for all directions are: variogram type, variogram ranges, and nugget. The parameters, range varies with the direction and the nugget value and the variogram type is same for the entire directions. An example of variograms ranges fitted with Minor direction and Major direction is illustrated as per Figure 3.27 and Figure 3.28 respectively.

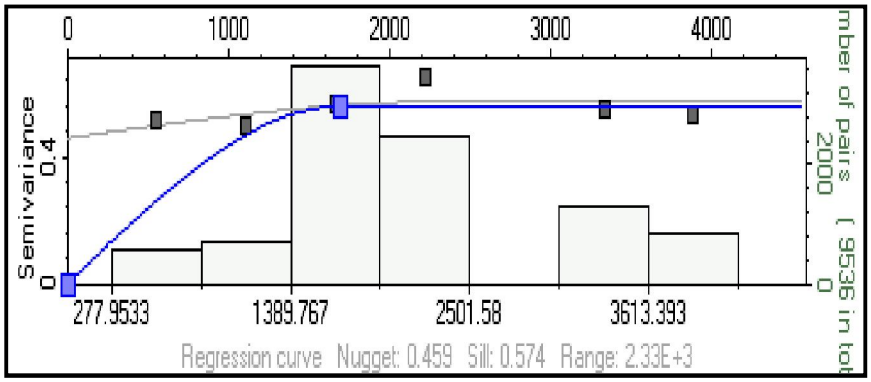

Figure 3.27: Example of variogram fitted with Minor direction

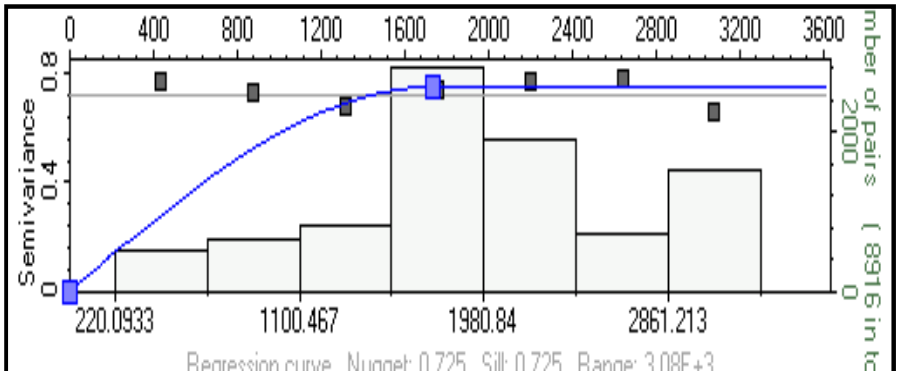

Figure 3.28: Example of variogram fitted with Major direction.

Several realizations have been done based on variogram ranges for SIS and TGS techniques and in the case of an object based on channel geometry; the focuses are on the realization models that represent the environmental concept. The pixel-based and object based techniques are able to provide a facies deposition model that represent the distribution phenomena with demonstrating facies transition. Table 3.2 shows the variogram parameters used for Pixel-based model.

Table 3.2: Example of a Variogram Range used for Pixel-Based Modeling

Pixel-Based	Realization-1	Realization-2	Realization-3
Function type	Exponential	Exponential	Exponential
Nugget	0	0	0
Major range/m	250	5000	1000
Minor ranges/m	150	2500	1000
Vertical range/feet	10	10	10
Major direction	43, 45 & 47	43, 45& 47	43, 4 & 47

Several scenarios have been applied to define the optimum lithofacies modeling approach, the pixel-based and object-based techniques realizations of lithofacies were computed in Petrel. The SIS and TGS realization are depending on the variogram fitting ranges. While the Object Based depends on width and thickness of the channel, three realizations were presented and the optimum was selected from each method and compared.

Stochastic uncertainties in facies modeling can be classified into three classes [30]. They are, (i) algorithm related that are derived from the mathematical parameterization (ii) assumptions (iii) simplifications of the modeling algorithm chosen, soft data derived from knowledge of the values of parameter for input to the modeling algorithm [31], [32], [33] and [34]. The soft data deals with uncertainties and stochastic related derived from the stochastic nature of the algorithms [35], [36], [37], and [38].

Vertical proportion curve (VPC) was applied to illustrate the probability of facies distribution in the reservoir zone. The objective of the VPC is to recognize the proportion of vertical variation of each facies in a stratigraphic zone. The pattern deposits appear as coarse sandy bar, lacustrine and delta front that are used to evaluate the facies distribution of the field by analyzing VPC where the reservoir heterogeneity was estimated by looking at the percentage of each facies at different layers in the proportion curves. Figures 3.29 and 3.30 show the probability curves from logs and up scaled facies data respectively.

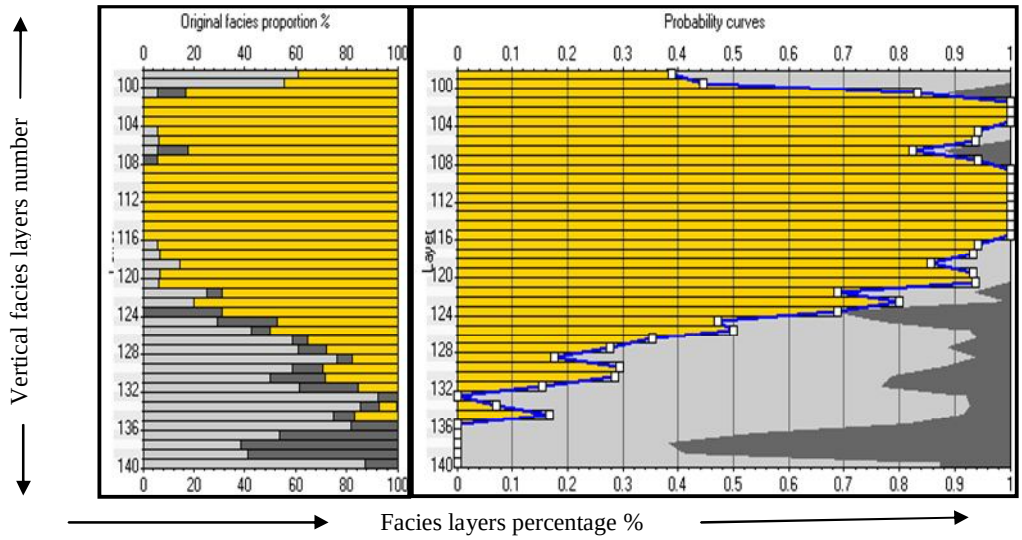

Figure 3.29: Facies in VPC origin and probability curves from Logs data.

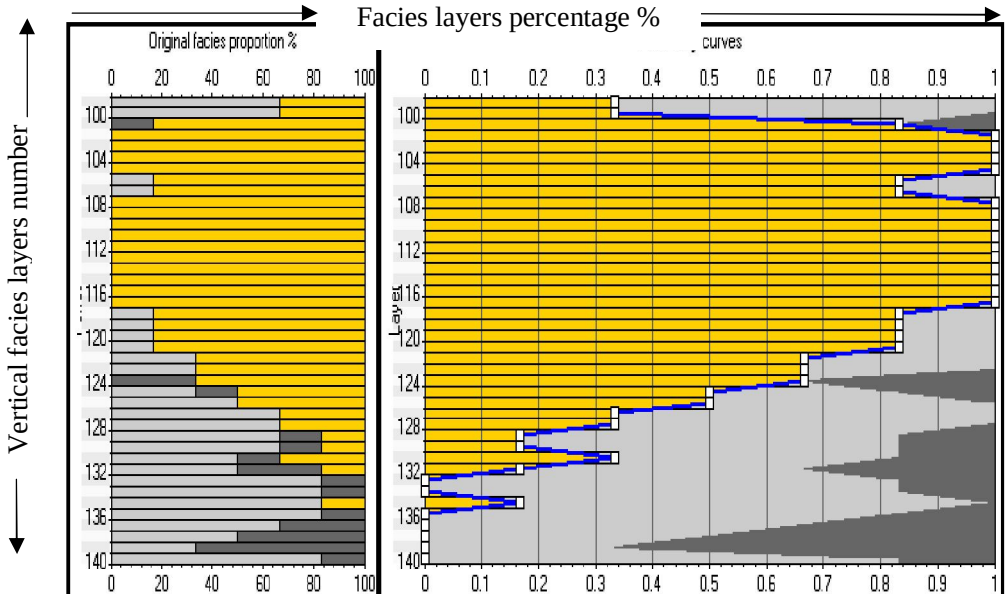

Figure 3.30: Facies in VPC origin and probability curves from up-scaling.

Legend

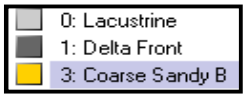

The facies in the VPC origin and probability curves show strong similarity and matching change between log data and up-scaling out-put as illustrated in Figure 3.29 and Figure 3.30. The probability for coarse sandy bar facies is dominant in the reservoir zone on the scaled-up zones through the grid interval whereas the lacustrine and delta front are less dominant.

In the reservoir, the channel is dominant in the middle and upper parts of the zone and here the probability to see more sand is good for that part. The reservoir facies are composed of approximately 60% coarse sandy bar, 25% lacustrine and 15% delta front.

In order to verify the percentage of matching between origin, Up-scaled, and model facies data, a histogram was constructed as shown in Figure 3.31.

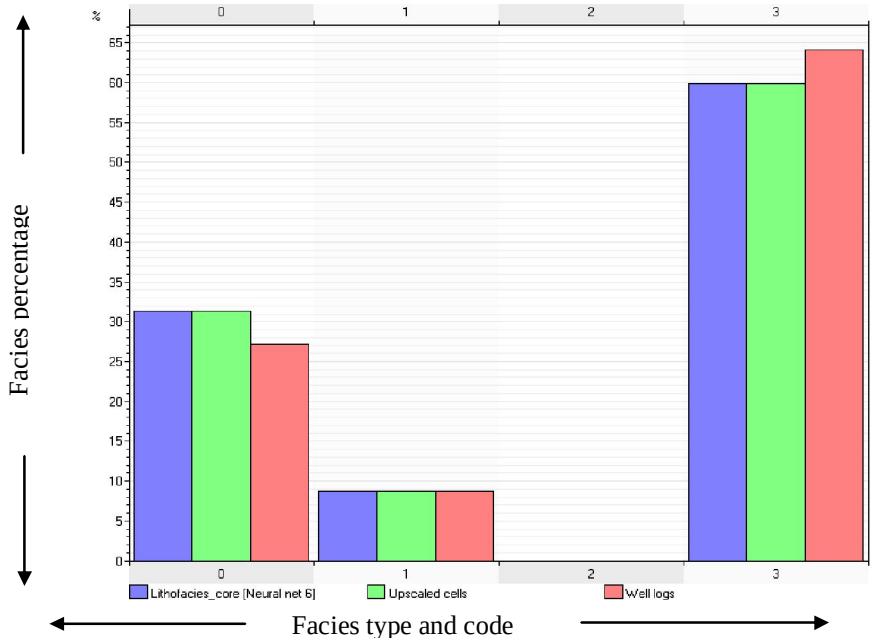

Figure 3.31: Histogram show matching between log facies, up scaled facies and model facies data for the three facies in the reservoir zone. The code 0, 1, 2 and 3 respectively represent lacustrine, delta front, sandy bars and coarse sandy bar facies, where the Z axis represent the facies percentage.

From the observation of the histogram and VPC for facies log and up-scaled data for the reservoir facies distribution proportionally, the reservoir zone shows a good matching between logs, up-scaled and model facies and may contain a good sand distribution.

The reservoir is here evaluated for the quantity and quality of the clean sand percentage, level of continuity and extension of the sand, thickness as visualized from the histogram, proportional curve, and cross-section map of the reservoir.

From observation of the reservoir facies distribution in the VPC the coarse sandy bar facies are dominant. In the histogram where the matching varies or is less similar, that could refer to the capturing of the facies layer in each reservoir and it will reflect into the histogram and shows sometimes scaled up facies data which is not similar to the model facies.

Both histogram and vertical proportion curve shows the reservoir facies distribution proportionally through the six wells up-scaled.

3.19 Facies Modeling

Facies modelling is important in static reservoir workflow which includes project unit setting, faults modelling, horizons modelling, 3D griding, wells blocking and data analysis as discussed earlier. Figure 3.32 shows the comprehensive workflow for facies modelling.

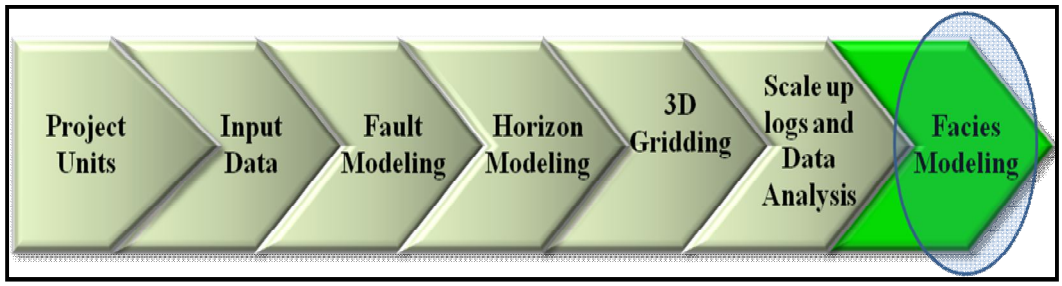

Figure 3.32: Static reservoir geological modeling workflow, showing the major steps for the facies modeling.

The reservoir modeling was defined as a process of quantitative analysis of reservoir properties by recognizing geological information and uncertainties in special variants [39]. The reservoir modeling goal has been to transfer quantitative information on reservoir property distribution with enough detail and accuracy to a numerical simulator so that the fluid flow simulation predictions would match reservoir performance. The application of reservoir modeling assists to assess the geometrical distribution, extension, and continuity of reservoir properties, which are important factors in predicting fluid flow and reservoir performance using numerical simulators [40].

In order to achieve the best picture of the reservoir and associated uncertainties, Stochastic modelling condition of well data is performed to generate several realizations of the geological parameter with base reservoir production simulation [41]. During the construction of the facies model, the parameters must honour the

well data and geological interpretations of the modelled zones besides the size, body shapes and spatial trends [39].

In this research geological modelling techniques were used to model reservoir facies distribution that are able to illustrate and reduce uncertainties of sand distribution, geometry and characteristic of braided system field.

3.20 Techniques in Modeling Braided System

As facies can be distinguished by different grain size or different diagnostic features and as well as distinction between sandstone and shale [42], the idea of choosing appropriate modeling methods depends on the environment of the depositional system, and facies type [43].

The stochastic methods have become widely accepted for reservoir flow studies, and are able to introduce the geometry of the flow units the spatial distribution of facies and fluid properties within each flow unit. Several stochastic methods existed in the Petrel software and are able to model braided environmental systems. To distribute facies properly in between the wells there are needs to consider interpolating methods, such as object based and pixel based techniques [44].

3.21 Object Based Modeling Method

The stochastic Object-based modeling technique was defined as a generation of point in space according to the Poisson process and sitting around these points of objects with a given shape based on density and geometry of object [45]. The general modeling operation with object-based method consists of the introduction of objects replacing a background, which commonly represents the most laterally extensive facies.

The introduced objects may have different geometries and dimensions, reproducing the variability of the elements in the depositional model [46], [47], [48], [49], and [50]. The object-based technique recognized as Boolean's Modelling is

appropriate for imposing geological illustration and good to produce heterogeneity within an object and within a channel in addition to introduce sharp boundary and flow features illustration. This method is able to in corporate reasonable and quantifiable 3D facies geometries to the static model. The method is able to build logical and reasonable geological shapes other than pixel-based techniques, but it is difficult to constrain the models to the actual wire-line log and seismic data sets [51].

The following processes have been used to choose and maintain the object modelling method for the reservoir facies model:

(i) The regional geology of the area shows that the environment of deposition is a fluvial channel system running in the northeast direction. The satellite images of the present day Shari river system take into consideration and illustrate braided delta. (ii) The cores images analysis indicates that the sand can be divided into coarse to very coarse sand which represents braided complex and the fine to very fine represent lacustrine deposits. (iii) The paleogeography map and log correlation confirm that the deposition trends in a SE-NW direction. (iv) Lithology and core descriptions indicate that the lithology is a channelized pattern of braided features; the finding is supported by the well to well correlation [52].

The input data on geometry are derived from the area map which shows the present day Chari River, the sand thickness from well correlation and the orientation of sediment were derived from paleogeography map of the area. The widths of the channel was determined from the analogs of similar environment and published papers by Robert, S. Tye, 2004 and Martin R. Goblin, 2006 as well as Marc. J. P. Jew and Henk Berendsen, J. A.2007 [53], [54] and [55].

Reservoir facies parameters set were done geometrically. The widths vary between 100 meters - 250 meters and the thickness, 10 - 25 meters, as interpreted from the correlation

In general stacking pattern of initial progradation, three realizations in object-based model were generated based on available geometrical data of the channel and deposition system, the example of the parameters used for geometry for the object-

based (one realization) for this study reservoir facies modeling are shown in Appendix B.

3.22 Pixel-Based Modeling Methods

The Sequential indicator simulation (SIS) and Truncated Gaussian simulation (TGS) techniques are a generation of spatial distribution of discrete variable facies and the main parameters are a proportion of discrete variable facies or trend map, vertical and horizontal variogram [27]. The pixel based techniques used are based on facies modeling algorithms [56]. These algorithms are fast and allow the iterative slow solution, where the value is assigned to each cell according to a probability distribution function. The methods give a variable result due to assumptions that deal with facies categories and compute the probability distribution function. The methods are based on variograms analysis and volume fraction as well as optional trend data to simulate the 3D facies model.

The SIS is a stochastic pixel-based technique which combines variograms and target volume fractions with the optional use of 2D or 3D trend data to simulate a 3D facies model. It is suitable when the shape of a particular facies body is uncertain or multiple trends control the facies type [57]. The SIS is based on the indicator approach [58], [59]. The estimation of the facies probability using the up scaled cells and variogram information is based on SIS [60]. The SIS provides the capability of using secondary probability data to adjust the SIS results. When dealing with categorical variables like facies, the indicator approach transforms each facies into a new variable, and the value of each variable corresponds to the probability of finding the related facies at a given position. It is used when the shape of the facies bodies is uncertain or controlled by a number of trends.

The TGS is an effective stochastic technique for modeling environments where there is a natural transition through a sequence of facies. Examples include progradational fluvial sequences [57]. The technique is used to describe the distribution of discrete or categorical variable facies. The method requires truncation of a continuous Gaussian function. It is a technique of distribution facies in ordering

following grain size criteria such as coarse sand, fine sand and clay [56]. The algorithm starts by calculating the thresholds between facies, assuming a Gaussian distribution.

The method is appropriate to model facies within a transition environment. An example of this case is the progradatioal sequence in fluvial environments. An example of facies parameters set in SIS and TGS realization-1 are included in Appendix C.

CHAPTER 4

RESULTS AND DISCUSSIONS

4.1 Introduction

In the previous chapter the methodologies of the reservoir facies modeling through SIS, TGS and Object-Based techniques were discussed. The modeling which started by setting the project unit followed by faults modeling, horizons modeling, 3D gridding, well blocking, data analysis and facies modeling. Included are three model realizations for each technique. The model results are verified and analyzed. This chapter illustrates the results of the main work done in this research such as correlation, environmental facies interpretation, and lithofacies prediction as well as well blocking, assessment and geostatistics analysis of the channel sands. In addition to the reservoir facies distribution models are described. These results output could help in reducing the uncertainties of the reservoir facies distribution.

4.2 Reservoir Lithofacies Modeling Concept

The lithofacies modeling is successful due to the contribution of the geology and the environmental studies of the reservoir interval. The model zone was conceptualized as a braided delta setting environment. As discussed previously in Chapter 2, the reservoir models were developed based on an analog of a braided delta system and the present day Shari river system as in Figure 4.1, Figure 4.2, and Figure 4.3.

The transition between the sub aerial braided plain and subaqueous braid delta is sharp, indicating that facies changes between the fluvial and deltaic facies belts are abrupt. The facies are established as coarse sandy bar, sandy bar, lacustrine and delta

front. The sedimentary structures observed in the sand facies are gravel, current bedding, and coarsening texture.

Traditionally, the fluvial deposits are sediments transported and deposited by rivers in a continental environment and there are several types of fluvial deposits, consisting of alluvial fans, deltas fan, braided-river deposits, and incised-valley fill. Each type of these deposits contains special properties that easily distinguished from the others in term of grain size, sand-body geometry, and orientations. An understanding of the differences is important for a subsurface reservoir evaluation as it affects fluid flow and reservoir. In this case the environment established is a braided delta system. It is characterized by a good reservoir quality with moderately good sorted coarse grain size and little clay matrix content. The four facies are inputs for lithofacies reservoir static modeling purposes following the conceptual deposition environment described previously in Chapter 2.

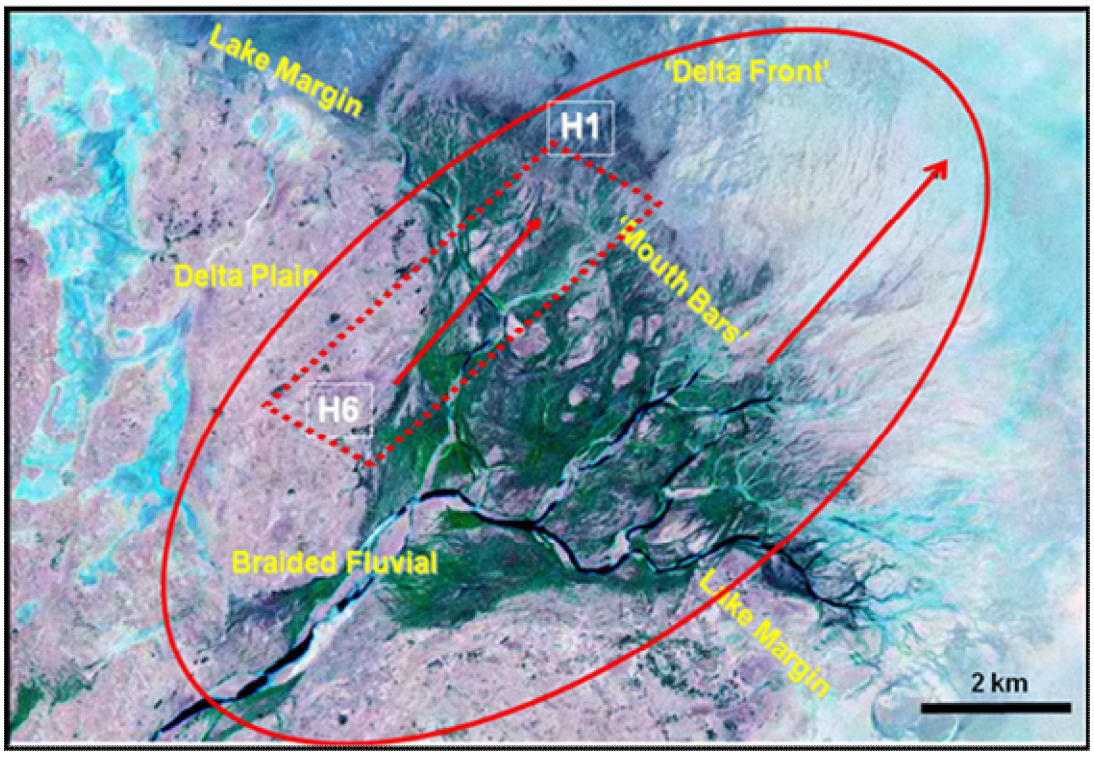

Figure 4.1: Analog for the braided delta depositional environment, Neales River Australia modified after [9].

Figure 4.2: A modern analog of a braided delta system, after L. Chignik Alaska.

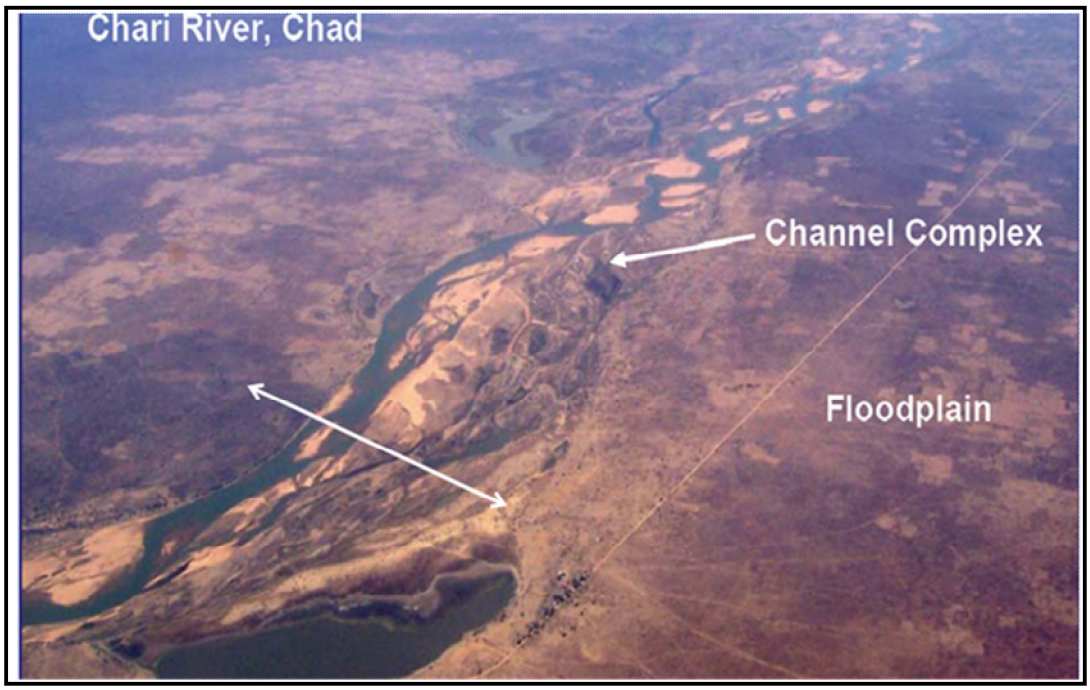

Figure 4.3: Example of present day braided channels, Chari River run from north to south, modified after [9].

4.3 Correlation and Lithofacies Distribution

The studied interval has a higher net to gross sand. The sands source for the interval is coming from southwest to northeast and the reservoir quality and thickness improved in the south as shown by the Figures 4.4. The sand was deposited as braided complex facies (coarse sandy bar and sandy bar), Lacustrine, and delta front (fine sand reach in mud). The sand distribution increases towards the northwest of well H1. The reservoirs facies are mostly continuous based on log data in all layers at well locations, and include the reservoir of H_5_a zone.

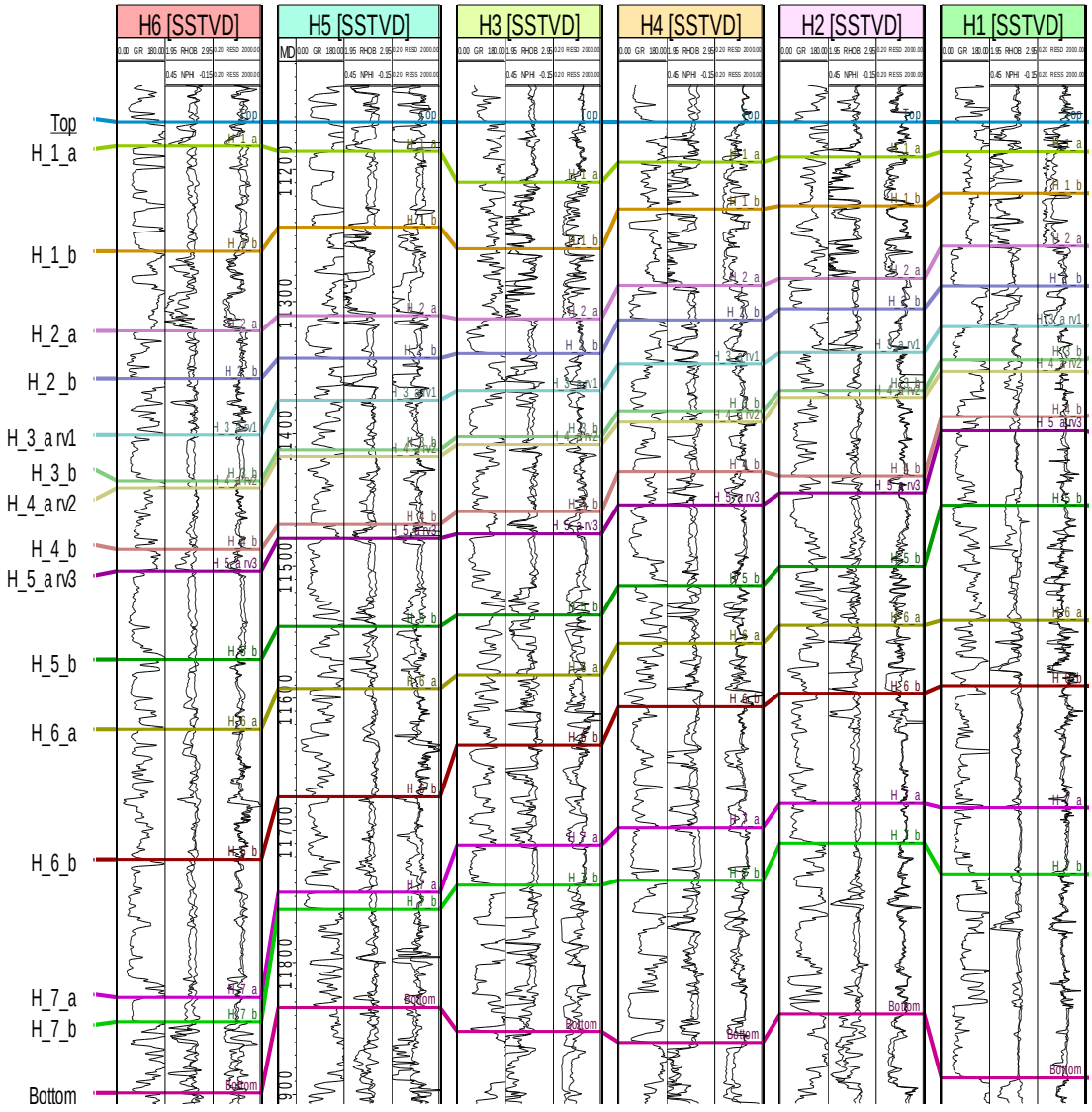

Figure 4.4: Well correlations of the study interval included the modeled zone (H_5_a and H_5_b). The thickest shale intervals under the datum zone exist in well H3 while less thickness are on both sides of H6 and H1.

From Figure 4.4 the columns in each well from left to right are represented Gamma Ray, density and Neutron Porosity and Resistivity Deep and Shallow curves.

The correlated sands are well connected lateral and vertical; it shows a thick and blocky pattern with low GR and fining upward. The H_5_a zone shows the sand varying in thickness as per Figure 4.5.

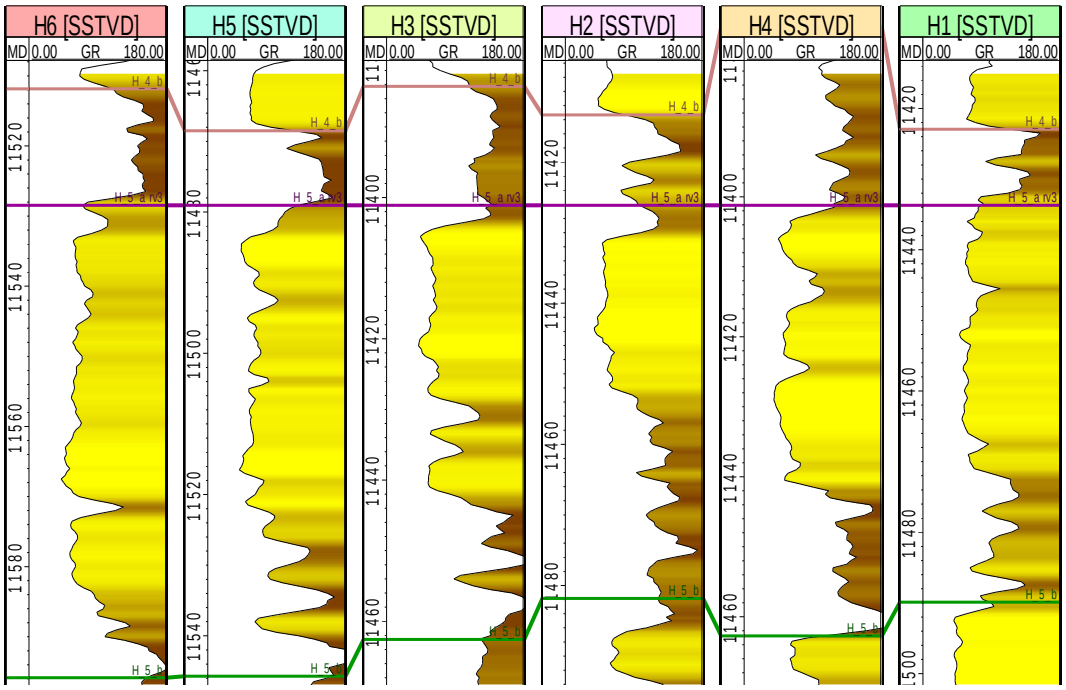

Figure 4.5: Gama ray motifs showing with different thickness for the six wells.

The sand deposits orientation increase towards north east of H1. The thickness improves to south and the well H1 proved that. The correlations had shown both the existing stratigraphy and facies correlation.

The thickness of the channel is observed from the correlation and the width from analog and published papers of similar environment.

From visual observation of the features in the core images and logs motives of a cored well, with considering a literature review of the lower Cretaceous as explained in the previous chapter, two environments are recognized and interpreted as braided delta complex (low Gamma ray, characterized by channelized deposition, coarse to very coarse sand grained and often pebbly grained formed in low sinuosity channels and associated by clay facies as well show cross bedding structure) and lacustrine

complex (high Gamma ray response, often continuous deposition vertically and characterized by fine sand grained with show lamination) as appeared per Figures 4.6, 4.7 and Figure 4.8 as well as Figure 4.9 and 4.10, where the Gamma ray motives shown in Table 4.1.

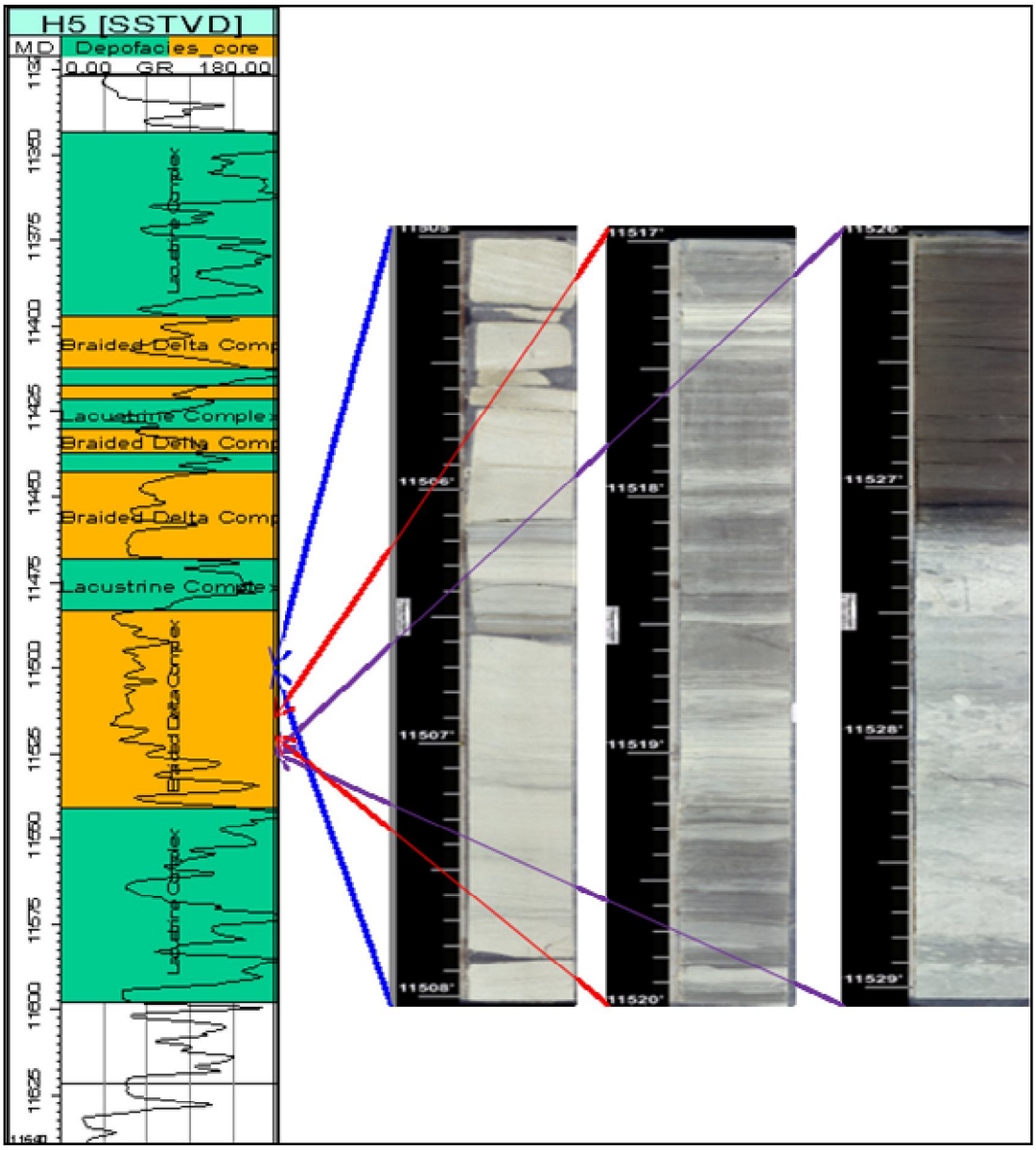

Figure 4.6: Example of cored zone depositional facies interpretation at well H5. Showing the braided complex facies depositional environmental in orange color.

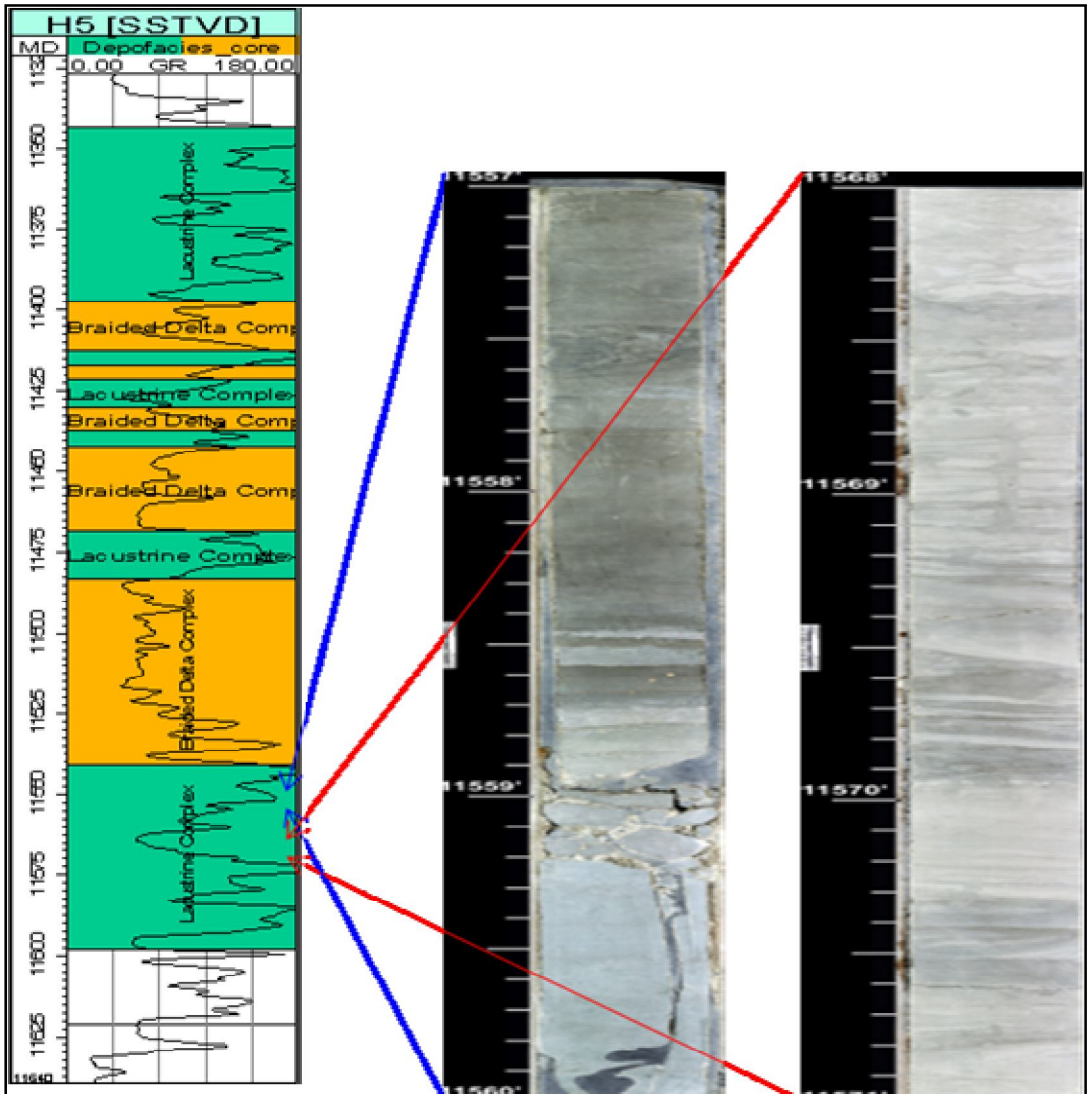

Figure 4.7: Example of cored zone depositional facies interpretation at well H5. Showing the lacustrine complex facies depositional environment in green color.

Legend:

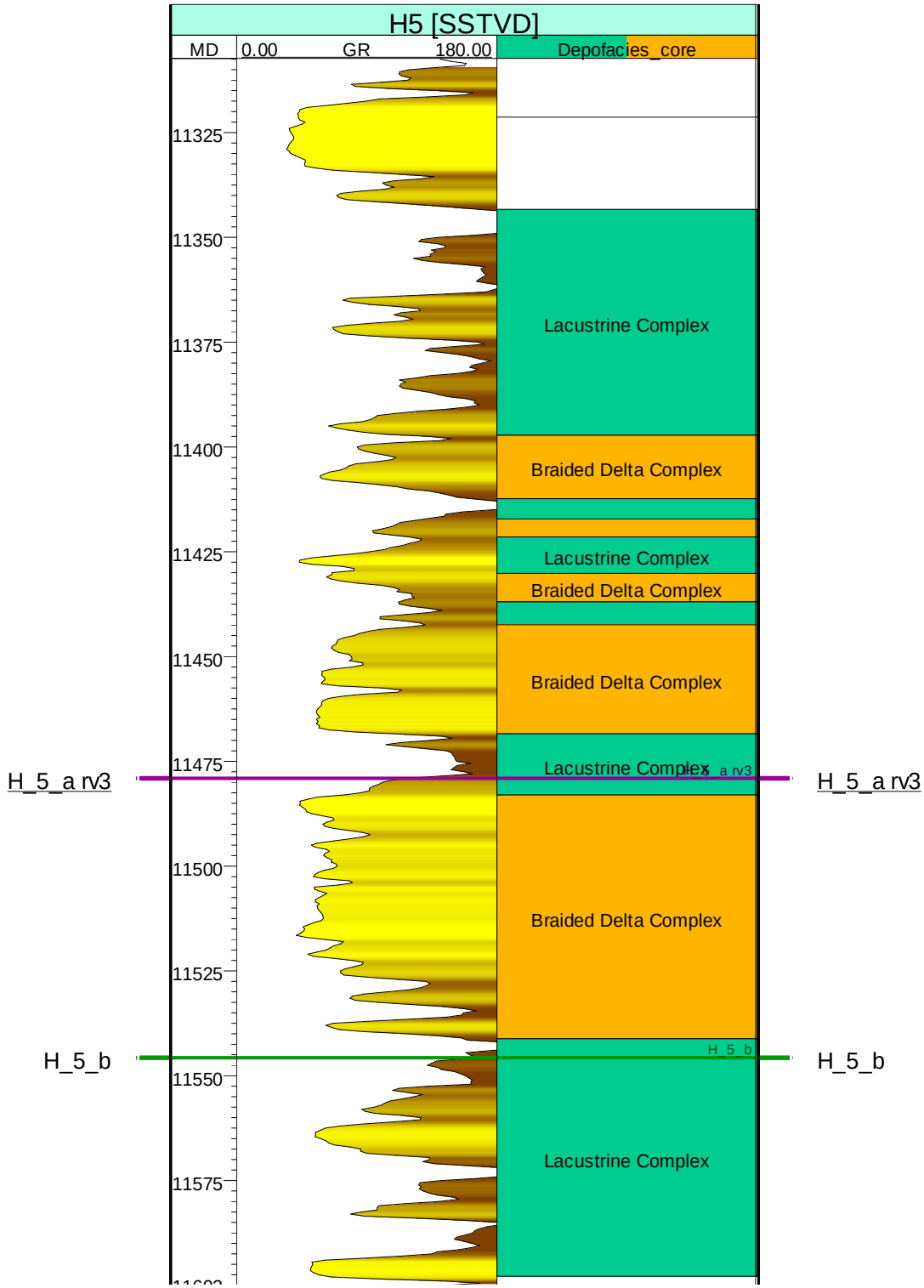

Figure 4.8: Result of cored zone depositional facies at well H5. Showing the braided complex and lacustrine complex facies depositional environment in orange and green color respectively.

Table 4.1: Showing an example of the Gamma Ray response within a braided complex and lacustrine complex environment.

Environment type	Gamma ray curve response
Braided Complex	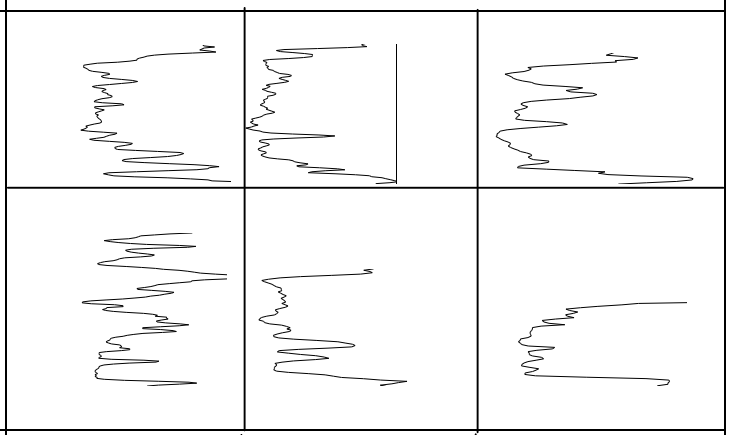
Lacustrine Complex	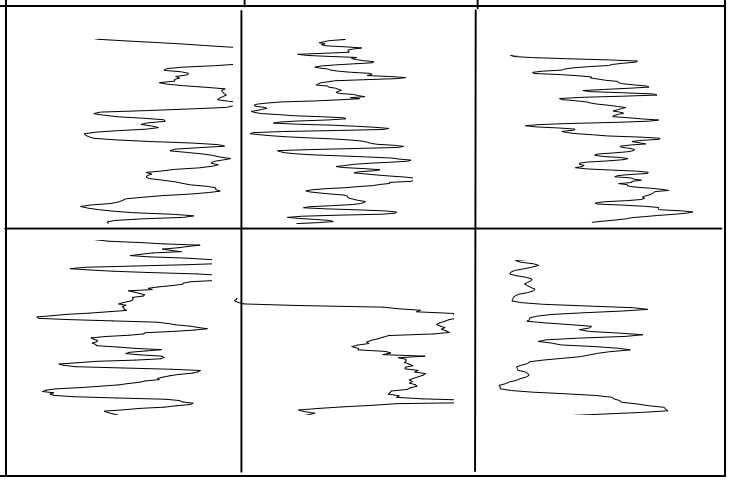

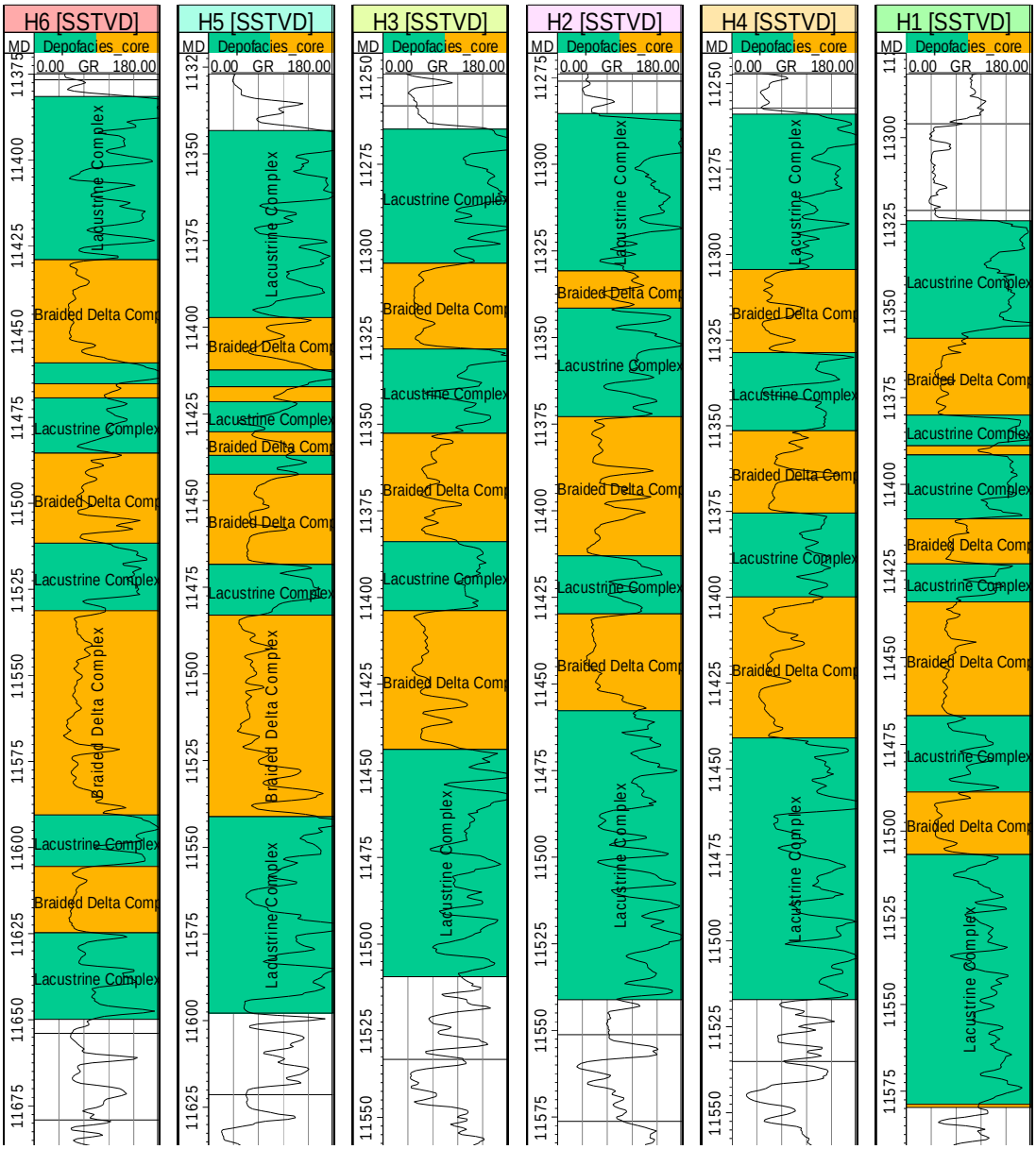

Figure 4.9: Result of study zone depositional facies at all wells. Showing the gamma ray calibrated to the depositional environment (braided and lacustrine complex).

Legend:

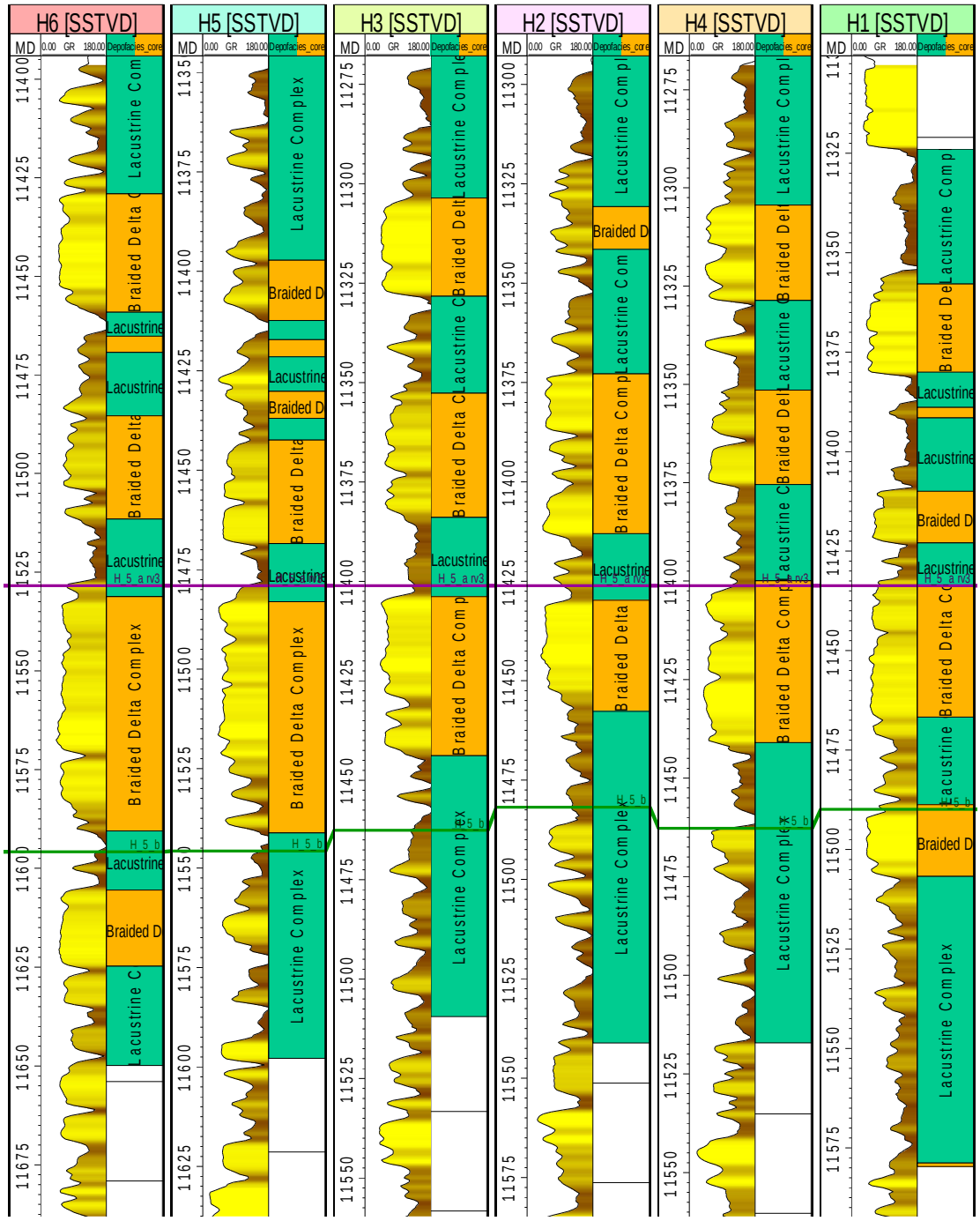

Figure 4.10: Depositional facies interpretation at wells position in the study interval.

Legend:

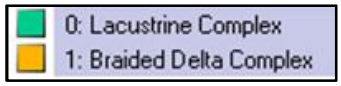

The observation from the environment facies section in wells position in Figures 4.9 and 4.10, are showing the lateral and vertical changes of the facies environment. The braided facies are dominant in a NW direction and lacustrine sediment is increasing within the NE direction. The GR is showing a low reading within sand zones and high within the shale zones. The sand bodies are ranging from the thin layers in the NE to the thick layers in the SW.

From the observation in core image features, Gamma ray logs response to the well H5 and review of the area, four lithofacies were reinterpreted (coarse sand bar, sand bar and delta front as well as lacustrine) and used as references to predict lithofacies for non cored wells as explained in Chapter 3. The sand interpreted as bar due to the observation of blocky to fining-upward, low Gamma ray and coarse to very coarse grained as well as cross bedded, bar, sand bar and delta front as well as lacustrine). The coarse sand is dominant. The sand in medium to fine grained, parallel laminated and show thin wave was considered as delta front facies, where the fine to very fine sandstone was considered as lacustrine , the four facies existed in the reservoir zone and the coarse sand bar is dominant as per Figure 4.11.

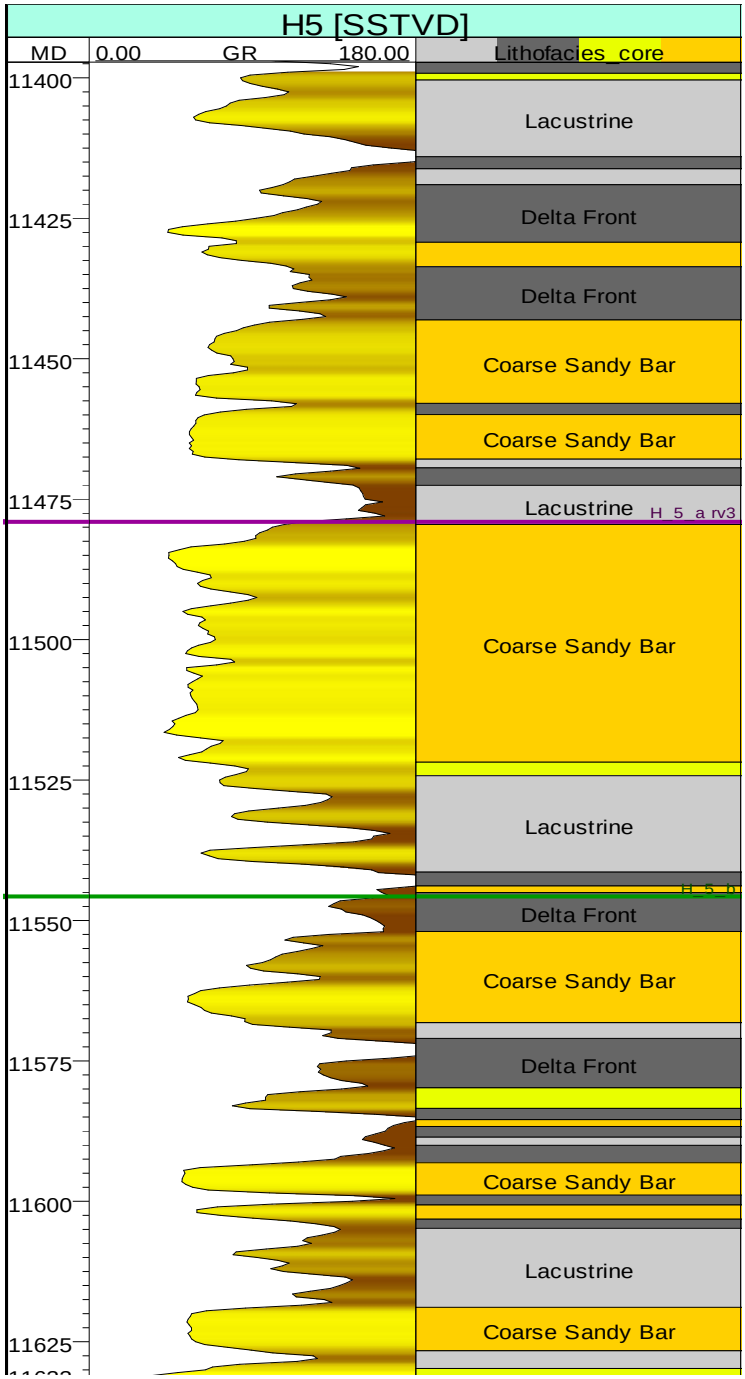

Figure 4.11: Lithofacies interpretation from core zones for well H5. The columns from left to right represent measure depth (MD) in feet, the logs in Sub Sea Total Vertical Depth (SSTVD), a Gama ray in API and lithofacies core).

Legend:

From a visual observation of the lithofacies trained according to the degree of similarity in the four tests seem acceptable and the optimum result comes from NN4 was run for the non cored wells, the sand bar facies are missed due to inability to capture thin layers that are less than 1 meter. Figure 4.12 and Figure 4.13 show the trend for the cored well to predict lithofacies and the predicted lithofacies at the locations of the non cored wells respectively.

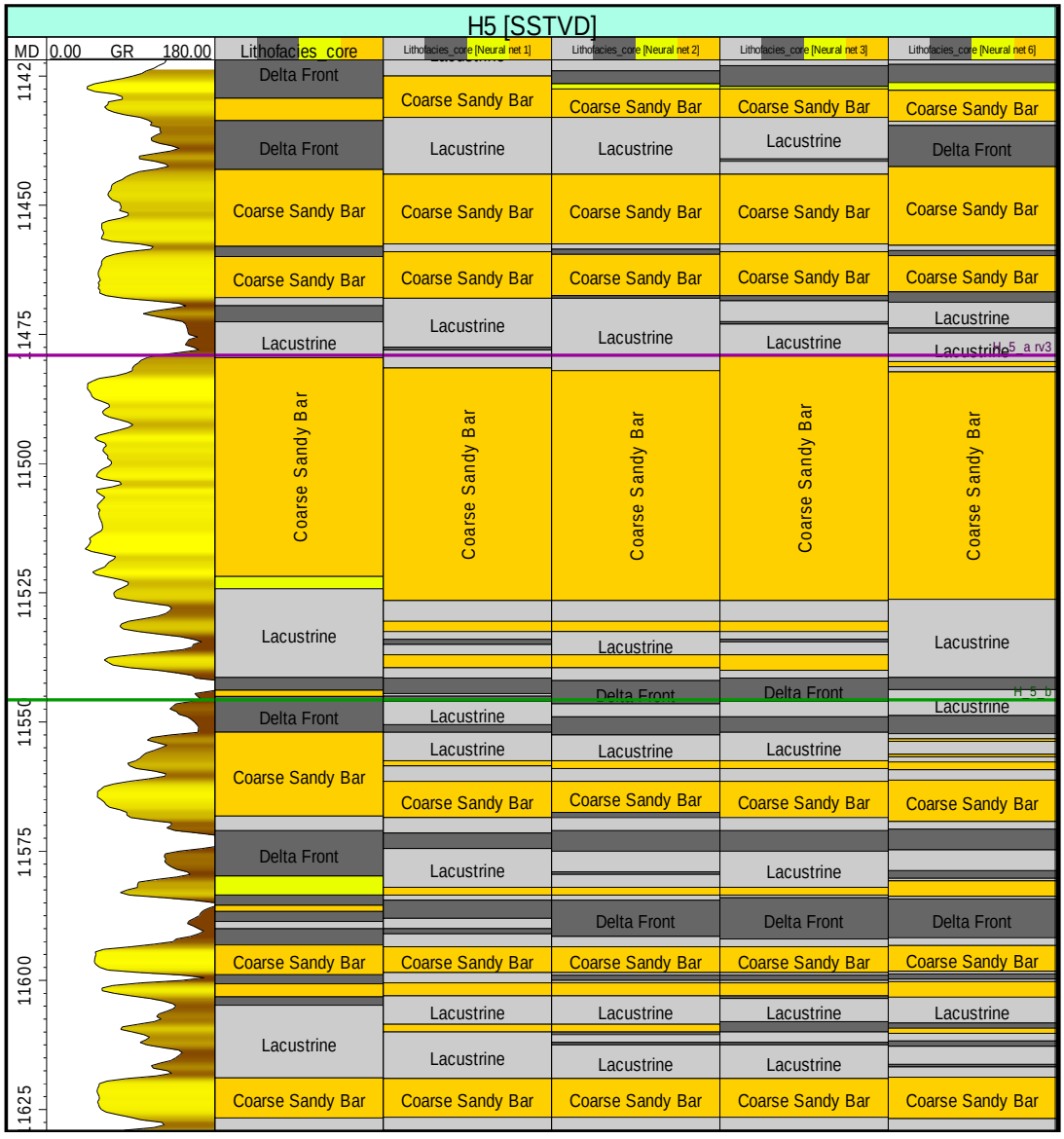

Figure 4.12: The core data for well H5 was digitized and used lithofacies neural network (NNW) to predict the lithofacies for non cored wells.

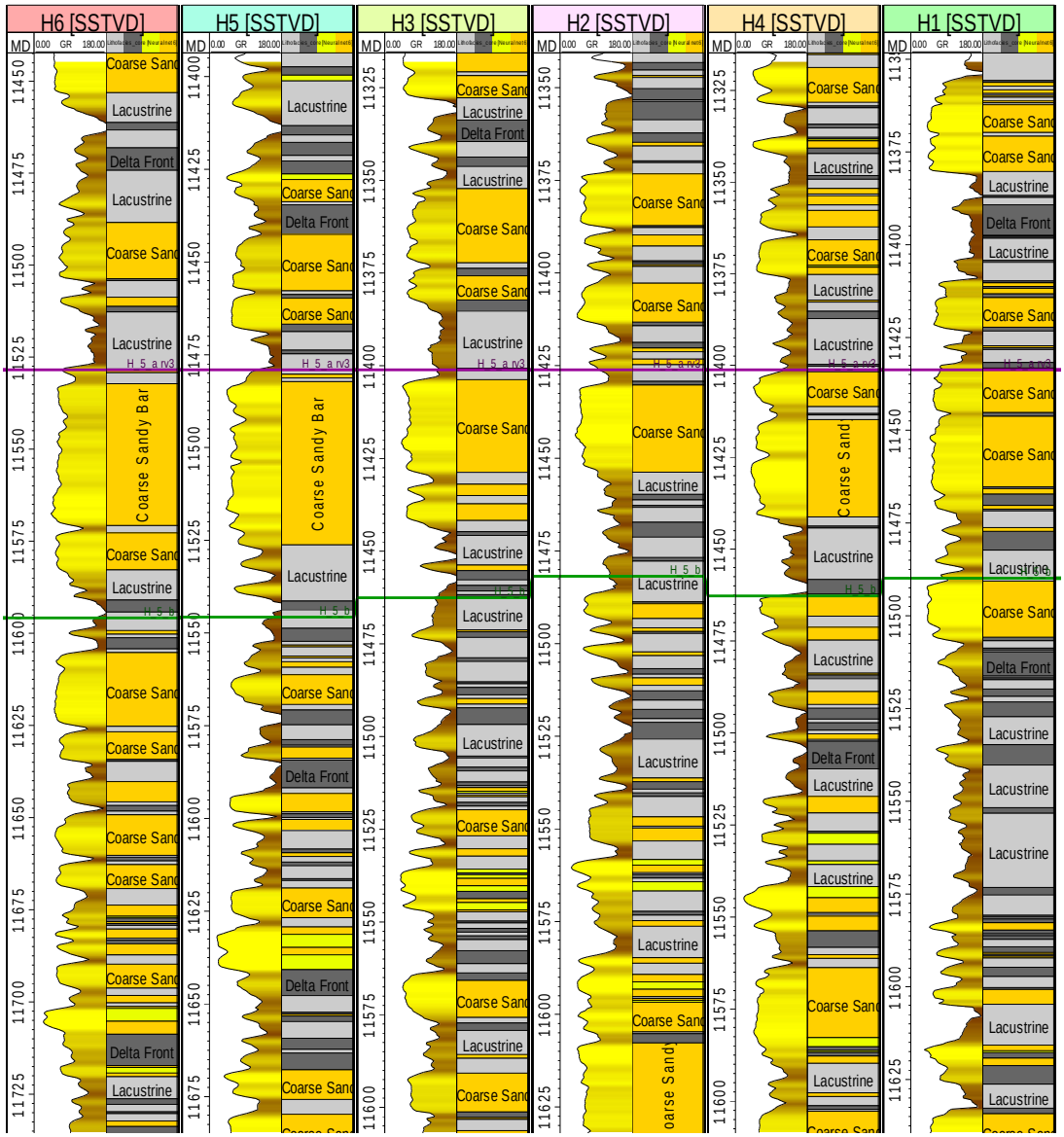

Figure 4.13: Predicted lithofacies for non cored wells by using NN4 (GR, NPHI, RHOB and SONIC are the input data for the Neural Net selected test).

From Figure 4.12, the log traces columns from left to right are: Measured Depth, Gama Ray, and Core facies, Neural Net one (NN1): (GR only), NN2 (GR and NPHI), NN3 (GR&RHOB), NN4 (GR, NPHI, RHOB and SONIC).

This predicted lithofacies established was used later as input for the modelling purpose.

From observation of the facies wells blocking result, which is calibrated to the original facies and Gama ray, it seems to be well identified with vertical geological information as it captures the important facies, as illustrated per Figure 4.14.

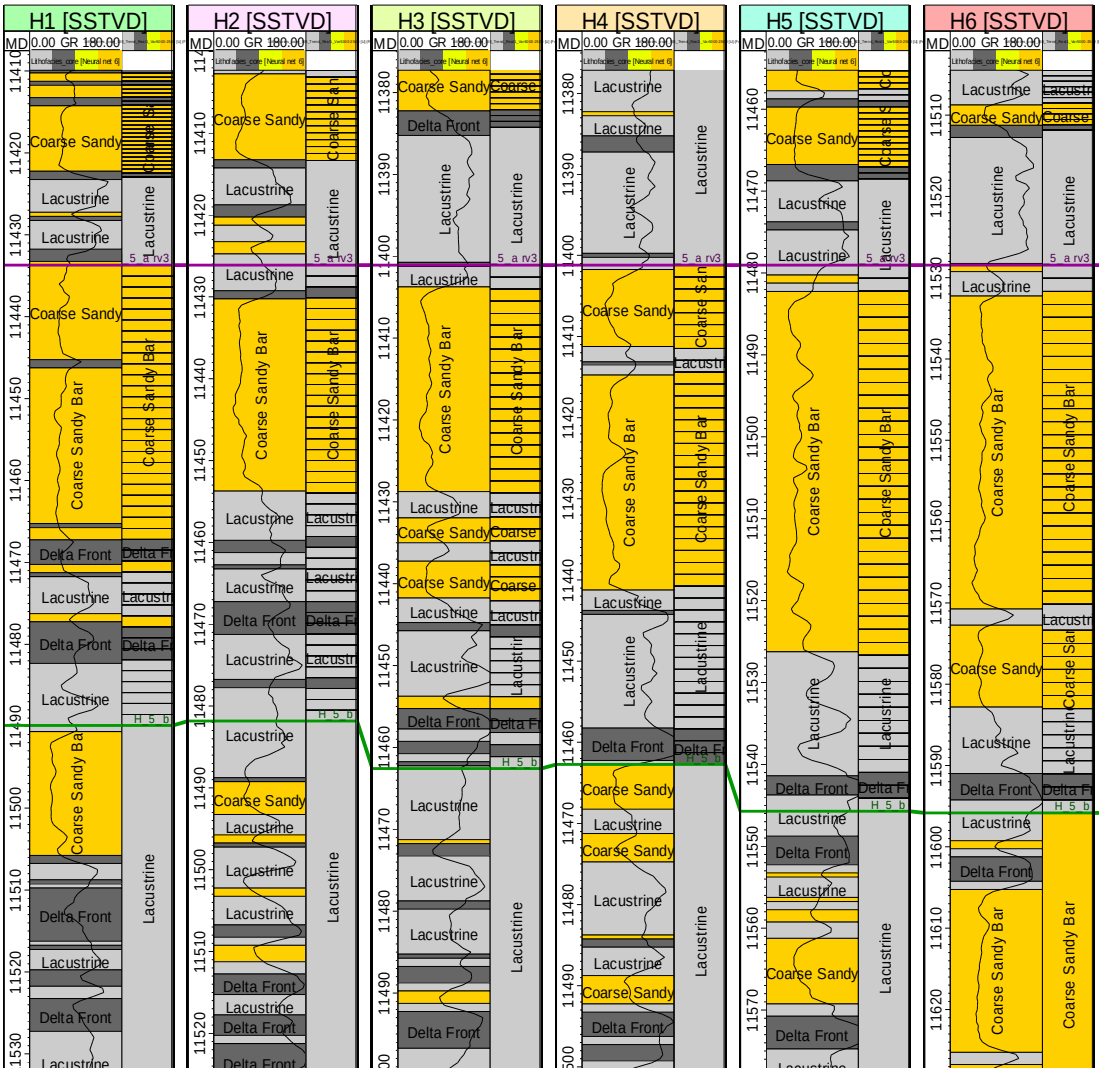

Figure 4.14: Scale-up well logs cross checking against the original logs.

Legend:

The resulting analysis of the facies blocked from the wells H6, H5 and H2 in the study zone, are showing that the major geological information is well captured as illustrated by Figure 4.15, Figure 4.16 and Figure 4.17.

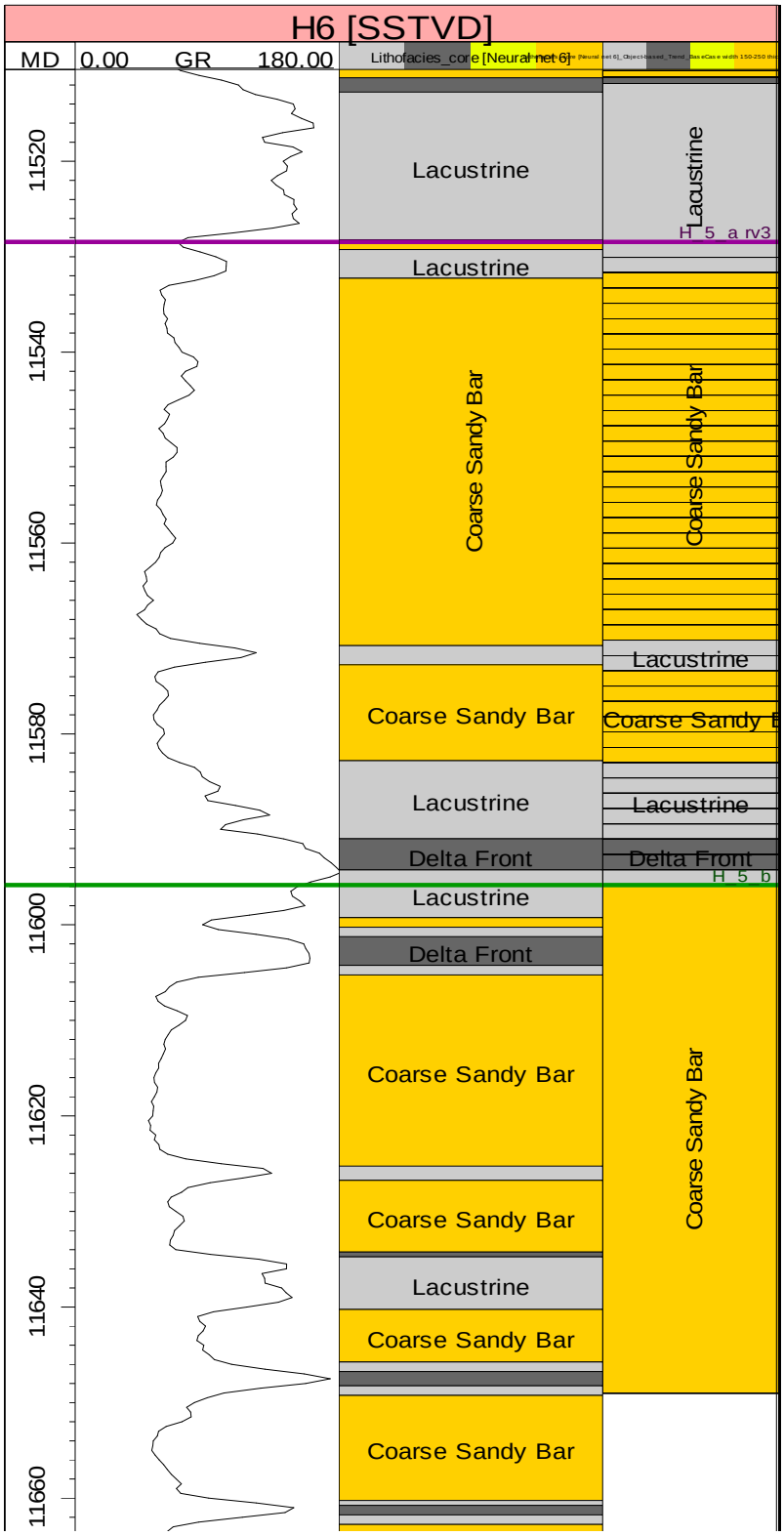

Figure 4.15: Example of scale-up facies well logs display on well section H6, Columns from left to right are representing measured depth (MD), Gama ray (GR), original facies and facies blocked respectively.

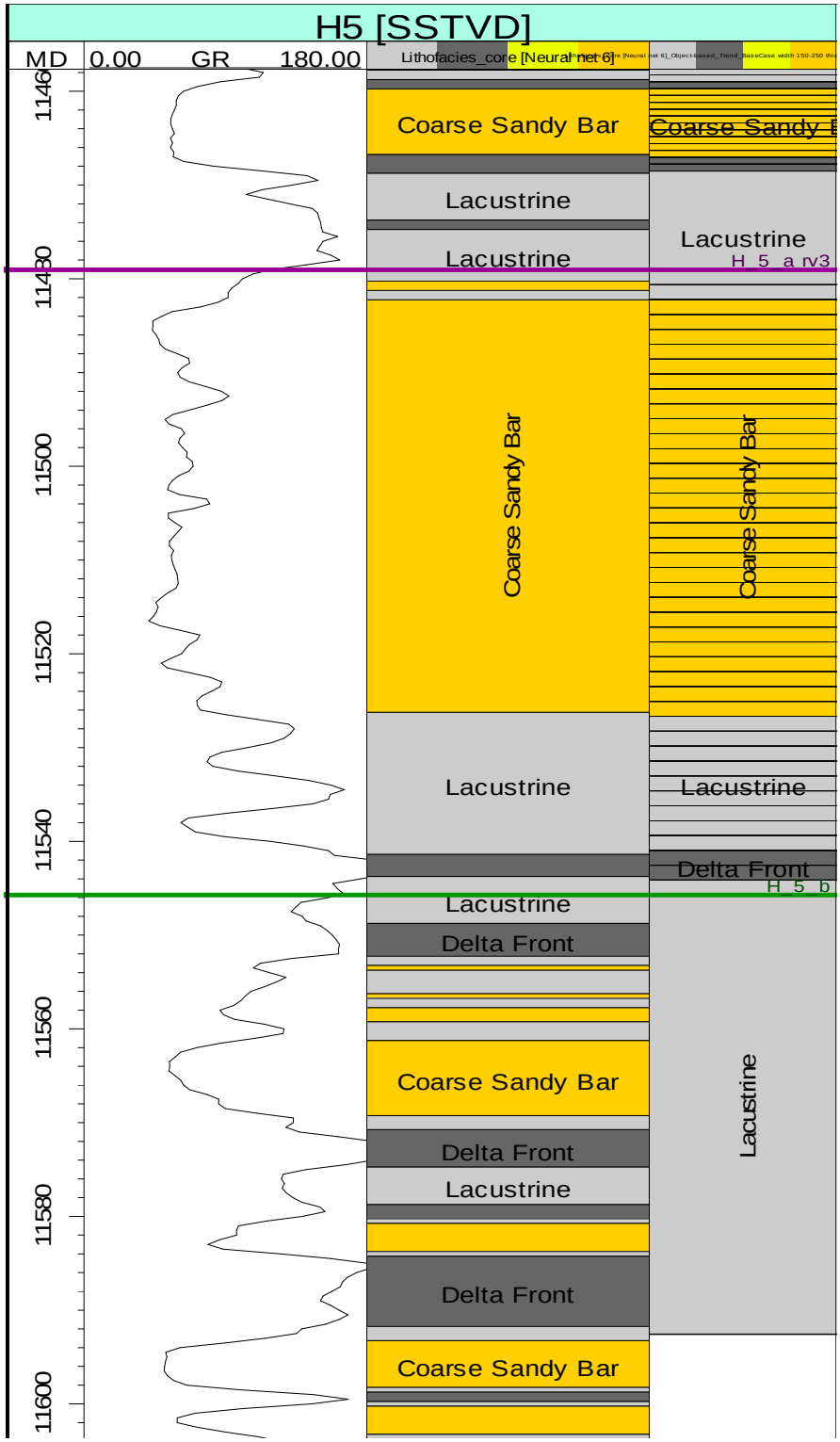

Figure 4.16: Example of scale-up facies well logs display on well section H5, Columns from left to right are representing measured depth (MD), Gama ray (GR), original facies and facies blocked respectively.

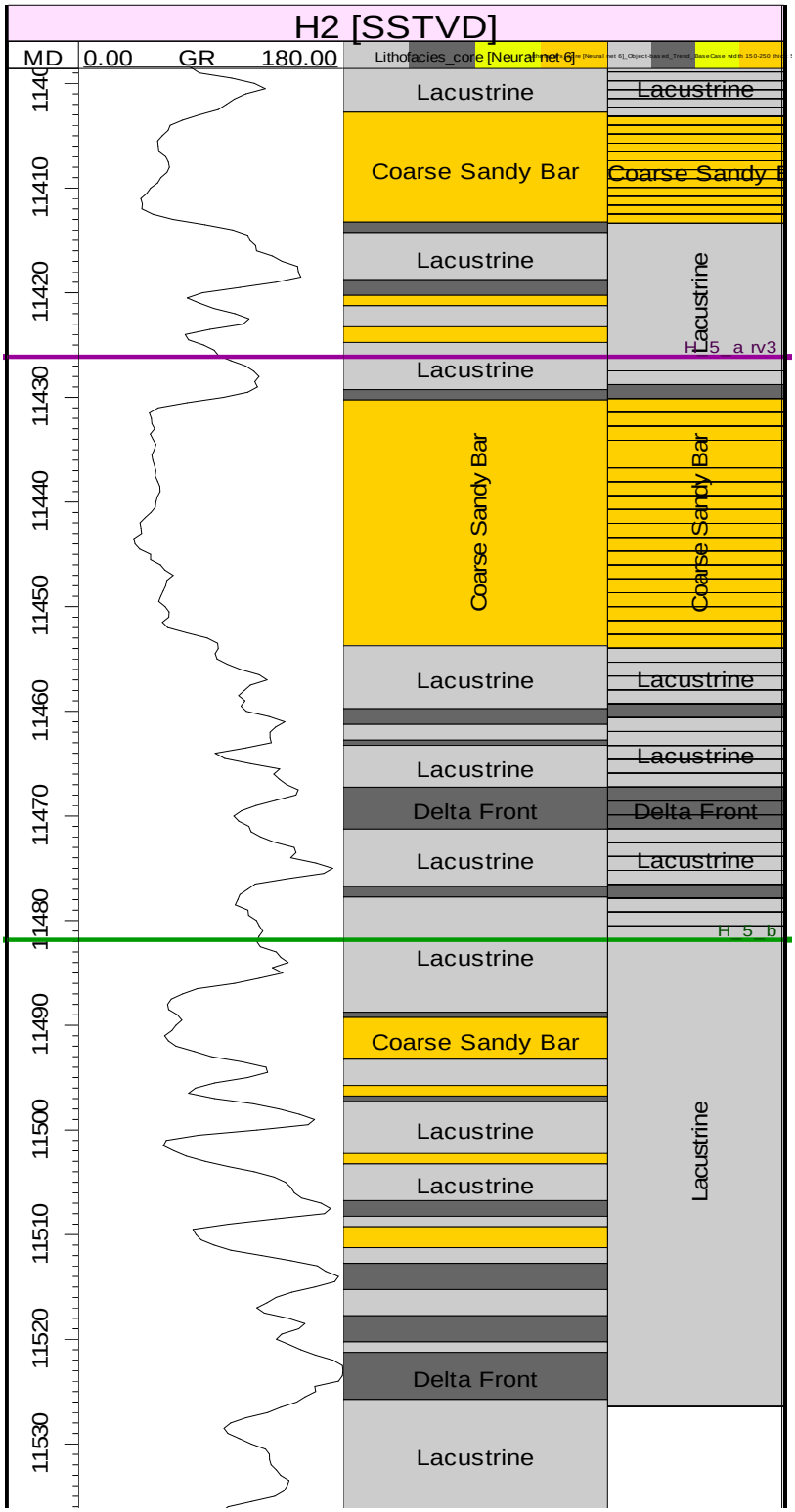

Figure 4.17: Example of scale-up facies well logs display on well section H2. Columns from left to right are representing measured depth (MD), Gama ray (GR), original facies and facies blocked respectively.

The result from the facies blocked is consistent with the original facies, and this proved that the vertical grid selected for the modeling purpose is normal since it captured the major geological information.

The blocked facies are in agreement with the classified facies. These indicated that significant facies are being well captured throughout facies modeling.

The observation of facies blocked in the reservoir zone in well H2 indicates to the missing of some thin layers of delta front facies and a few missing of the coarse sand bar facies in well H5. The lithofacies are well captured in the well H6.

4.4 Lithofacies Architecture

The four types of lithofacies selected, which included coarse sandy bar, sandy bar, lacustrine sandstone and delta front lithofacies are not showing specific characters. The sandy bars are the reservoir facies with delta front and lacustrine are non reservoir facies.

In the modeling the lacustrine facies form the background, delta front as body and the course sandy bar as channel reservoir facies. This facies is representing a good reservoir due to the high braided energy that produced channel rich in sand with coarse grain size. The delta front sands are considered to be lower quality than the sandy bar due to the grain size and degree of porosity and permeability. Most of the sands are coarse to very coarse grains with sharp top and base in GR motives (fining upward).

The thicker shale on the datum zone in well H3 and the less thickness in both sides of H6 and H1 is the maximum flooding surface interval thickness of about 609.6 meters to 1371.6 meters. Details are in previous Figure 4.4.

The channel is dominant in the middle and upper parts of the zone and the probability to see more sand are promising on that part. The reservoir facies are composed of approximately 60 % coarse sandy bar, 25 % lacustrine and 15 % delta front.

4.5 Reservoir Facies Models

The output model results for this study area are represented in 3D, 2D, and 1D for reservoir lithofacies distribution models which reflect the lateral and vertical continuity and extension for the reservoir sand. Both model results come from pixel based methods and object based method are consistently appearing to be logical in terms of facies distribution as displayed in the different three realizations described in the following paragraphs. The realization of the reservoir zone was captured in align along the vertical direction (K) where the K is in the layer number 124. Subsequently the layer 124 illustrated all facies sand dominate in the NW and very fine sand in the NE portion of the area which typically represents the braided delta system.

4.5.1 SIS Model Realization-1

From the observation of the SIS model realization-l in Figure 4.18. The braided complex has sand but not as a channel filling character. In the southwestern portion the sandy bar reservoir is dominant and initially replaced by lacustrine, less connected, delta front facies appear in the northeast of the area within the layer 124 in the vertical direction (K), where fine sands are dominant. This may indicate to the possible lake facies will appear on continuing going in that direction.

Figure 4.18: 3D facies models lateral distributions in k 124 based on SIS, realization-1, showing domination of sandy bar facies on the southwest part.

4.5.2 SIS Model Realization-2

The model shows the reservoir sand distribution that is partially replaced by the lacustrine and delta facies in the whole area. The coarse sandy bar (channel filling) reservoir is dominant in the northeast portion of the area and a transition among the three facies is shown. That indicated to the prospect of the lake appearing in the north eastern part of the field. In this realization the delta front non reservoir facies is extensively observed in the northeast portion of the field with the existing coarse sand facies, but the model may represent the analog in some way as shown in Figure 4.19.

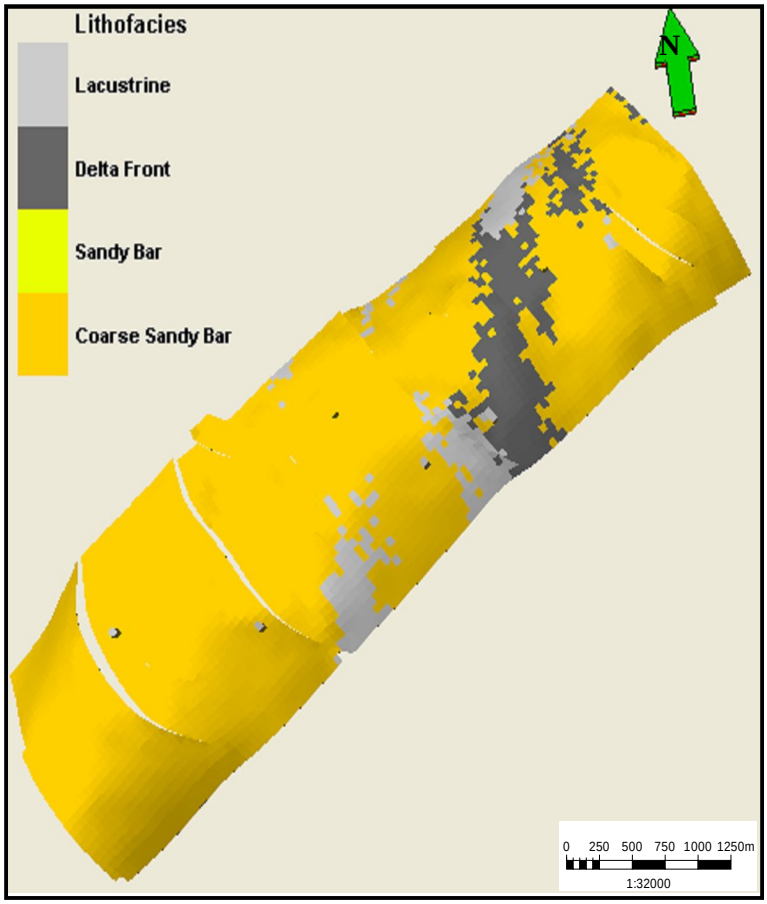

Figure 4.19:3D facies model lateral distributions in k 124 based on SIS realization-2

4.5.3 SIS Model Realization-3

The model shows the reservoir sand distribution that is partially replaced by lacustrine and delta front which shows a facies transition in the north east. In this realization the braided complex distribution in the southwest is dominant. The non reservoir facies occur as a patchy shape in the northeast, weakly connected and are not well represented the environmental deposition in the area. Figure 4.20 shows the 3D reservoir facies models distributions in SIS realization-3.

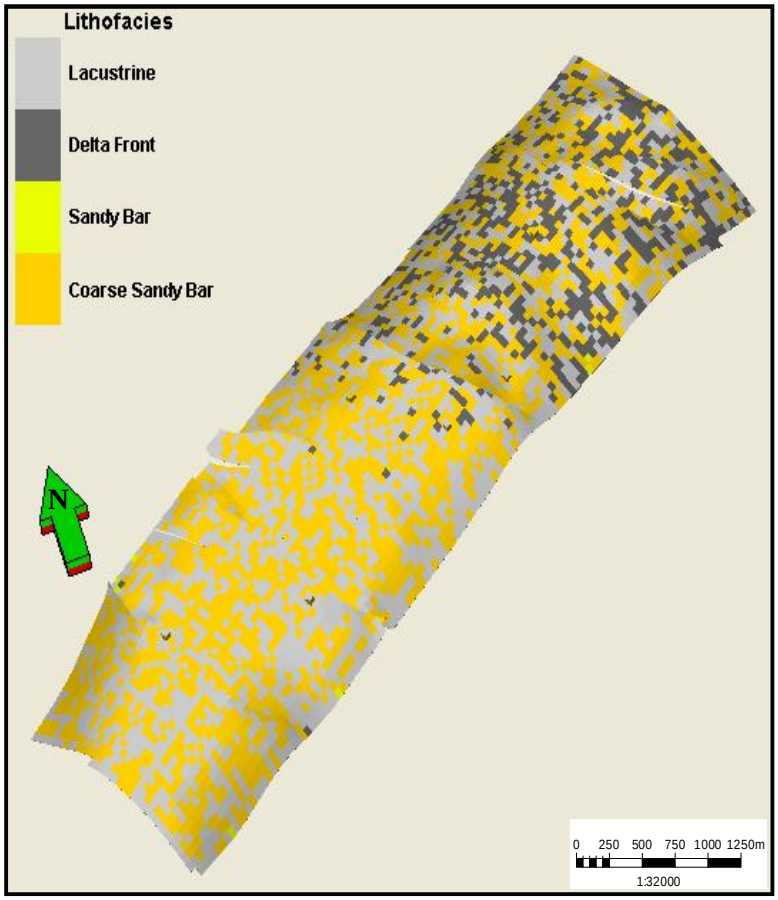

Figure 4.20:3D facies model lateral distributions in k 124 based on SIS realization-3.

4.5.4 TGS Model Realization-1

The coarse sandy bar distribution is not properly connected and is partially replaced by lacustrine. The facies does not show a proper transition between coarse sandy bar, lacustrine and delta. The braided complex distribution in the southwest is dominant over the delta front and lacustrine respectively. The coarse sandy bar distribution is not properly connected and partially replaced by lacustrine as shown in Figure 4.21.

Figure 4.21: 3D facies model lateral distributions in k 124 based on TGS, realization-1. View from above.

4.5.5 TGS Model Realization-2

The braided complex facies distributed in the southwest are showing that coarse sandy bar, lacustrine and delta front show a transition between the three facies. This indicates that the lake facies will appear on going to the northeast direction. Figure 4.22 shows the model with distribution of the facies.

Figure 4.22: 3D facies model lateral distributions in k 124 based on TGS realization-2

4.5.6 TGS Model Realization-3

From the observation of Figure 4.23, the braided complex distribution in the southwest is dominant. The deltas front and lacustrine in the northeast direction are well distributed. The patches are weak connected and does not represent the typical modern analog for the environment of deposition in the area.

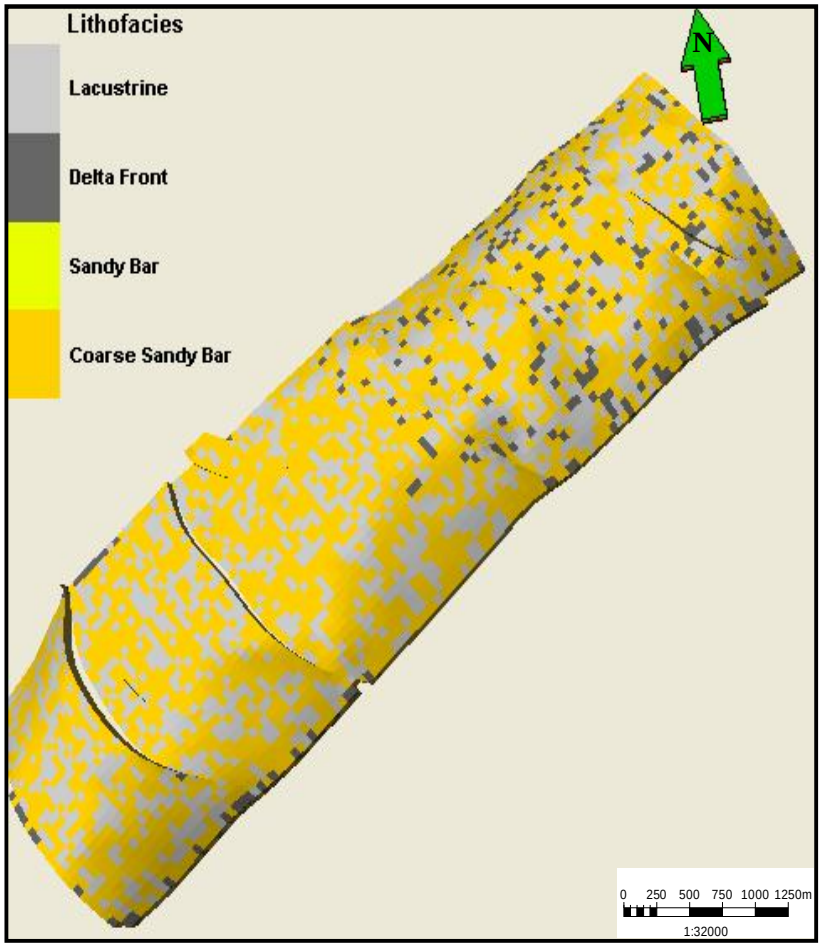

Figure 4.23: 3D facies model lateral distributions in k 124 based on TGS realization-3

4.5.7 Object-Based Model Realization-1

The coarse sand facies are more abundant and thicker within the channel belt in the southwest portion and is partially replaced by lacustrine sediments which are well connected and dissected by NW- SE trending normal faults. The sediments contain significant porosity and permeability. In the NE portion, the coarse sand is less abundant and the less porous delta front facies which is aligned in the NE are found. The model is showing a close similarity to the braided delta analog that is used for this research as illustrated per Figure 4. 24.

Figure 4.24: 3D facies model lateral distribution in k 124 based, on Object-based realization-1.

4.5.8 Object-Based Model Realization-2

The coarse sandy bar facies distribution in the southwest area are dominant, well connected and replaced partially by lacustrine sediments. At the northeastern portion of the area the coarse sand are still dominant with the appearance of delta front and lacustrine facies in between the channels. The delta front facies are aligned northeast - southwest in an elongated manner as shown in Figure 4.25. It does not show a strong similarity to the analog of the deposition environment compared to the realization-1. However, it still can represent the analog.

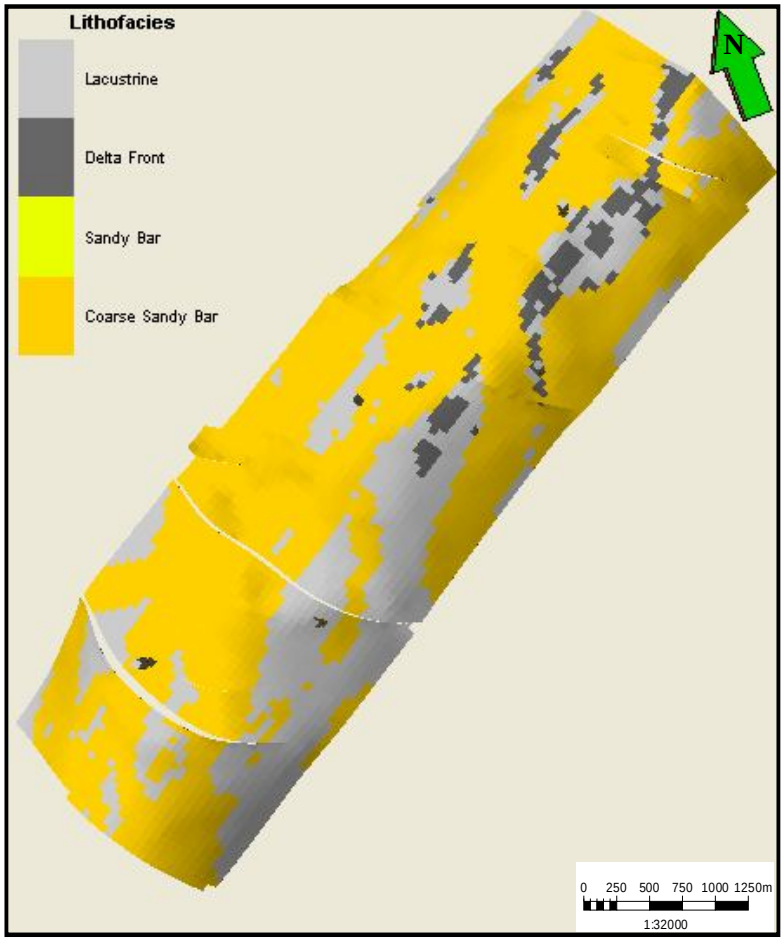

Figure 4.25: 3D facies model lateral distribution in k 124, based on Object-based, realization-2.

4.5.9 Object-Based Model Realization-3

Figure 4.26 shows the coarse sandy bar facies distribution are dominant in the southwest followed by lacustrine and delta front which are aligned in a southwest direction. The reservoir facies distribution is showing little similarity to the model analog as well.

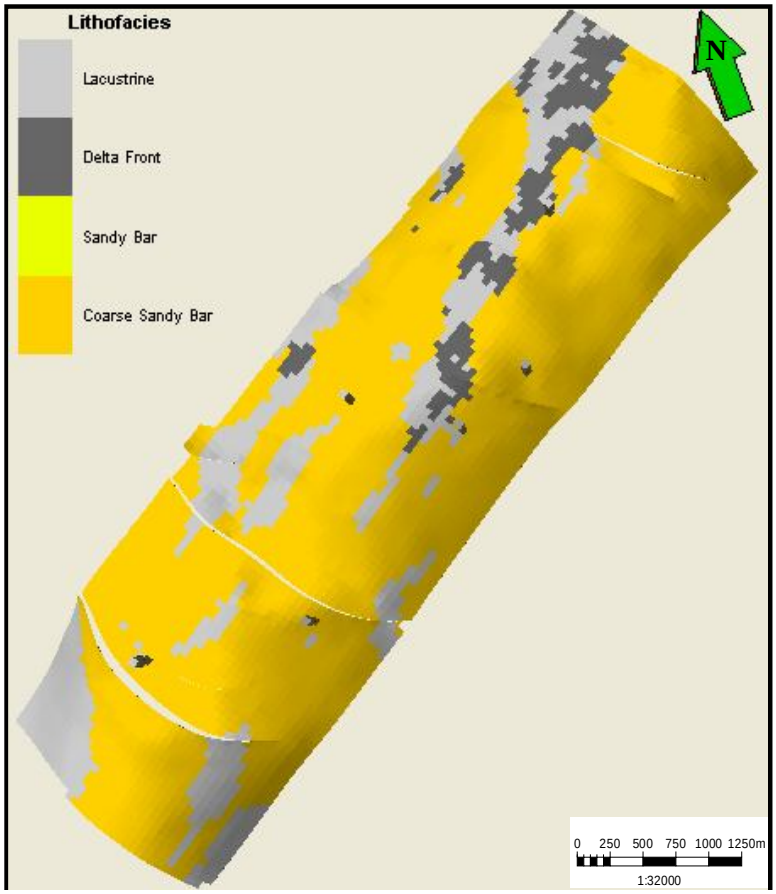

Figure 4.26: 3D facies model lateral distribution in k 124, based on Object-based, realization-3.

4.6 Comparison of Models

Facies modeling technique was applied in the consideration of the braided delta depositional system. As the nature of the braided channel facies deposition and existence of the high net gross sand interval that are linked to the braided deposition system covers a wide area in low sinuosity which probably is the beginning of lake facies within the channel belt, usage of different modeling techniques such as object-based and pixel-based could represent the facies distribution of braided delta reservoir system. The results from the three models are showing wide distribution of coarse sandy bar facies throughout the area with some lacustrine and delta front in the NE part. All the models confirm that the coarse sandy bar facies are dominant in the entire

area. The Figure 4.27 shows the optimal facies model realizations produced from the three techniques.

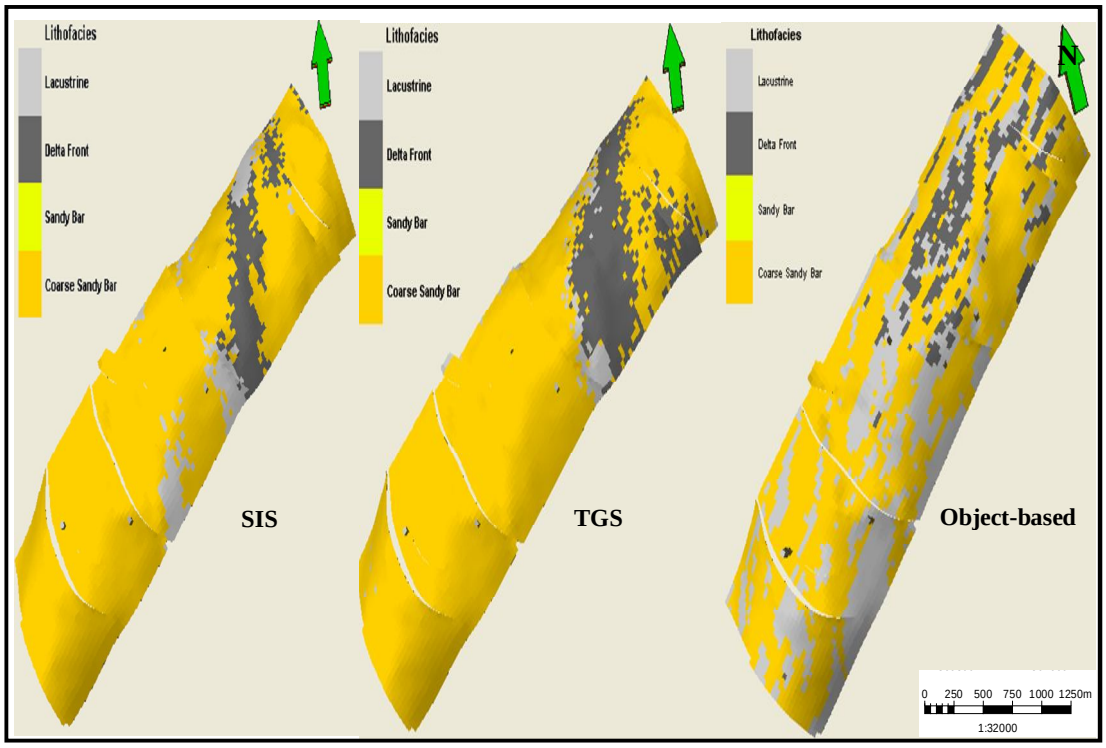

Figure 4.27: 3D facies models selected in stochastic Pixel-based and Object-based techniques.

Comparison of the three models shown in Figure 4.27, seem to be reasonable in terms of facies distribution, due to the similarity to the braided delta depositional system. However the facies model produced from the object-based technique is the optimum model as it shows a high similarity to the analog below in Figure 4.28.

The reservoir sand distribution and geometry of the selected models reservoir in the K-Oil Field are re-summarized in Table 4.2.

Table 4.2: A summary of reservoirs and distribution and geometry for the selected stochastic model realizations.

Modeling Techniques Types	Reservoir distribution	Reservoir geometry
SIS Realization -2	At SW portion the Coarse sand bar facies are dominant, well connected and partially replaced by lacustrine facies as well as containing good reservoir properties. At the NE portion the coarse sand facies are abundant replaced partially by thin less porous delta front facies compared to TGS, elongated in a NE direction.	In SW consist of sands associated with channels occur between delta front. Facies bodies are narrow and aligned to N - S and characterized by a fine facies
TGS Realization -2	In SW portion the Coarse sand bar facies appear strongly within the channel belt which is well connected, dissected by NW - SE normal faults and contain significant reservoir properties. At the northeast portion the coarse sand facies are less abundant, replaced partially by a less porous facies which is elongated in a NE direction. The transitions between the three facies are observed.	The variogram ranges are between 5000 - 250 meters and the vertical is 10. At the SW the delta front facies are thicker, triangle shape, elongated between 90 - 2380 meters. The width is between 100 - 900 meters, and elongated between 90 - 2380 meters
Object-Based Realization -1	In the SW K-Oil Field, the Coarse sand is more abundant within the channel belt which is partially replaced by lacustrine which is thicker, well connected and dissected by NW SE normal faults as well as containing significant porosity and permeability. At the NE portion the Coarse sand is less abundant and associated with none or less porous delta front facies which is aligned in a NE direction.	In the K-oil field, the channel width is about 150 - 250 meters, and thickness of 5 - 20 meters with orientation of 43 - 47 degree, the body shape of the delta front as deltaic alluvial with thickness from 10 - 20 meters, and elongated.

The optimal facies model realizations produced from the three techniques are analyzed and compared based on the similarity represented by the conceptual analog of the deposition environment of the area. The analysis shows that the model resulting from the object based is more representative of the analog. Figure 4.28 illustrates the consistency between object based reservoir facies model and modern analog.

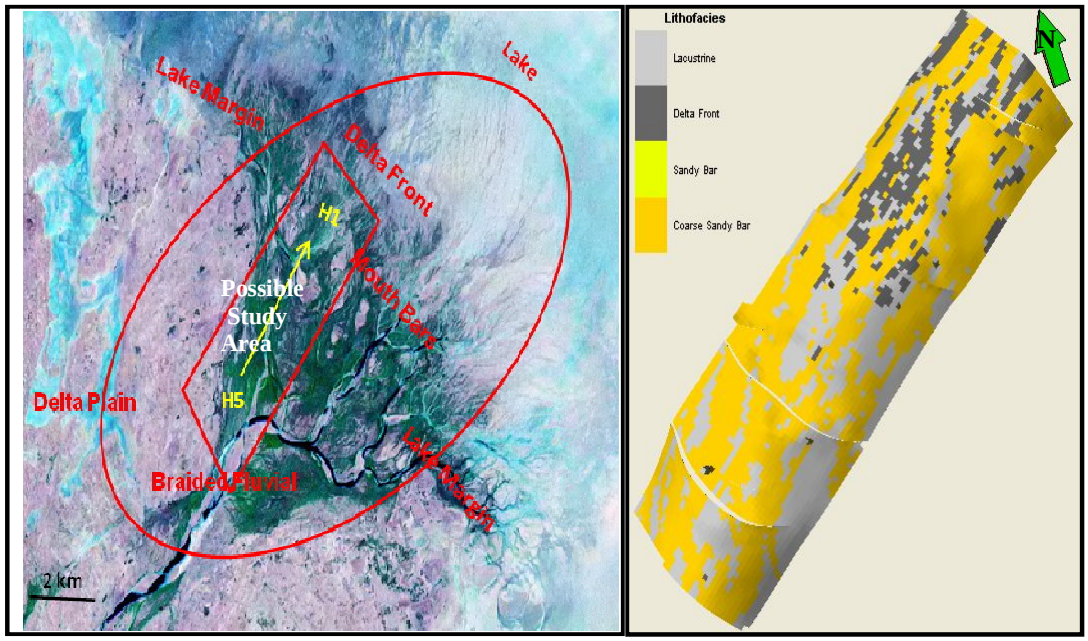

Figure 4.28: Comparison between conceptual models from the left braided delta Neales River Australia and Object-based facies model on the right. It shows well consistent between the model and the Analog.

4.7 Reservoir Heterogeneity

The lateral and vertical distributions of the sands are shown by the cross section of the reservoir zone. The cross section of the reservoir with the six well logs demonstrate that the coarse sandy bar facies are dominated in the southwest sector. Figure 4.29 illustrates the variability of facies in vertically as well as laterally. The coarse sand bar is widely extended, connected, and thicker compared to the other facies of the reservoir rock.

Hence the reservoir is more uniform in the southwest and becoming more heterogeneous toward the northeast. However the reservoir facies is very much in connection and may be in communication over the reservoir zone.

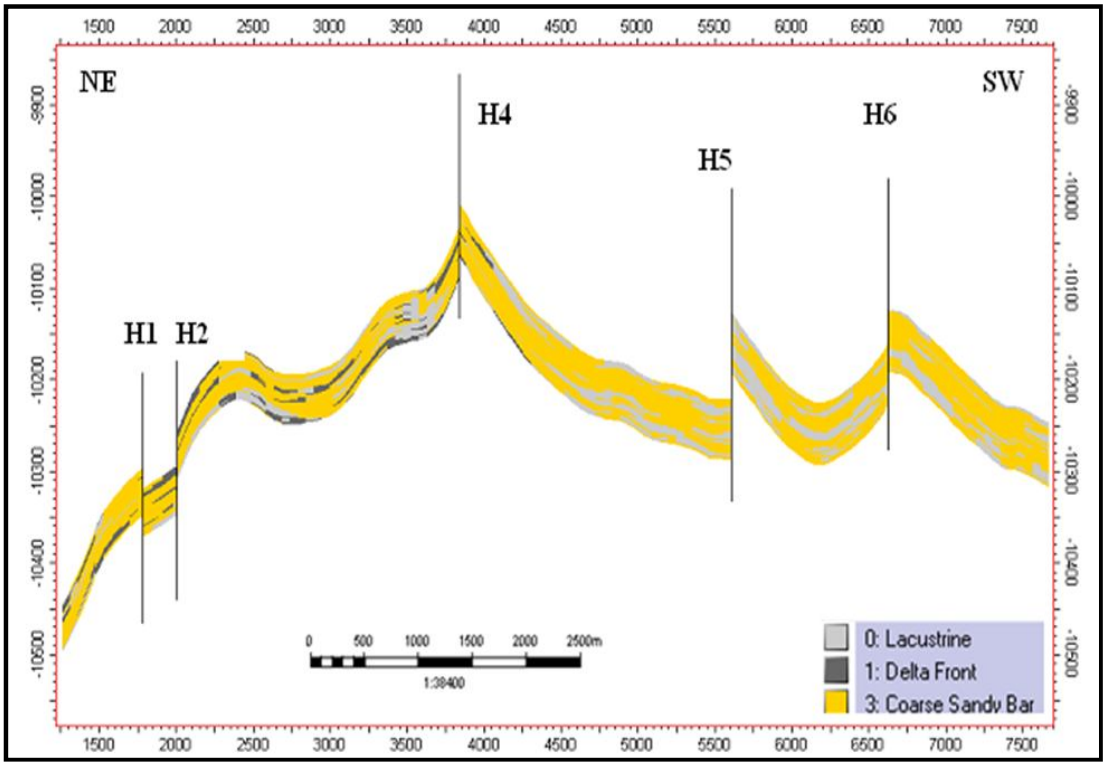

Figure 4.29: Cross Section map of reservoir zone, view from west. The cross section shows that risk on sand distribution in the channel belt is low and the reservoir sand expected to have better porosity and permeability.

The average thickness of the reservoir interval varies from 17.07 meters to 20.42 meters. The facies distribution in the reservoir shows that the channel depositions are from the southwest - northeast direction into the lake. The channel width varies from 150 meters - 300 meters. The upper section of the reservoir shows continuity of coarse sand in all wells and the lower part is showing more lacustrine and delta front.

The GR curves have shown a coarsening trend that represents an increase in energy and decrease of channel sinuosity characterizing the braided delta system environment.

The reservoir is continuous within the channel built and the sand thickness of 17.07 meters - 20.42 meters is proven by all the six well logs data. All the six wells penetrate the reservoir. The model of a braided deposition system is consistent with the model, shown in Figure 4.24. The heterogeneity of the reservoirs is contributed by the internal geometry of the reservoir in term of the connectivity of the entire facies, and represents a barrier of fluid flow and sensible characterizing of the reservoir. The

heterogeneity of the reservoir estimated from the net sand distribution, by visual observing to the percentage of facies types at different levels in the proportion curves and by the pie diagram is shown in Figure 4.30.

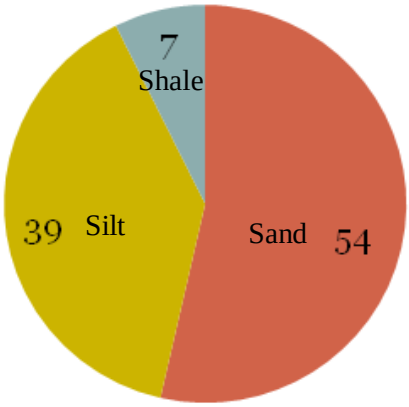

Figure 4.30: A statistical pie diagram of the facies shows net to gross sand in percentage % for the reservoir zone.

The reservoir heterogeneity exists within the channel built and it varies in different zones. The braided complex facies are dominant, approximately 65% (coarse sandy bar facies), and lacustrine complex about 35% (delta front facies and lacustrine sediment).

4.8 Implication for Development K-Oil Field

In static reservoir modeling, facies modeling is the important stage to prepare for the volume calculation by introducing facies distribution, such as the heterogeneity and the porosity as well as permeability properties can be considered in terms of fluid flow factors. Having an idea about the deposition environment of reservoir based on facies distribution, continuity and extension, although the reservoir facies distribution in the study area was modeled by the stochastic techniques.

The realizations are important in modeling reservoir to test and compare due to different interpretation as multi interpretations are possible in case of few observations and high uncertainties. In order to understand the reservoir facies distribution and heterogeneity, the different results based on the modeling techniques have been considered.

In the SIS and TGS techniques the distributions of facies are based on their probability distribution function (PDF) assumptions and the changes of the variogram fit (ranges from major, minor, and vertical direction) and the facies fractions are affecting the results.

The variogram fitted in the pixel-based methods failed to capture the environment concept in the case of contract facies models realizations from ranges 100 meters - 250 meters as the models appear as discreet facies with less connectivity and continuity of reservoir facies as illustrated in Figure 4.20 and Figure 4.23.

In the case of expanding the variogram ranging from 2500 meters - 5000 meters, both the techniques are showing the wide connectivity of sand within the facies models realizations as appeared in Figure 4.19 and Figure 4.22.

In the case of object-based technique the parameters affecting the results are the channel geometry, facies fraction and the trend map.

The model fitted well with the analog when the parameter is set for the channel geometry with the 150 meters - 250 meters, and a thickness of 1.5 meters - 6.1 meters as illustrated in Figure 4.24.

Reservoir sand distributions for the future development of the K-Oil Field is demonstrated and shown by the models, theory in object-based technique. As most of the reservoir sand is in the northwest sector, well placements are suitable within that sector. The model all suggests that the reservoir is well connected and there is continuity in the southwest sector as well.

CHAPTER 5

CONCLUSIONS AND RECOMMENDATIONS

5.1 Summary

The results were obtained with the support of having important parameter concepts in this research. The lateral and vertical lithofacies distributions by using statistical information were illustrated and the geometry and heterogeneity of the reservoir facies in three dimensions were predicted. Reservoir lithofacies of several models of the distributions of the braided delta system using stochastic methods have been made and the optimal model was determined. However the conclusion reflects that the objective of this research has been achieved.

5.2 Review of Results

In the previous chapter the reservoir lithofacies modeling for braided delta have been documented and discussed. In this chapter, the contributions from reservoir facies modeling of the Cretaceous braided delta system by using object-based and pixel-based techniques are summarized. The objectives were achieved and further studies for future research in this field are also recommended. The following items have been completed with a discussion on the field products.

5.3 Conclusions

The result from reservoir litho-facies models of braided delta are summarized as follows:

1 Static 3D reservoir lithofacies modeling of the braided delta system using SIS, TGS and Object-based modeling techniques for the Cretaceous reservoir in the K-oil field of the Doba basin were carried out to understand facies distribution. The length and the width of the channel varied from 1500 meters - 2500 meters and 150 meters - 300 meters respectively in the area of about 4500km^2. The thickness of the reservoir varied from 17.07 meters - 20.42 meters. The reservoir lithofacies distributed illustrated that the channel depositions are from SW - NE toward the lake. The reservoir heterogeneity was contributed by the internal geometry and estimated to be less within the NW direction and is high toward NE of the area due to the presence of lake facies trace on that direction. The uncertainties to see non reservoir facies is less in the southwest of the area which may be the possible location of a development well.

2 The three lithofacies used for this modeling are coarse sand bar coarse to very coarse grained sandstone, delta front facies medium to fine grained sandstone, bedded and lacustrine sediments fine sandstone grained. The coarse sand bar facies fraction are dominant, approximately 54%, delta front facies and lacustrine fraction are about 46%. Based on modeling techniques for this study, train estimation model and object-based modeling techniques are useful tools in predicting lithofacies and generating a braided reservoir model.

3 The reservoir lithofacies for the Cretaceous in the K-oil field of the Doba basin are distributed laterally and vertically in the study interval based on the object-based modeling technique. The results illustrated that the coarse sand bar are dominant in the reservoir zone especially in southwest direction of the area. Reservoir properties such as porosity and permeability may improve laterally and vertically southwest of the area as the grain size of the sands facies are increasing. The reservoir porosity and permeability are expected to be good within the coarse sand bar facies in the SW portion of the area.

4 The model`s realizations of the reservoir in the K-oil field demonstrate that the selection of techniques, facies fraction and variogram range that are affecting

the result were correct. The pixel-based methods failed to capture the environment concept in the case of contracting facies models realizations (when the variogram range is less, the models appear as discreet facies with less connectivity and continuity) but in the case of expanding the variogram ranges, it shows the wide connectivity of sand within the facies models. The results show that the reservoir is continuous from NE - SW within the channel built and environmental changes laterally and vertically in the wells position and the coarse sandy bar facies are dominant. The model selected is from the object-based technique, and consistent with the conceptual analog of a braided system as coarse sandy bar dominates in the SW and lacustrine appear in NE. The risk of the sand distribution within the channel belt is low.

5.4 Contributions

Therefore the contributions of reservoir lithofacies modeling research in the K-Oil Field of Doba basins are:-

- Prediction of lithofacies for the study interval in the K-Oil Field uses the train estimation technique and well logs data.
- New models of braided delta reservoir lithofacies of Cretaceous distribution by using Sequential Indicator Simulation (SIS), Truncated Gaussian Simulation (TGS) and Object-based modeling techniques are created.
- Risk of sand distribution within the channel belt is low. The optimal model established the one that is produced from object-based as it represents a typical environmental system of a braided delta analog. In terms of reservoir quality it suggests a better sand distribution in several cases, compared to the models produced from SIS and TGS techniques.

This research has established that for modeling of braided delta systems, the object-based model is most optimum due to a well representing the analog of the area.

5.5 Recommendations

The report ``Lithofacies modeling of Cretaceous reservoir in Doba basin, Southern Chad``, can be improved with the following:-

- Facies model may be integrated with seismic attribute data to improve the estimation of facies quality and distribution.
- Reprocessing of seismic data to produce seismic impedance that can be integrated within the facies model.
- The reservoir model with input from lithofacies model can be used to update the dynamic reservoir model for future management of reservoir performance and reservoir assessment.
- In the present work only cored well data were used. If there are any additional core data it should also be included.

REFRENCES

[1] Mohammad A. Al-Khalifa, Tobias H.D. Payenberg, and Simon C. Lang, 2007. "Overcoming the challenges of building 3D stochastic reservoir models using conceptual geological models: A case study". SPE Middl east Oil and gas show and conference, 11- 14 march 2007, Bahrain.

[2] Schlumberger Petrel Online Help, 2004. Petrel 2004 Version.

[3] Seifert. D and J.L Jensen, 2000, "Object-based and pixel-based reservoir modelling of braided fluvial reservoir", Mathematical geology, V. 32, No.5.P. 581 - 603

[4] Haldorsen, H. H and E. Damsleth, 1990, "Stochastic modelling", Journal of Petroleum Technology, AAPG, p 404 – 412.

[5] Genik, G. J. 1993. "Petroleum geology of Cretaceous-Tertiary rift basins in Niger, Chad, and Central African Republic", AAPG, p 1405 - 1434.

[6] Petroleum in Chad 2001. Source: Resistance Oil Watch Network Bulletin Number 12 – January 2001. The Document Available from internet: *http://www.oilwatch.org/doc/paises/chad/chad2001ing.pdf*

[7] Fairhead, J.D. 1986. "Geophysical Controls on Sedimentation within the African Rift Systems", in L.E. Frostick, R.W. Renault, I. Reid, and J.J. Tiercelkin, Eds. Sedimentation in the African Rifts, Geological Society, London, p 19 - 27.

[8] Reynolds, D.R. And Jones, C.R, 2004, "Structural Evolution of Doba Basin, Chad: Controls on Stratal Architecture of the Three Fields Area", AAPG Hedberg, p.

[9] Patterson, P.E and Abba Kaka, A, 1997, “Reconnaissance Study of Cretaceous & Tertiary Outcrops, Mayo Kebbi & Logone Oriental Provinces”, Chad: April 20-25, 1997; EPR.36ES.97.

[10] Jenny Joyce (EMDC), Clive Jones (EMEC), and Ray Skelly (EMEC) with contributions by Jonathan Zybala, Damian O'Grady, Rebecca Crompton & David Lowe, 2005, “Core Description and Facies Analysis of the K4Lower Cretaceous Core, Doba Basin, Chad”, PETRONAS, Report no R025251.

[11] John G. McPherson and GanapathyShanmugam Richard J. Moiola, 1987. “Fan-deltas and braided deltas: Varieties of Coarse-Grained Deltas”. Geological Society of America Bulletin, 99, p. 331-340.

[12] David J. Reynolds1 and Clive R. Jones, “Tectonic evolution of the Doba and Dosio Basin, Chad Controls on Traps formation and Depositional setting of thethree fields area, Chad”. Exxon mobile from the internet:

http://www.searchanddiscovery.com/documents/abstracts/2004hedberg_baku/extended/reynolds/reynolds.htm

[13] Roger M. Slatt, 2006, “Stratigraphic Reservoir Characterization for Petroleum Geologists”, Geophysicists, and Petroleum Exploration, Handbook of Volume 6.

[14] Atkinson, C.D., J.H. McGowen, S. Bloch, L.L. Lundell, and P. N. Trumbly, 1990.“Braid plain and Deltaic reservoir, Prudhoe Bay Field, Alaska: in Sand Stone Petroleum Reservoirs”, p 205-224.

[15] Schlumberger, 1989, “Cased 3/34 Hole Log Interpretation Principles/Application", p 3/32 3/34.

[16] Asquith and Krygowoski, “Basic Well Log Analysis”. AAPG Method in Exploration No. 16. (2004).

[17] Tearpock and Bischke, 1991. “Principal of well log correlation, well log correlation techniques”. Geosciences research document, available from the internet.

[18] Reed, KJ, 1999. “Environment deposition of source beds of high-wax Oil”: AAPG Bulletin, 53: P, 1502 - 1506.

[19] Asquith, G. And Gibson, C., 1982. “Basic Well Log Analysis for Geologists” AAPG Publications, Tulsa, OK 216 pp.

[20] Heidar. M and Jeffrey B, “Determination of Lithofacies from Well Logs Using Neural Networks," Journal of Engineering Technology, pp. 33 - 35, 1994. Lithofacies Prediction.

[21] Heidar Malki and Jeffrey Baldwin, “On the Comparison Results of the Neural Networks Trained Using Well-Logs from One service Company and Tested on Another Service Company’s Data,” pp. 1776 - 1779, IEEE International Conference on Neural Networks, Vol. III, 1993.

[22] Caudills, M. 1987. “Neural Networks Primer, Part I”, Alex part 2 (12); P, 46 52.

[23] Bishop, C.M, 1995, “Neural Networks for Pattern Recognition”, Oxford University.

[24] Mustapha,M. R, R. B. Rezaur, S. Saiedi and M. H. Isa, 2012. “River Suspended Sediment Prediction. Using Various Multi Layers Perceptron Neural Net Work Training Algorithm, A case study in Malaysia”, UTP, P, 3 - 5.

[25] Schlumberger Software, 2008. “Train estimation model”, Petrel helps.

[26] M. H Hissein and W. I. Wan Yusoff, “Reservoir Lithofacies Prediction from Well Logs and Core Data Using Train Estimation”, (ICPEG2013), 2013, Malaysia.

[27] Anderton, R.1985, “Clastic facies models and facies analysis”. Geological Society, London, v. 18.

[28] Hunt, J.M. 1990. “Generation and migration of petroleum from abnormally pressured fluid compartment”. AAPG Bulletin 74, 1 - 12.

[29] Knipe, R. J. 1997.” Juxtaposition and seal diagrams to help analyze fault seals in hydrocarbon reservoirs”. AAPG Bulletin 81,187 - 185.

[30] Dubrule, O.1994, Estimating or choosing a geostatistical model, in R. Dimitra kopoulos, Ed. Geostatistics for the next century: Dordrecht, Holland, Kluwer Academic Publishers, p. 3 - 14.

[31] Dreyer, T., L. M. Falt, T. Hoy, R. Knarud, R. Steel, and J. L. Cuevas, 1993, Sedimentary architecture of field analogues for reservoir information (SAFARI): A case study of the fluvial Escanilla Formation, Spanish Pyrenees, in S. Flint and I. D. Bryant, eds. The geological modelling of hydrocarbon reservoirs and outcrop analogues: International Association of Sedimentologists Special Publication 15, p. 57 - 80.

[32] Cossey, S. P., 1994, “Reservoir modelling of deep water clastic sequences: Mesoscale architectural elements, aspect ratios, and producibility, in P. Weimer, A. H. Bouma, and B. F. Perkins, Eds., Submarine fans and turbidity systems”: Gulf Coast Section SEPM 15th Annual Research Conference, p. 83-93.

[33] Mijnessen, F. C. J., 1997, “Modelling of sandbody connectivity in the Schooner field, in K. Ziegler”, P. Turner, and S. R. Daines, Eds., Petroleum geology of the southern North Sea: Future potential: Geological Society (London) Special Publication 123, p. 169 - 180.

[34] Satur, N., A. Hurst, B. Cronin, G. Kelling, and K. Gurbuz, 2000, “Sand body geometry in a sand-rich, deep-water clastic system, Miocene Cingoz Formation of southern Turkey”: Marine and Petroleum Geology, v. 17, p. 239 - 252.

[35] Dalrymple, M., 2001. “Fluvial reservoir architecture in the Stratfjord Formation (northern North Sea) augmented by outcrop analogue statistics”, Petroleum Geoscience, v. 7, p. 115 - 122.

[36] Johnson, S. D., S. Flint, D. Hinds, and H. D. V. Wickens, 2001, “Anatomy geometry and sequence stratigraphy of the basin floor to slope turbidite systems, Tanqua Karoo”South Africa: Sedimentology, v. 48, p. 987 - 1023.

[37] Larue, D., 2004, “Outcrop and water flood simulation modelling of the 100-foot channel complex, Texas and the Ainsa II channel complex, Spain: Analogs to multistory and multilateral channelized slope reservoirs, in M. Grammer, P. M. Harris, and G. P. Eberli, Eds., “Integration of outcrop and modern analogs in reservoir modelling”: AAPG Memoir 80, p. 337- 364.

[38] Larue, D., and F. Fried mann, 2005. “The controversy concerning stratigraphic architecture of channelized reservoirs and recovery by water flooding” Petroleum Geoscience, v. 11, p. 1310 -146.

[39] Lake, L. W and Carroll, H. B. 1986, “The role of reservoir characterizations in the reservoir management process I”, P, 665 – 676.

[40] Seifert, D and Jensen, J.L, 2000. “Object-based and pixel based modelling of braided fluvial reservoirs, Mathematical Geology”, Springer.

[41] Jean-Paul Bellorini, Johnny Casas, Patrick Gilly, Philippe Jannes, Paul Matthews, David Soubeyrand, and Juan-Carlos Ustariz, 2003, “Defining of a 3D Integrated Geological Model in a complex and Extensive Heavy Oil Field, of iciana formation, Faja de Orinoco, Venezuela”. AAPG,.

[42] Deutsch C. V, 1999, “Reservoir modelling with publicity available software: Computer and geosciences”, P, 355 - 363.

[43] Oriol Falivene, Pau Arbués, Andy Gardiner, Gillian Pickup, Josep Anton Muñoz and Lluís Cabrera, 2006, “Best practice stochastic facies modelling

from channel-fill turbidities sandstone analogue (the quarry outcrop, Eocene Ainsa basin, northeast Spain)". AAPG, p 1003 - 1029.

[44] M. H Hissein, W. I. Wan Yusoff and Siti N. M. N, " Stochastic Lithofacies Modelling of Cretaceous Braided Delta Reservoir using Wells and Core Data", Second International Conference on Integrated Petroleum Engineering and Geosciences (ICIPEG2012), June 12 - 14, 2012, Kuala Lumpur, Malaysia.

[45] Doligez, B. 2008, "Reservoir Characterization and Modelling". UTP and IFP, P, 26, Academic material.

[46] Haldorsen, H. H., and D. M. Chang, 1986, Notes on stochastic shales - From outcrop to simulation model, in L. W. Lake and H. B. Carroll, Eds., Reservoir characterization: Orlando, Academic Press, p. 445 - 485.

[47] Clementsen, R., A. Hurst, R. Knarud, and H. Amir, 1990, "A computer program for evaluation of fluvial reservoirs, in A. T. Buller, E. Berg, O. Hjemel and, J. Kleppe, O. Torsaeter, and J. O. Aasen, eds., North Sea oil and gas reservoirs II": London, Graham and Trotham, p. 373 - 385.

[48] Tyler, K, A. Henriquez, and T. Svanes, 1994, "Modelling heterogeneities in fluvial domains, a review on the influence on production profile, in J. M. Yarus and R. L. Chambers, Eds. Stochastic modelling and geostatistics" Principles, methods and case studies, AAPG Computer Applications in Geology 3, p. 77-89.

[49] Deutsch, C. V., and L. Wang, 1996, "Hierarchical object-based stochastic modelling of fluvial reservoirs": Mathematical Geology, v. 28, p. 851 - 880.

[50] Deutsch, C. V., and T. T. Tran, 2002, "FLUVISIM: A program for object-based stochastic modelling of fluvial depositional systems": Computers and Geosciences, v. 28, p. 525 - 535.

[51] Caers, J., 2005, "Petroleum Geostatistics": Soc. for Petro. Eng. Richardson, Texas, p 88.

[52] M. H Hissein, W. I. Wan Yusoff, 2012, " 3D Object-based Reservoir Facies Modelling of Cretaceous Braided Delta using Core and Wells log Data", Malaysian Journal of Science (MJS), 2013, Malaysia.

[53] Robert, S. Tye, 2004, "Geomorphology: An Approach to determine subsurface reservoir dimensions Roberts". AAPG, p 1123 – 1147.

[54] Martin R. Gilbling, 2006, "Width and thickness of fluvial channel body and valley fills in the geological record: a literature completion and classification". Journal of Sedimentary Research, p, 731 - 770.

[55] Marc. J. P. Gouw and Henk Berendsen, J. A. 2007, "Variability of Channel-belt Dimension and the consequence for alluvial Architecture": Observation from the Holocene Rhine-Meuse Delta (The Netherlands) and lower Mississippi Valley (U.S.A.)", Journal of Sedimentary Research, p, 124 - 138.

[56] Deutsch, C. V. 2002, "Geostatistical reservoir modelling: Applied Geostatistics Series", Oxford University Press, 376 p.

[57] Schlumberger, "Petrel Facies Modelling" The document available from the internet:

http//:www.slb.com/services/software/geo/petrel/geomodeling/facies_modeling.as.

[58] Journal, A. G., 1983, "Non parametric estimation of spatial distributions": Mathematical Geology, v. 15, p. 445 - 468.

[59] Gomez-Hernandez, J and R. M. Srivastava, 1990, "ISIM 3D: An ANSI-C three-dimensional and multiple indicator conditional simulation programs": Computers and Geosciences, v. 16, p. 355 - 410.

[60] Khaled BENZAOUI and Tom COX,2009, "Integration of Multi Scale Data in Facies Modelling using Neural Network" CSPG CSEG CWLS Convention 801. Schlumberger, Calgary, Alberta, Canada.

APPENDIX A: INPUT DATA

A1 Data Importing Background

The process of preparing a 3D map started from scanning, the contours and faults were digitized, imported and register in Petrel. The position of four corner locations in the world were set by fitting the x, y and z coordinates. X and Y in each corner were calculated and displayed in the exact place over the world coordinates as well as registered in the 2D window.

A2 Importing Map

The map was imported properly after scanning and using import on selection as following steps: Create folder, right click on the folder and select import on the selection and select Bitmap image format then choose the file and click open as in Figure A1.

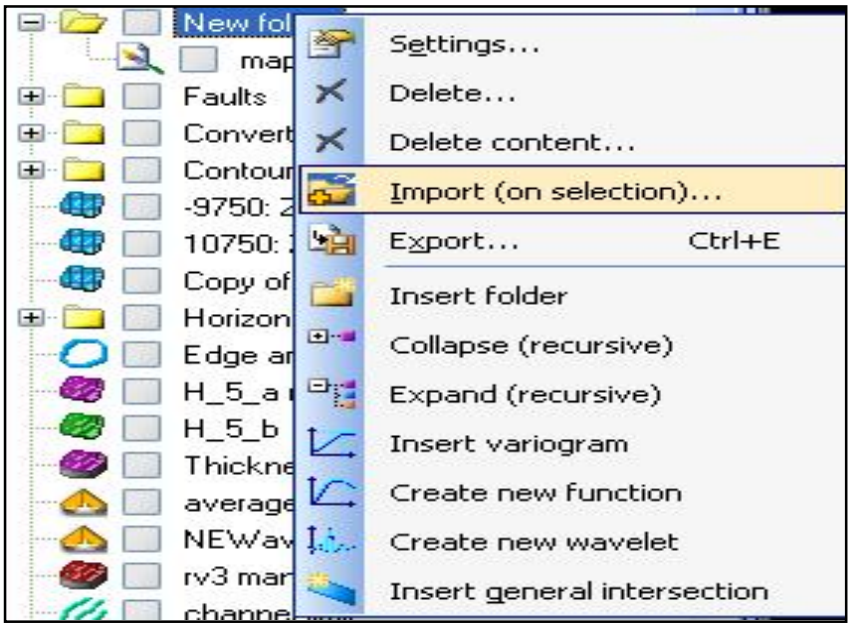

Figure A1: Window tab first step of Importing map image.

A3 Assign Coordinate

Coordinates were inserted into the image by double clicking on import file, selected setting tab and checked the box in world location as well as the coordinates XY min and max for the four corners, and Z value as shown in Figure A2.

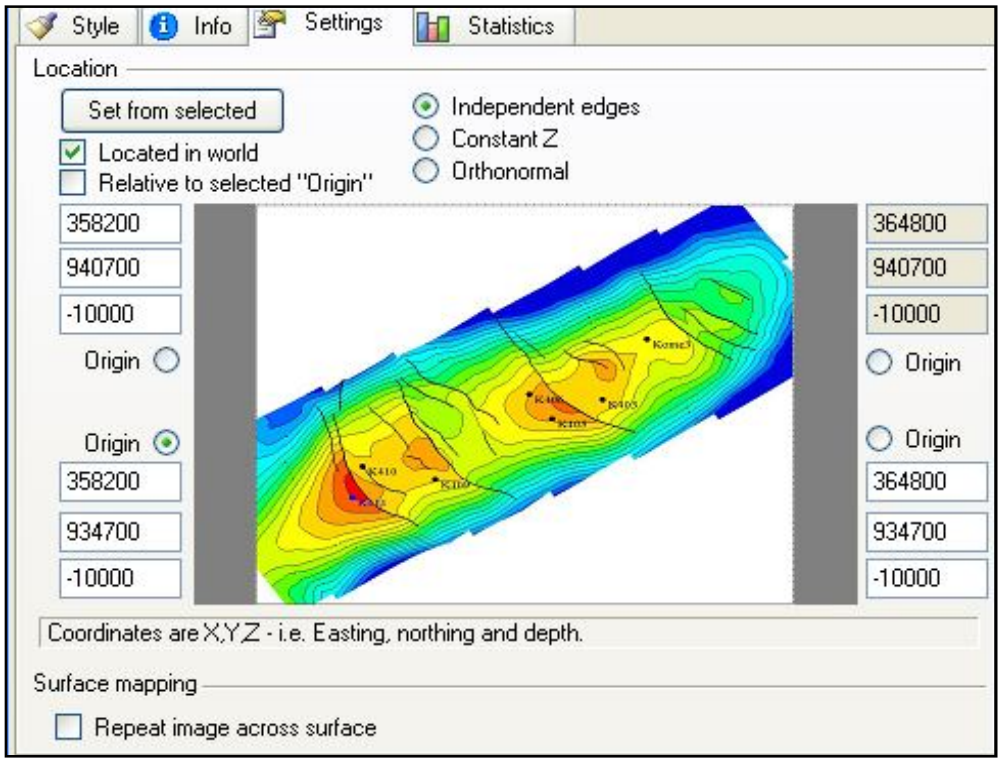

Figure A2: Assigning X, Y in the world located, and Z in Petrel.

From the earliest the map inserted on depth of 3352.8 meters and later moved to proper depth, then by clicked apply and Ok to complete the process as show in Figure A3.

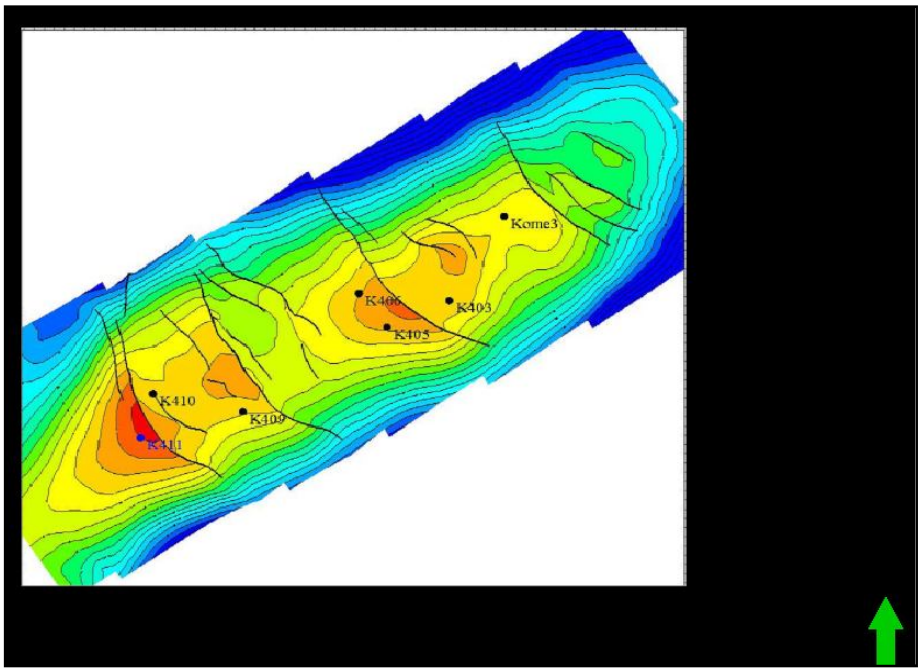

FigureA3: Final displayed on the maps on the 2D window ready to start digitizing.

A4. Contours and Faults Digitizing

Contours and faults were digitized properly and converted as polygons and line respectively in Petrel by using the following steps:

- Click open to display a 2D window and display objects to conduct digitizing
- Tick Make/edit polygon process and click up Z value icon on the right side.
- Start digitizing the contours by clicking the start new set of polygon icon, then Click on the points and keep them in wide spaced, close the polygon by stop digitizing, and clicking on the close selected polygons icon and insert the Z value of each contour and click apply. Figure A4, Figure A5 and Figure A6 are shown the process of digitizing contours, in case of faults it is needed for selected convert the system into polygon.

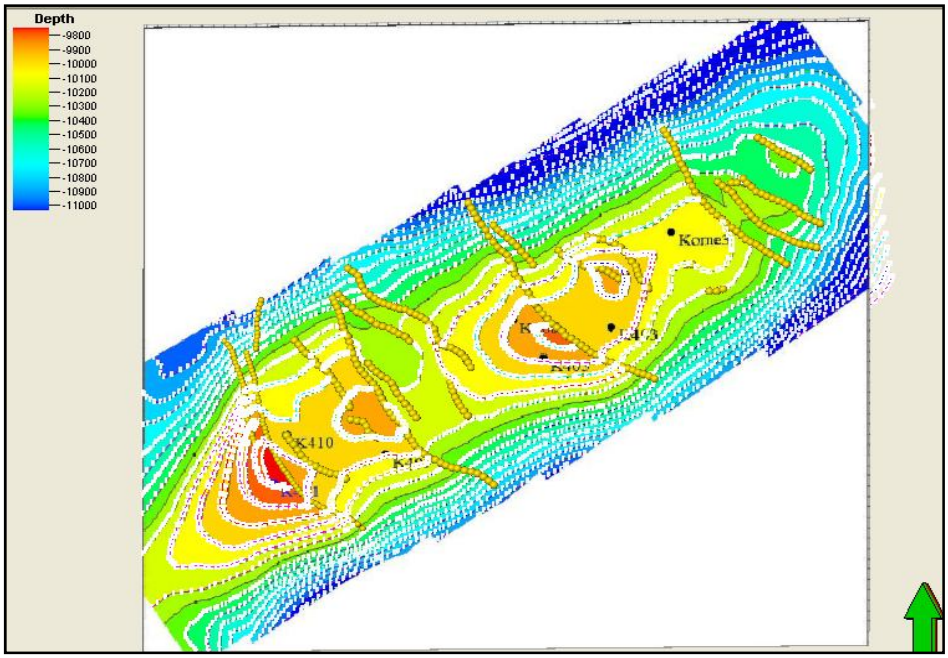

Figure: A4: Window for contour and faults digitized from the image.

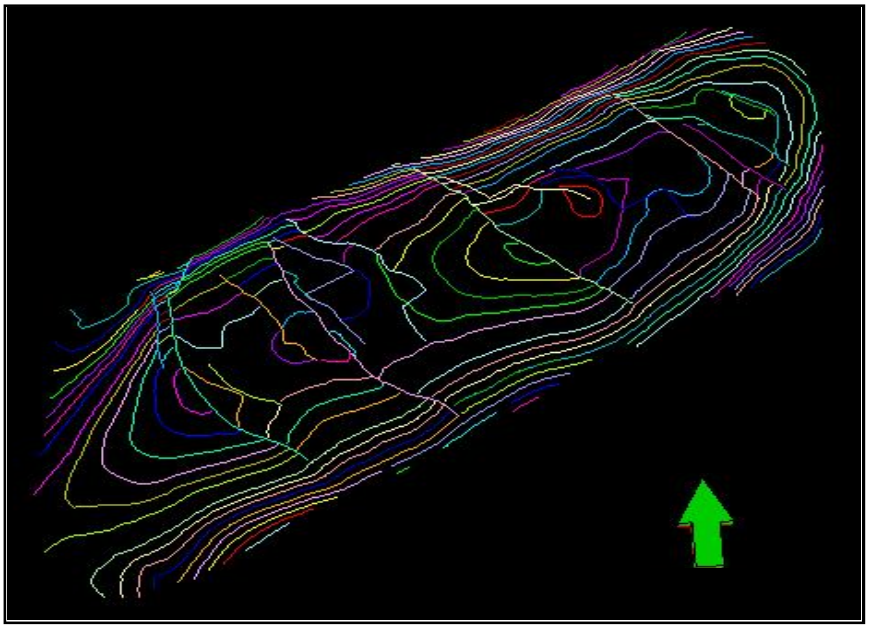

Figure A5: 2D Window with contour and fault converted.

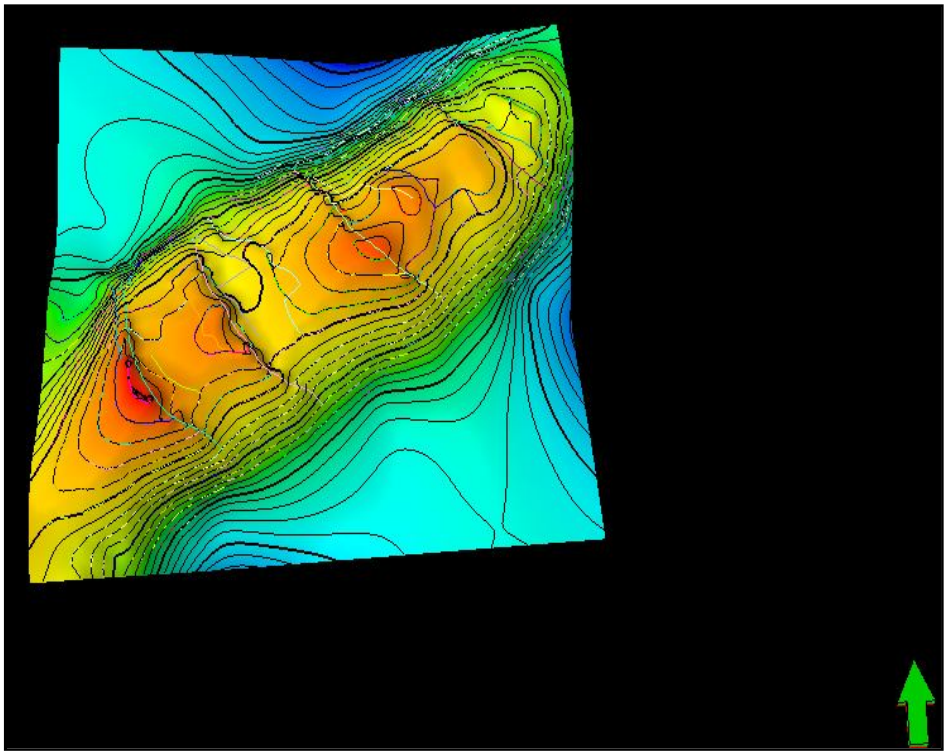

Figure A6: 2D window of surface maps made by digitizing contour/fault data.

A5. Data Importing

The combined wells and depth map data were imported to the Petrel Version.2008 for modeling purposes as illustrated in Table A1.

Table A.1: Different data, type and format used and imported

Data	Format	Type
I. Well Data		
-Well Headers	Well heads *. *	Well
-Well Deviations	Well Path deviation ASCII *. *	Well
-Well Logs	Well Log LAS 3.0 *. Las	Well
II. Well Tops	ASCII *. * Well Tops	Well top
III. Depth map Data	Horizon Pick ASCII *. * Lines	Surface
-Fault	Digitized	Polygon
- Contour	Digitized	Lines

The well logs data and depth map of the top H_2_a interval have been digitized and imported to the Petrel through Z-Map ASCII format. The fault polygons associated with these surfaces were also imported as line data. Sets of well point data in X, Y and Z. Well name for all top reservoir layers were imported using points format, data from six well were imported(Well Heads, Well Name and X Y as well as KB) and well trajectories (Measured Depth, Inclination and Azimuth) in ASCII file the trajectories were automatically calculated in Petrel. The well trajectories were checked against the well point data followed by the associated log data in LAS format many log curves were imported as well log data, but only some of them were used in this modeling process. Table A2.

Table A2: Well data imported in petrel and used for this study

Well Deviation	Well Coordinate	Well Top	Well Logs Curves
MD	Well Name	Well	GR
Deviation	X	UWI	CALI
Azimuth	Y	Surface	RESD
-	KB	MD	RESS
-	-	TVDSS	ROHB
-	-	-	NPHI

However, the data from GR, CALIP, NPHI, RHOB, MD, TVDSS and RE curves were used for liability well cross sections, well log correlations and facies log that will be blocked later for the modeling purpose.

A5.1 Well Data

The Well data consist of three main categories of data type: Well Headers, Well Deviations, and Well Logs.

A5.11. Well Headers

Well headers were created by using a text editor the Notepad and inserted into the project by the following steps:

- Click the Insert menu and choose New Well Folder.
    - Choose New Well Folder, a new Wells folder will be added and appear in the Project as in Figure A7

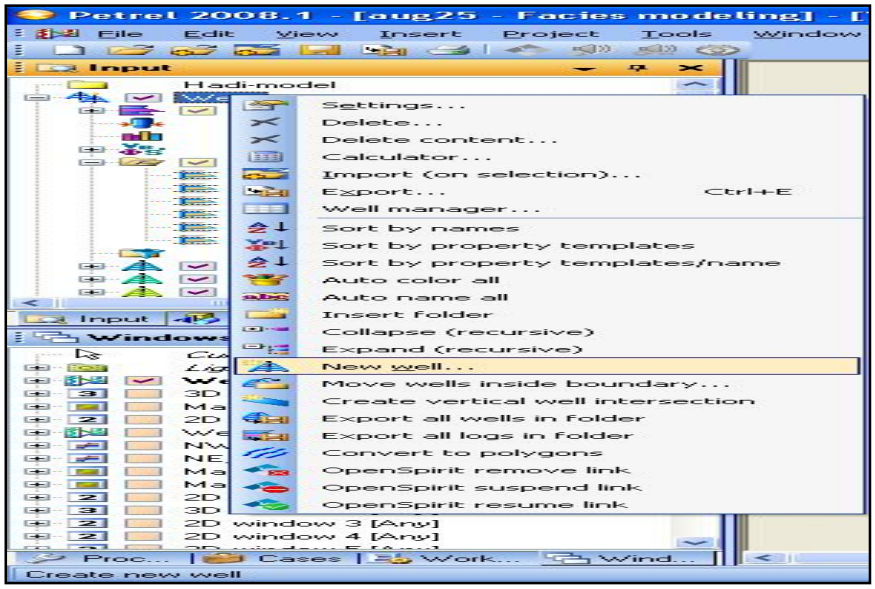

Figure A7: Window tab of creation new well.

The data consist of Well Name, X and Y coordinate and Kelly Bushing as well as Top and Bottom Depth in addition to Symbol of each well, as shown in Figure A8

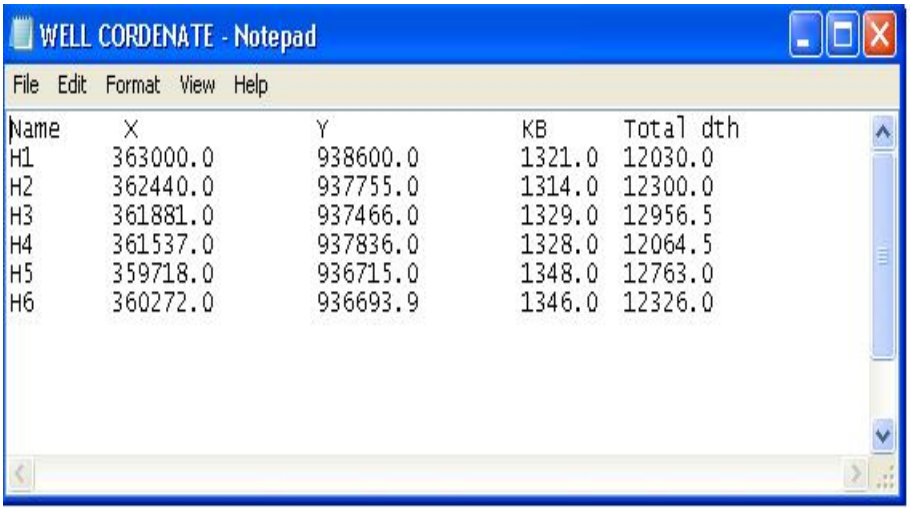

Figure A8: Well headers data file open in a notepad.

- Right click on this item and select import on selection. The import file form appears as in Figure A9.

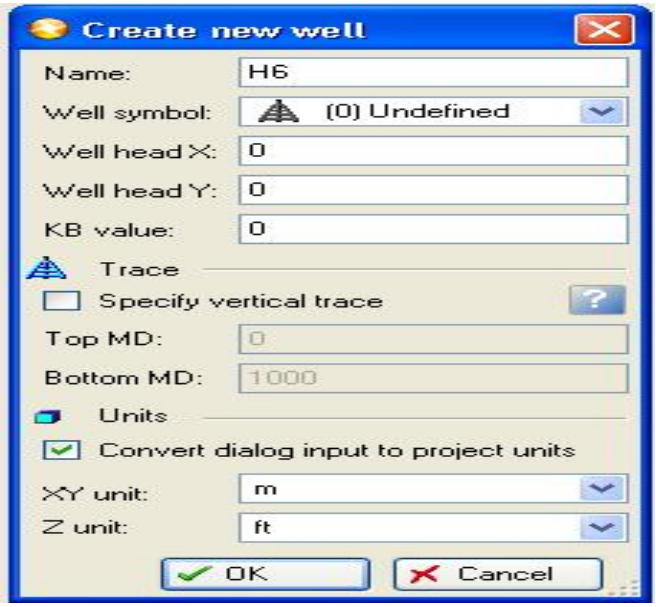

Figure A9: New well creation tab of well headers

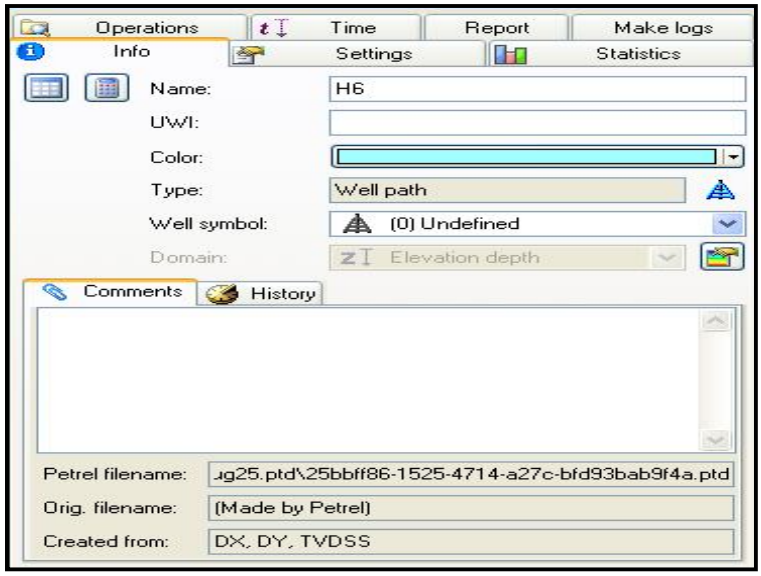

Figure A10: Setting tab of import well headers info.

- Press Ok, the wells will already add to the Wells folder.

The Well Name column contains names of the wells; X and Y coordinate. KB is referring to the elevation of the Kelly bushing at this well, the top and bottom depth

refers to the depth of the top and bottom zones in the well. The symbol refers to the type of well, which is set to any number and later changed in Petrel to the proper well type. The units of x-y and z were converted into the meter, after inserting well headers into the project and later edited in Petrel.

A5.1.2 Well Deviations

Well Paths can be read in Petrel within a specific format. A deviated well is traced along its path for each point MD, X & Y and Z as well as TVD in addition to DX, DY, AZIM, INCL and DLS data is required. The MD represents the positive value of the measured depth for each point. X and Y values are the coordinates of each point and Z refers to the negative value of the depth of each point. TVD is the true vertical depth of each point. DX is the difference between the X value of the points and the well's X coordinates. DY is the difference between Y value of the points and the well's Y coordinates, but in this case MD, Deviation, and Azimuth are used as they are available in all the wells.

The well deviations were inserted into the project by the following steps:

- Click right on wells folder and choose import on selection, the import file form will appear as per figure A11.

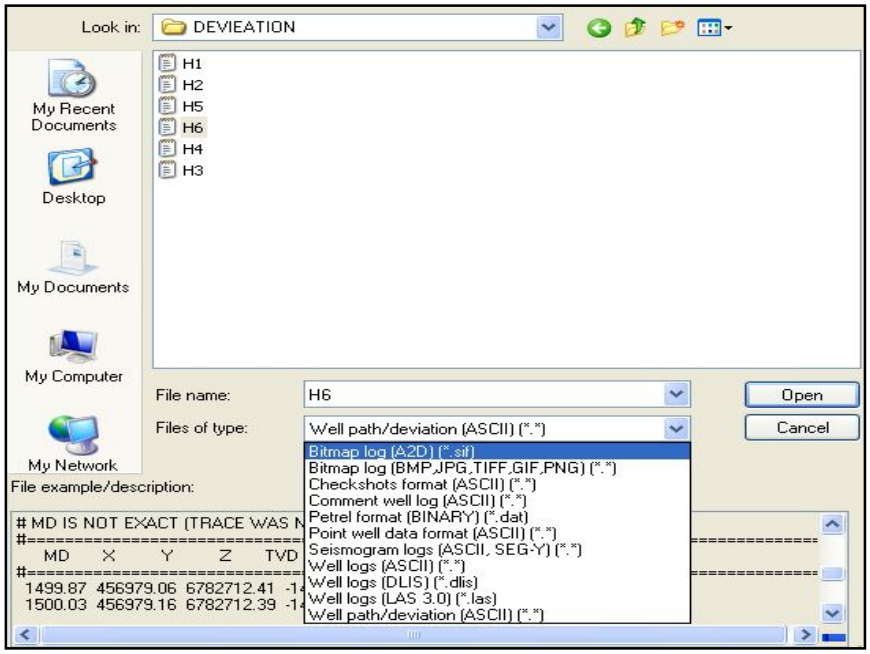

Figure A11: Well path deviation appropriate file type and format selected.

- Chose Well deviation from files type and type *.dev In the file name

- Click Open to see deviated wells listed as per Figure A12.

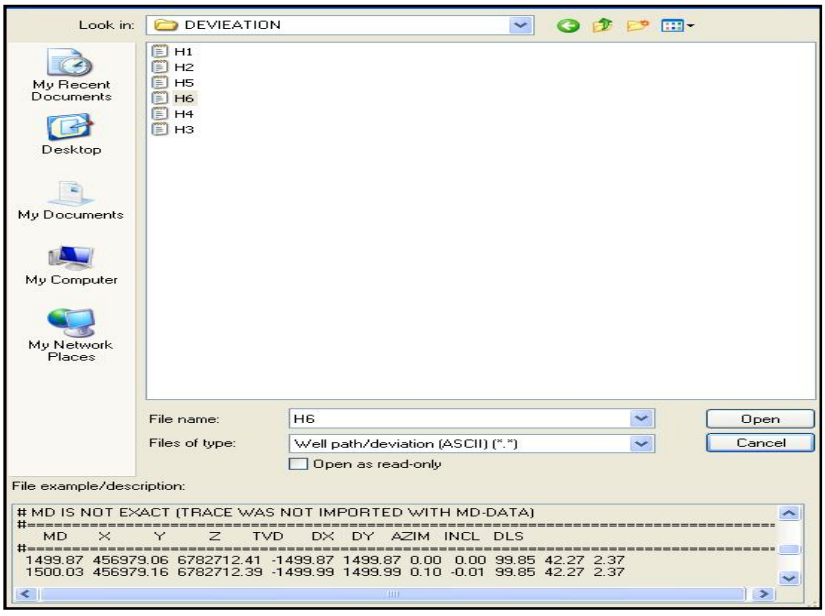

Figure A12: Tab format and file type of wells inputted.

In the file example we can see and verify the data type (MD, XY, Z, TVD, etc.).The filename and Well window will appear as per Figure. A14

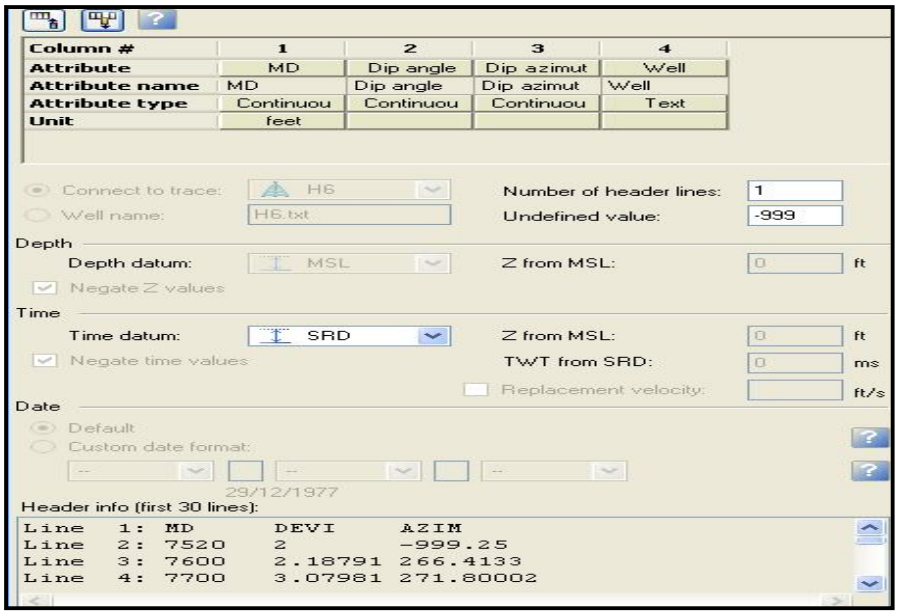

Figure A14: Tab imported point data for well header.

The file name and well trace names were matched together,

- Select correct well name in the well trace column from the box and press Ok.
- Click the Input data tab and select the MD, INCL, TVD and giving them numbers from 1, 2, 3 respectively and then select a KB from MD and TVD elevation reference as per figure A15

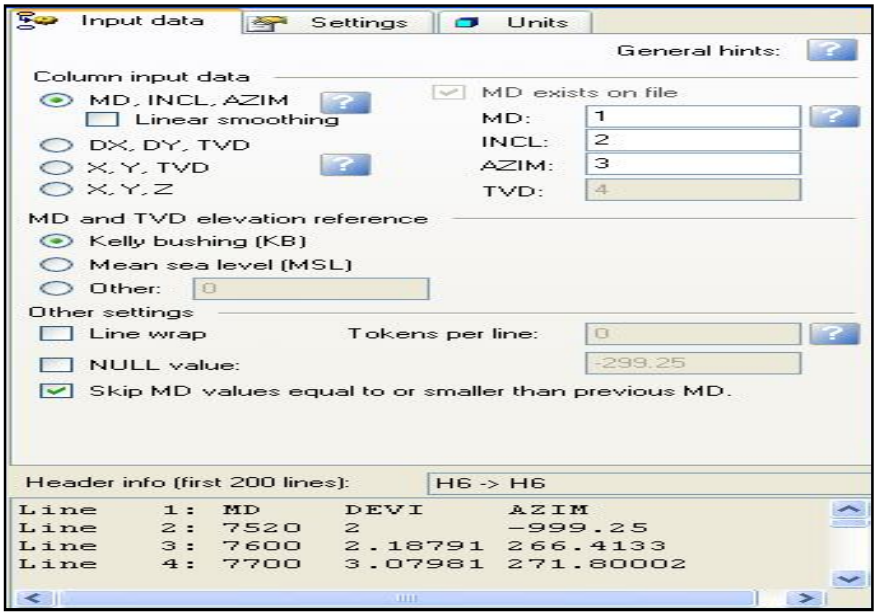

Figure A15: Imported well deviation form.

- Click units and select - specify the unit base on data unit input unit Z in the feet and XY in meter and the project unit are similar, the angle is in degree and the well is from onshore as seen per Figure A 16.

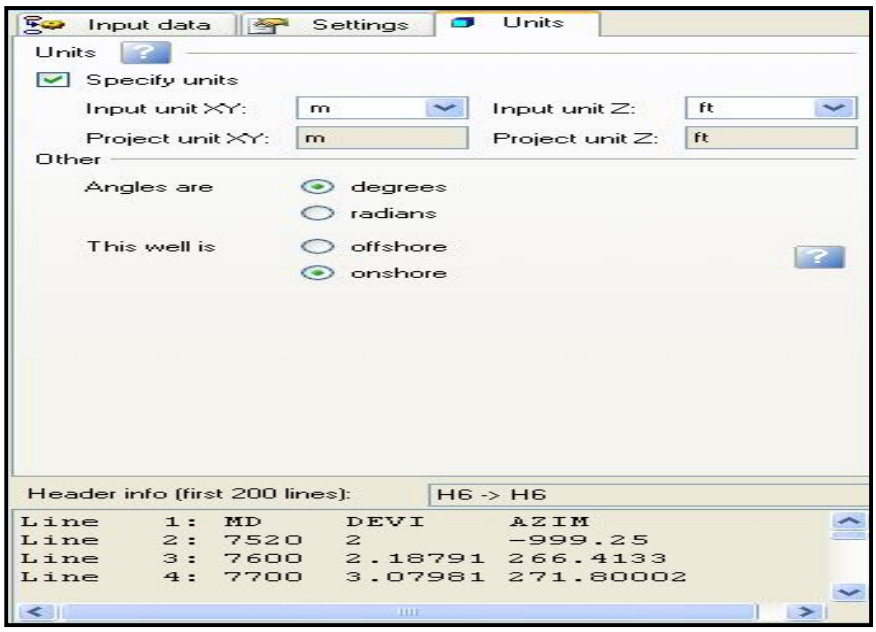

Figure A16: Specify unit data and other of import well deviation.

After that by pressing Ok for all, the wells with their deviations were displayed in the 3D Window as appear in Figure A 17.

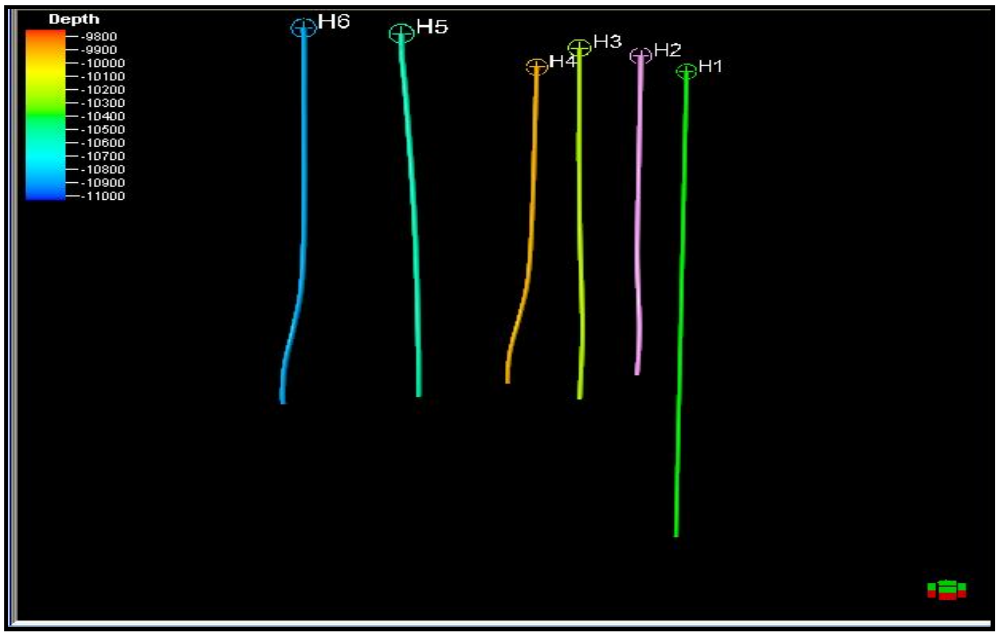

Figure A17: Wells deviations are displayed in the 3D window looking from the south.

A5.2 Well Logs

The imported well logs data in Petrel were read in a LAS format 2.0 and are supported in this case by a LAS 3.0 format. The log data were inserted into the project by the following steps:

1- Right-clicking on the Wells folder and select Import on selection as shown in Figure A 18.

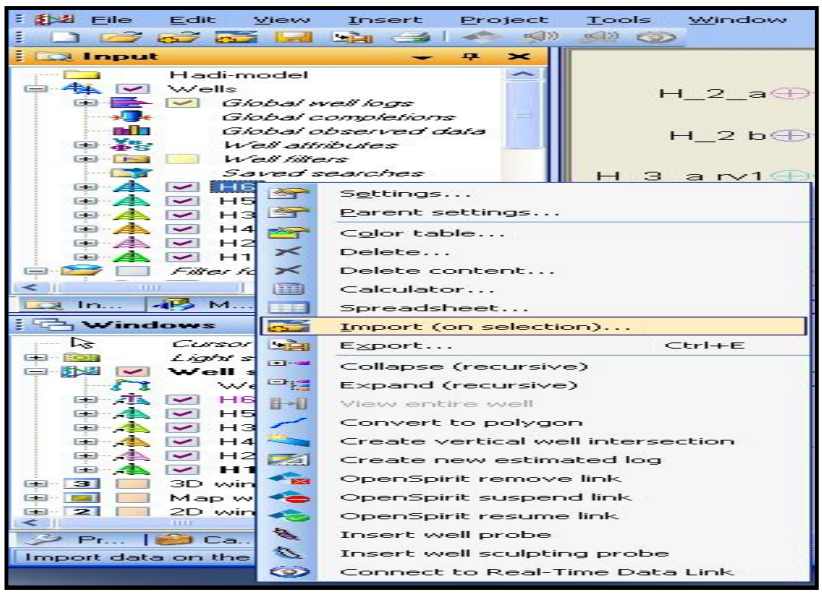

Figure A18: Tab of importing well logs.

1- Select Well logs LAS 3.0 from the files of type in the file name on box type Figure A19 and Figure A20.

2- Select well logs LAS 3.0 *. Las from the files of type in the file name as shown in Figure 20 and Figure 21.

3-

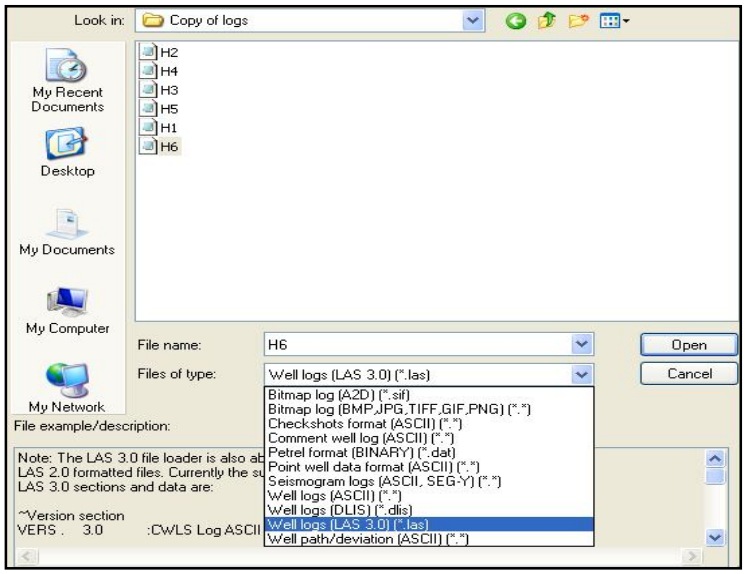

Figure A19: Tab well logs format file type.

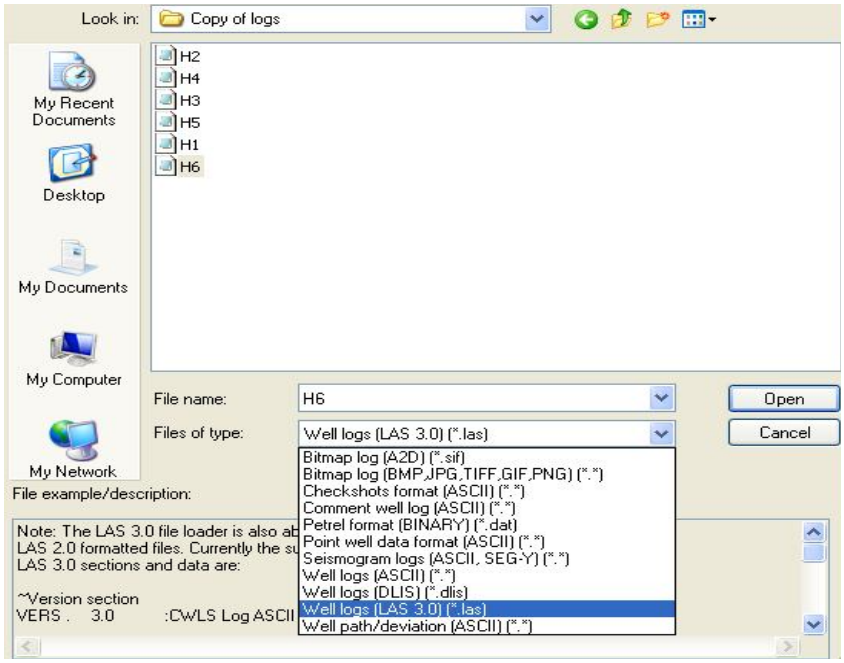

Figure A20: Tab shows well logs format file type.

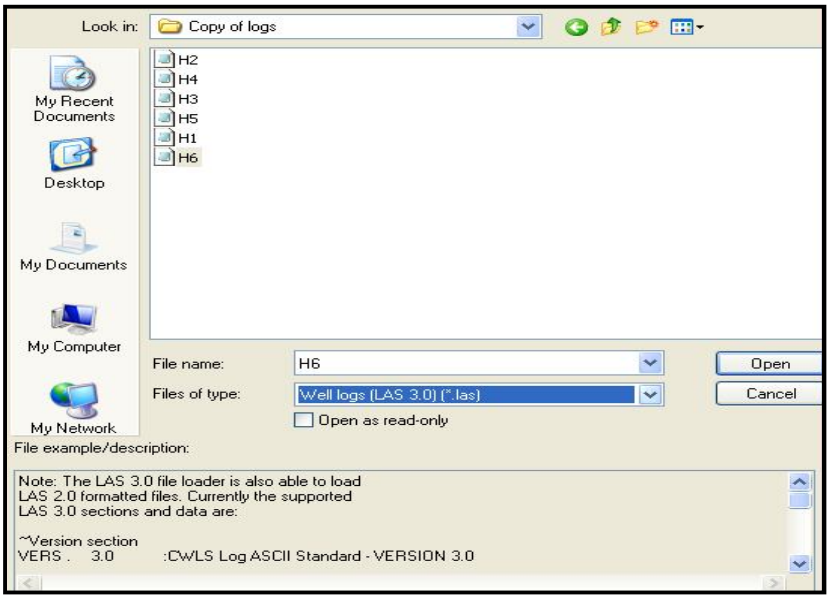

Figure A21: Tab well logs file type LAS format selected.

Select all files then press open, the file and well window will appear as in Figure A22.

File	File name	Well trace
1	H2	H2 ()
2	H4	H4 ()
3	H3	H3 ()
4	H5	H5 ()
5	H1	H1 ()
6	H6	H6 ()

Figure A22: Window of match filename and well trade names.

Subsequent to that match file name and Well Trace names together. If it is a wrong match, select the correct well name in the well trace column from the box and click OK.

4- Press open window of Las input data it will open, and then from the general well logs item select the logs to be displayed for all wells as seen in Figure A 23.

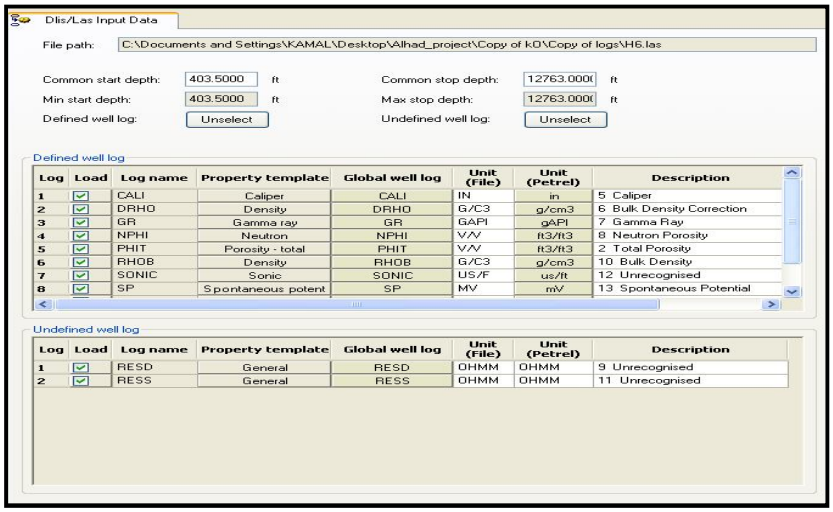

Figure A 23: Total number of logs items imported into the petrel

The steps make the logs attached to the well deviation similar to the attachment of the wells path and the wells header as in Figure A 24.

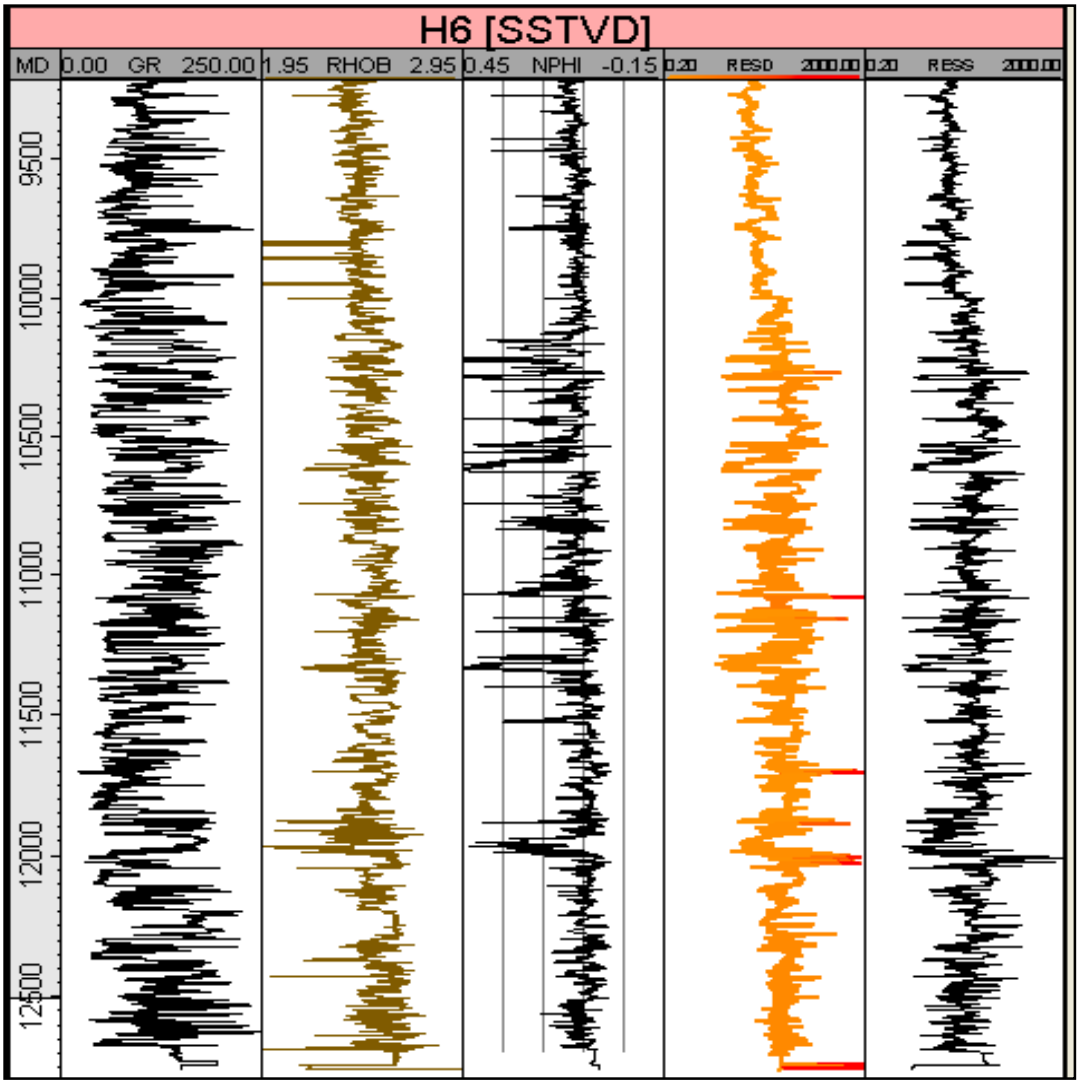

Figure A24: Well H6 logs data displayed in 1D window. The image shows 5 columns from left to right Gama ray, density, neutron porosity, and resistivity.

A5.3 Well Tops

A well tops data file was created by using a text editor notepad file. The well tops data include horizon name, well name, X, Y, Z, Type, Symbol, measured depth, Pick name, Interpreter, Dip Angle, and Dip Azimuth of each well. The X, Y is the well's coordinates and Z is representing the horizon's depth.

The type refers to the type of the stratigraphic sequence horizon, Zone, and Layer. Horizon name and well name refer to the horizon and well names.

The symbol refers to the type of wells. Measured depth refers to the depth of the horizon, the well tops inserted into the project by clicking the insert from icon. Select new well tops and the new well tops folder will be added as in Figure A25.

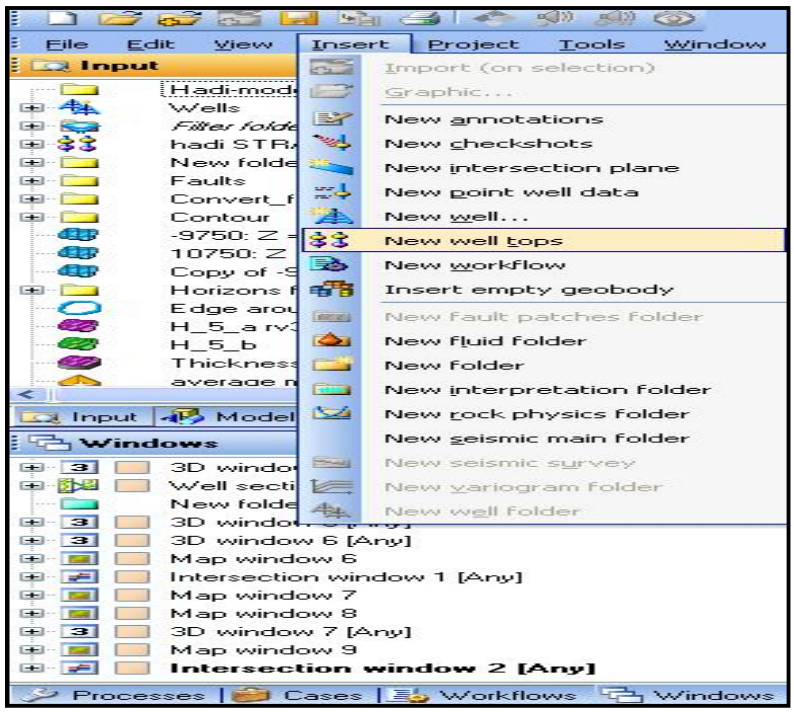

Figure A25: Window tabs, shows the first steps of importing well tops.

- By using the right click on this item and select import on selection, the import file form will appear as in Figure A26.

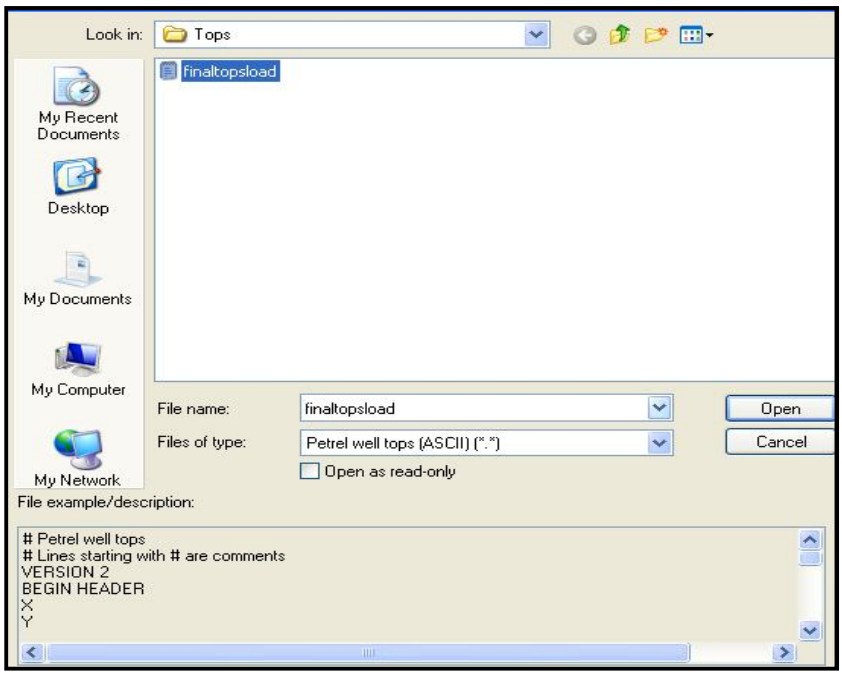

Figure A26: Well tops selection format file type.

- Select Petrel well tops ASCII from the file type tab & specify location and name of the well tops data file and press open, as in Figure A27.

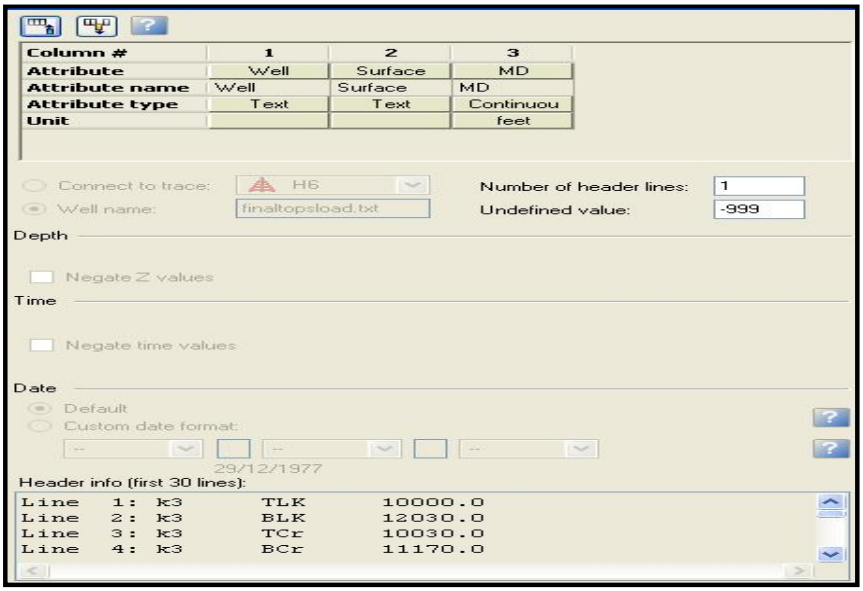

Figure A27: Well tops file ASCII format selected.

- Select the appropriate well tops for each of three columns and number of header line (in this case 1), and so press Ok for all, the logs will appear as in Figure A 28.

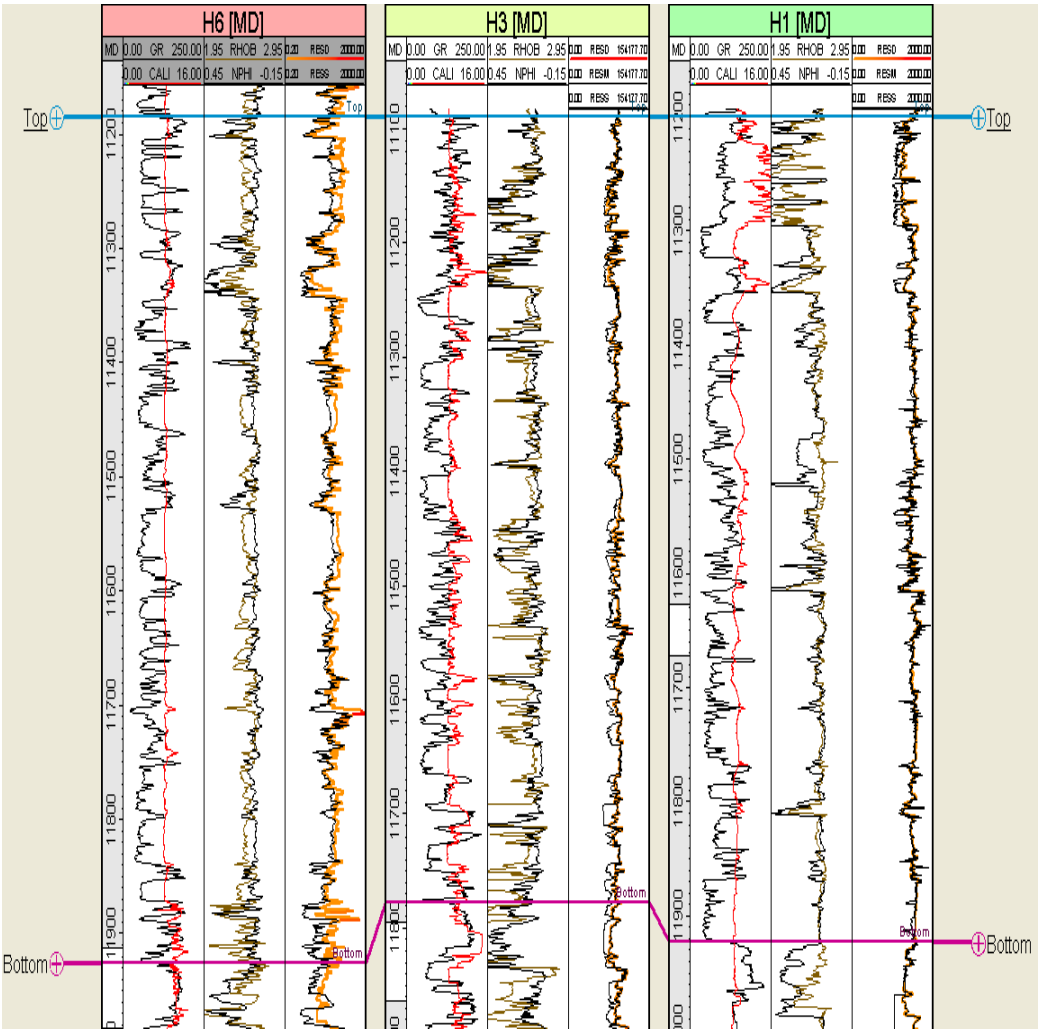

Figure A 28: 1D window tab, show top, and bottom of the 3 wells in Petrel.

A6. Quality Control of Imported Data

Subsequent to the data imported into the Petrel, the quality control was applied by using rapid data verifications in modeling and displayed in the statistical domain to guarantee whether the data are as expected after importing.

The depth map and faults imported to the Petrel clipboard normal and degraded set. The import grid surfaces in the horizon griddling are consistent with the project

boundary. The resultant maps were compared to the originals and quality checked through 3D visualization techniques and cross sections. The well picks for the top of each reservoir and non reservoir zones were imported into the horizons directory and placed in the appropriate depth locations for the wells. This process automatically enters the well tops data into the Petrel well intersection framework to build the 3D model.

Layer thicknesses of SSTVD data were calculated in the well intersection database to provide thickness data for isochors mapping for the reservoir facies and average thickness from well position was considered as shown in Table A3.

Table A3, showing the reservoir thickness in the wells position.

Wells Nam	H6	H5	H3	H4	H2	H1
Thickness	63.4	62	*63*	50	40	30

APPENDIX B, SETTING OF FACIES PARAMETER PANE

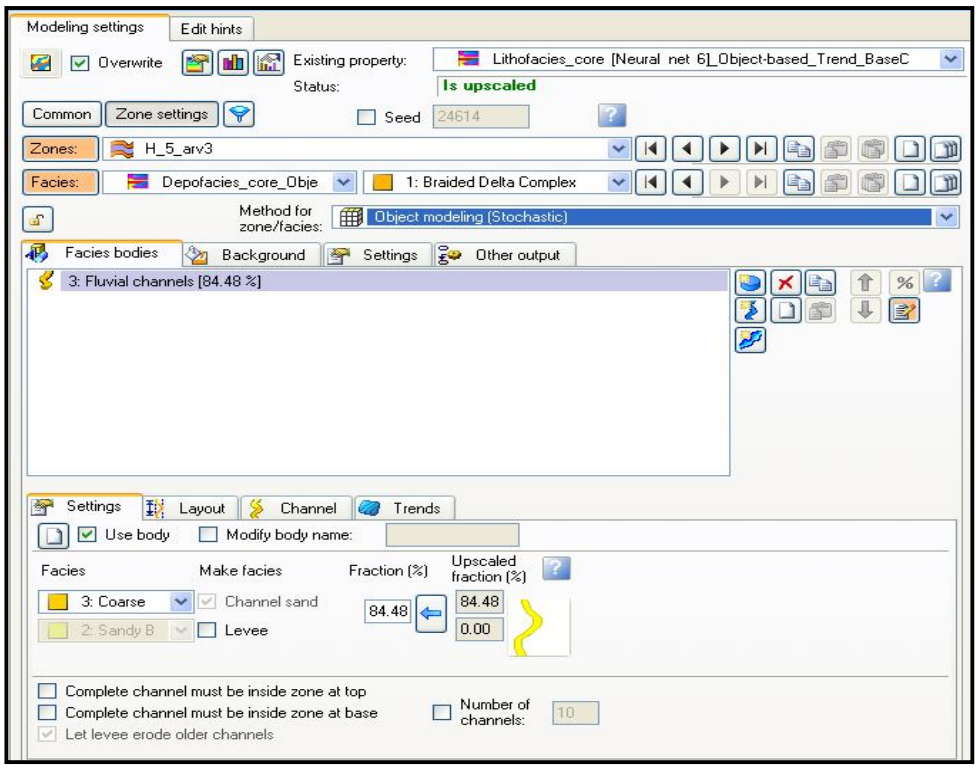

Figure B1: Object-based setting reservoir facies parameters set for coarse sandy bar.

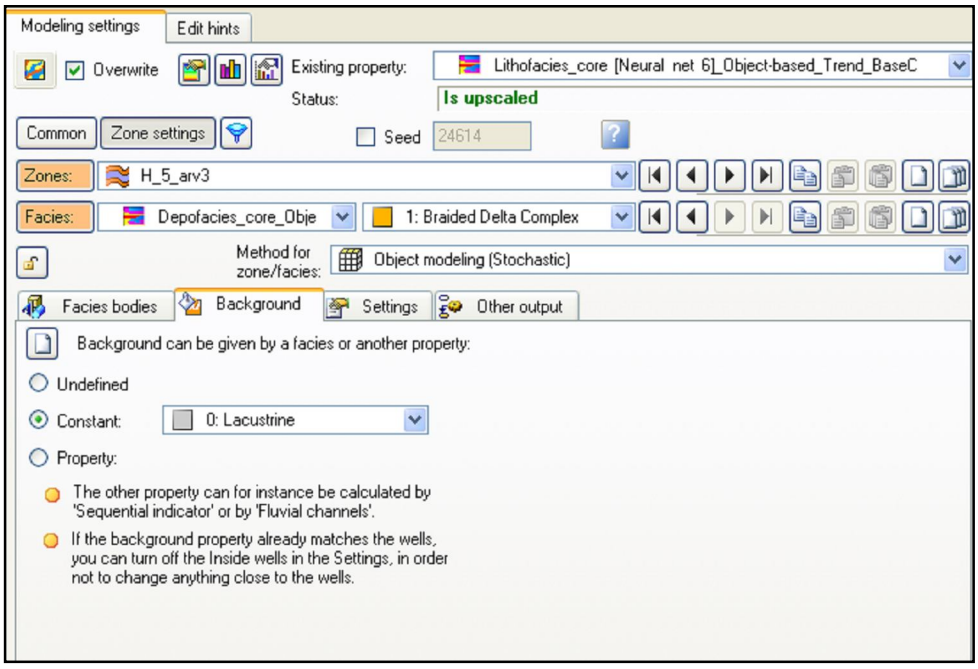

Figure B2: Object-based facies parameters set for reservoir zone lacustrine.

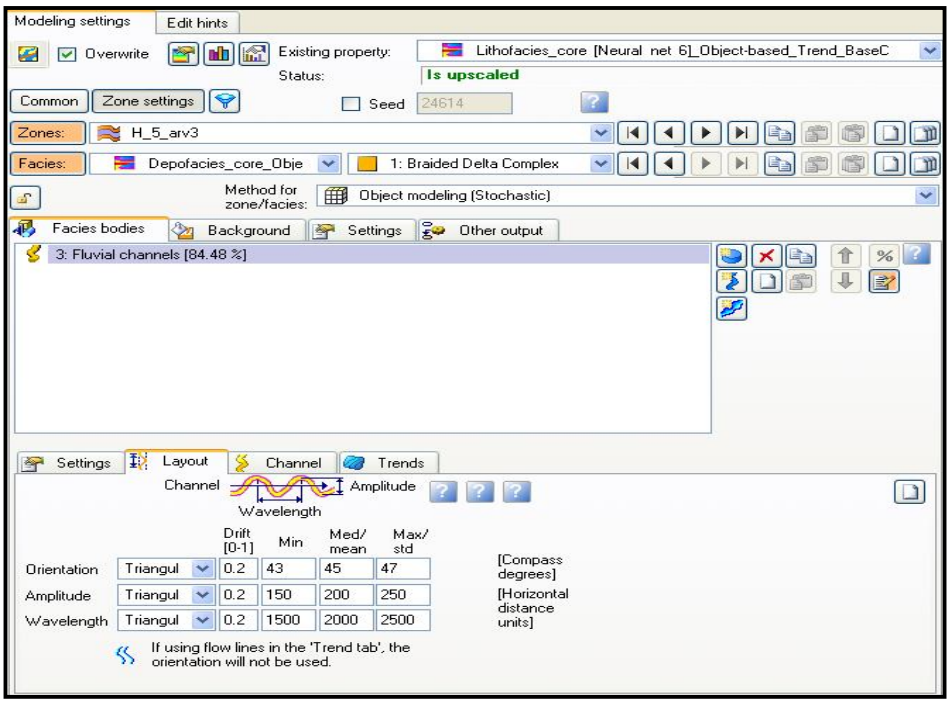

Figure B3: Object-based setting facies parameters set for reservoir zone braided delta channel.

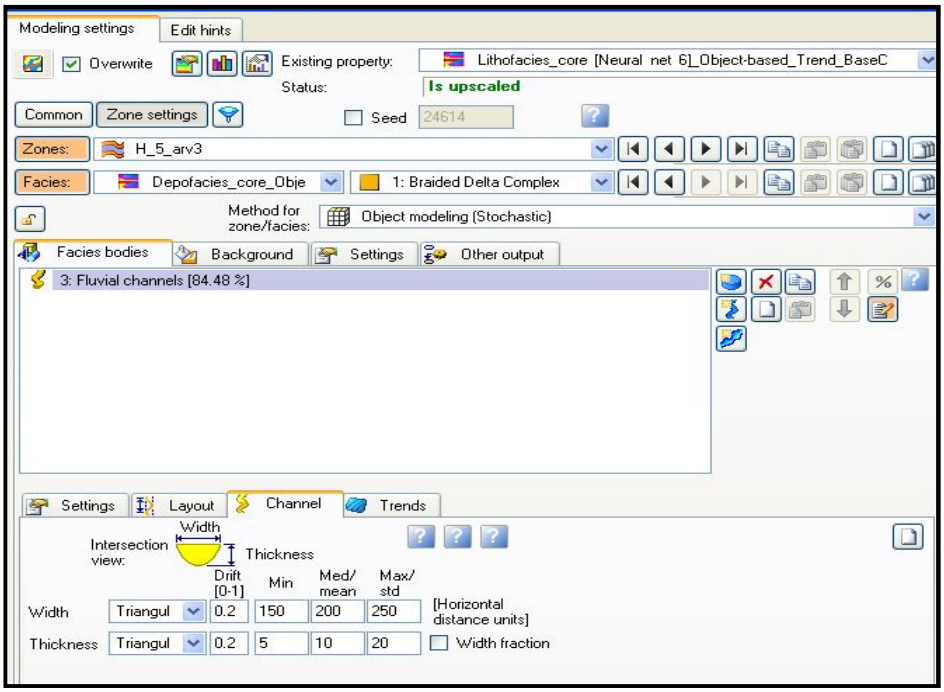

Figure B4: Object-based facies parameters set for reservoir zone fluvial channel.

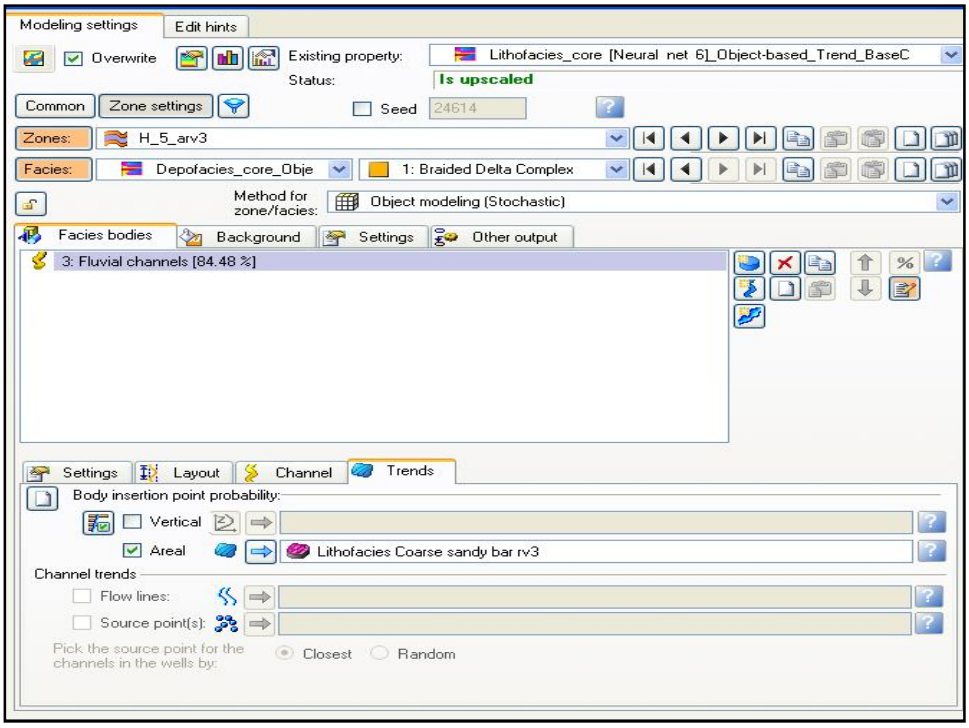

Figure B5: Object-based facies parameters set for reservoir zone channel trained

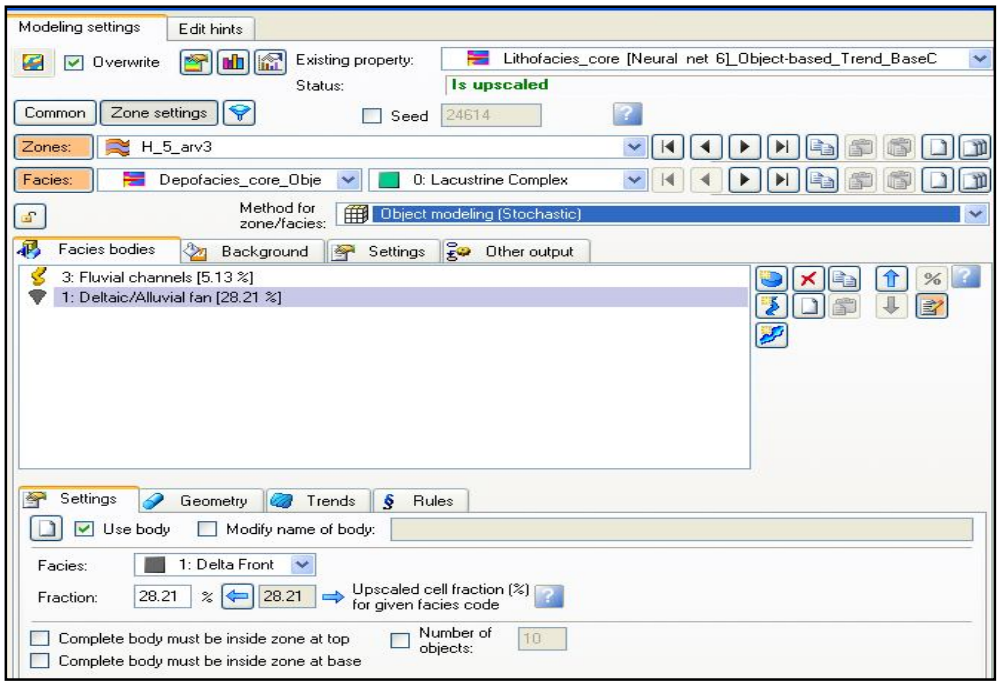

Figure B6: Object-based facies parameters set for reservoir zone delta front setting.

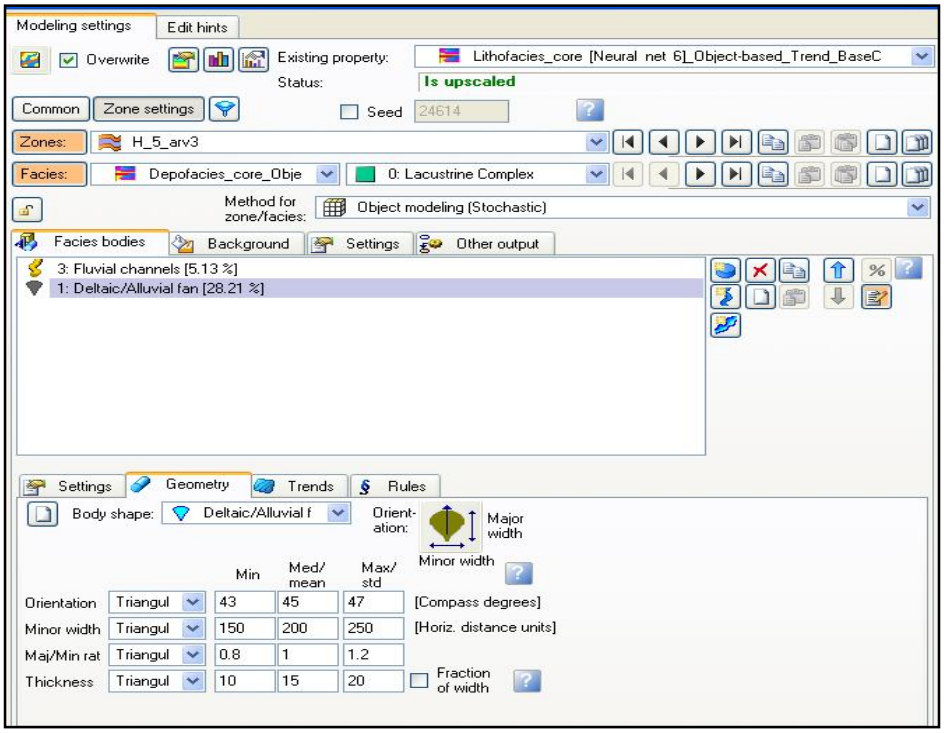

Figure B7: Object-based setting facies parameters set for reservoir zone delta front geometry.

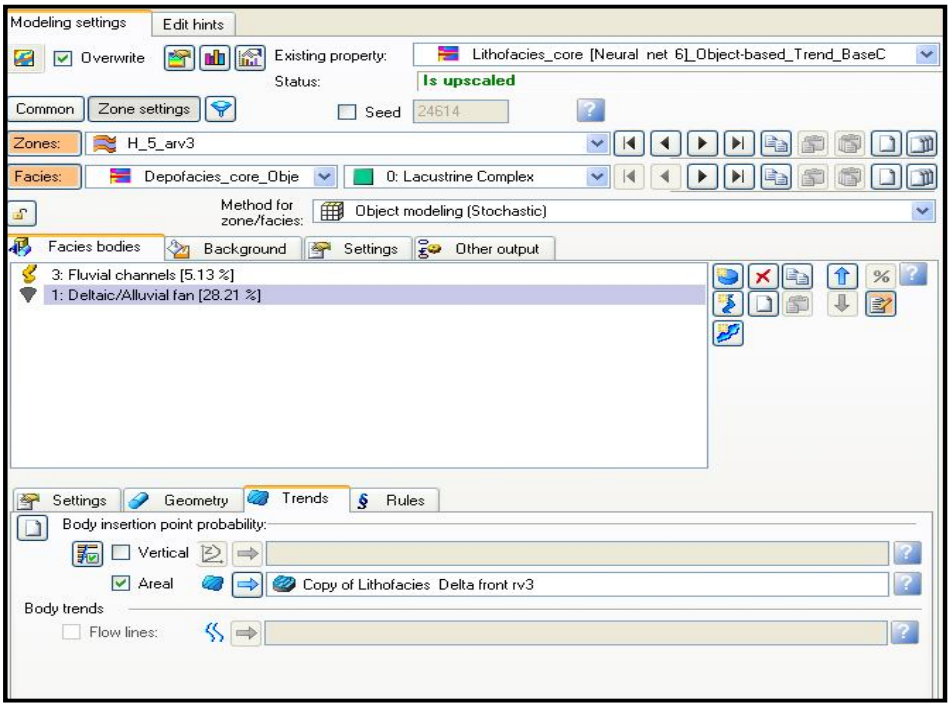

Figure B8: Object-based facies parameters set for reservoir zone delta front trained.

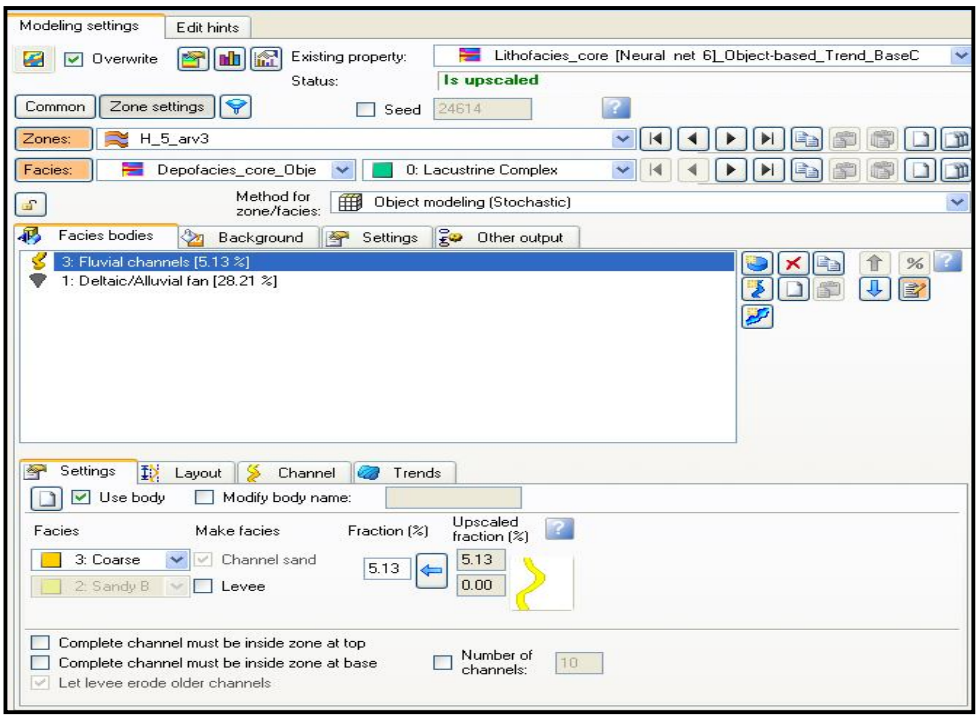

Figure B9: Object-based facies parameters set for reservoir zone lacustrine channel.

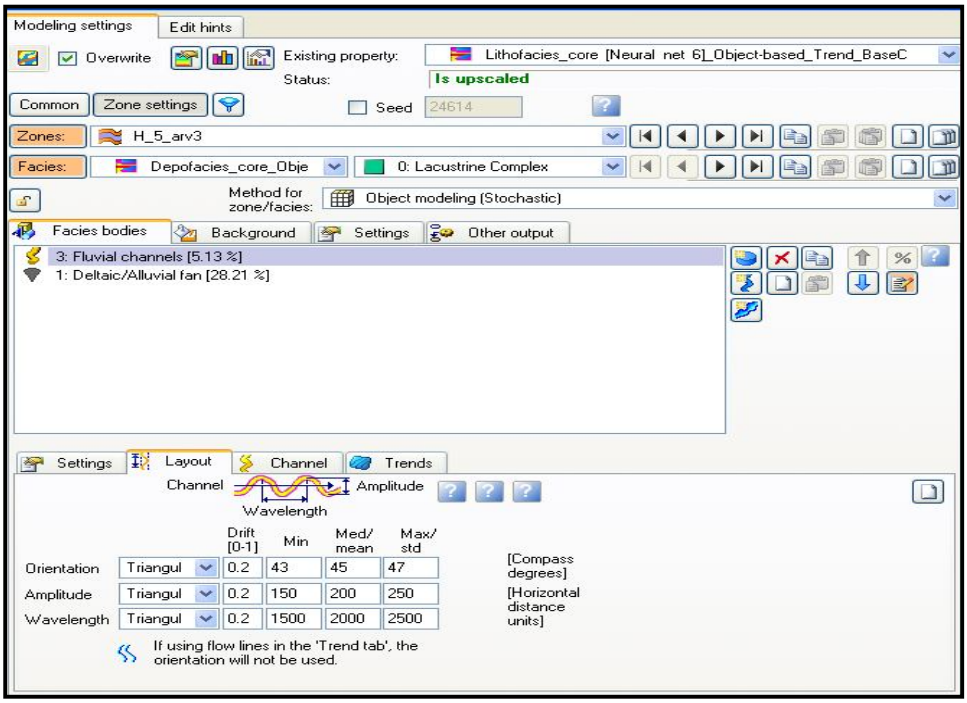

Figure B10: Object-based facies parameters set for reservoir zone lacustrine channel layout.

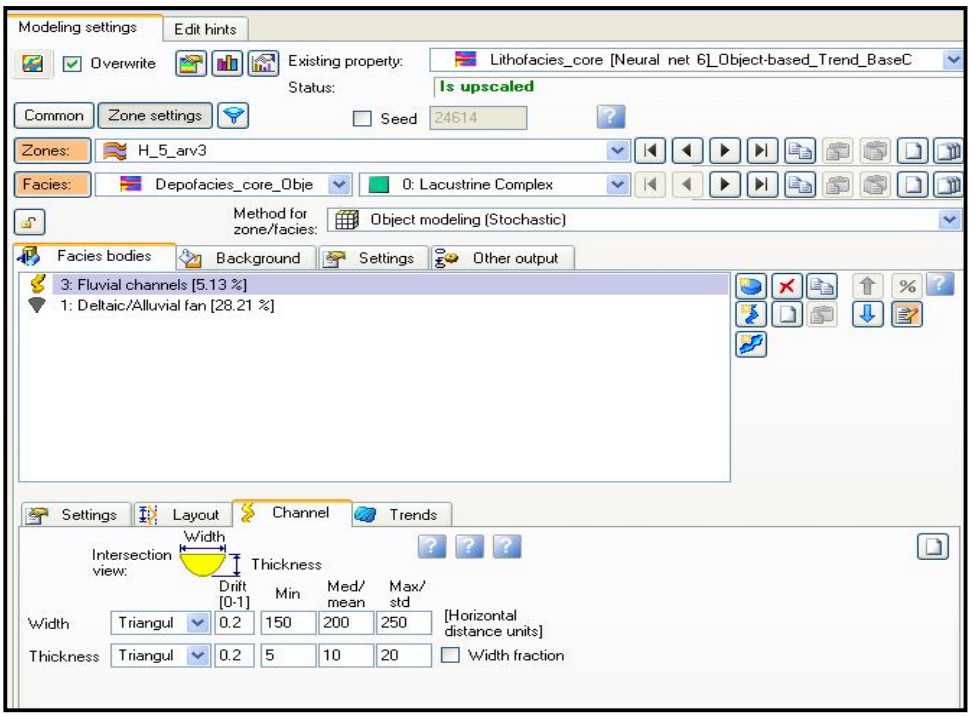

Figure B11: Object-based facies parameters set for reservoir zone lacustrine channel layout.

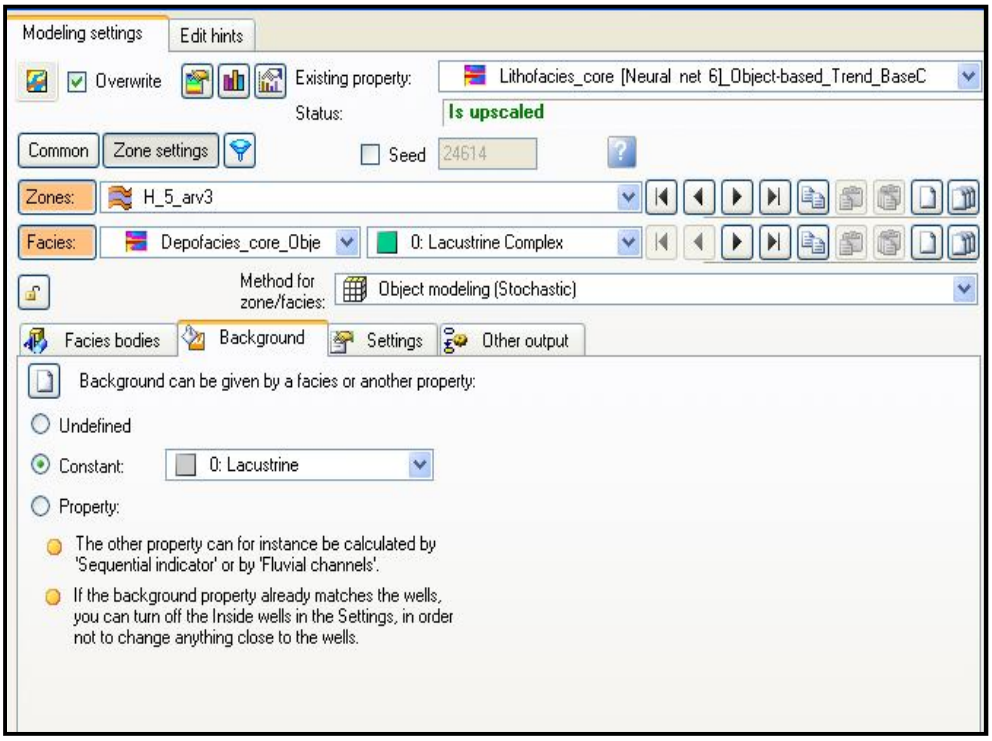

Figure B12: Object-based facies parameters set for reservoir zone lacustrine.

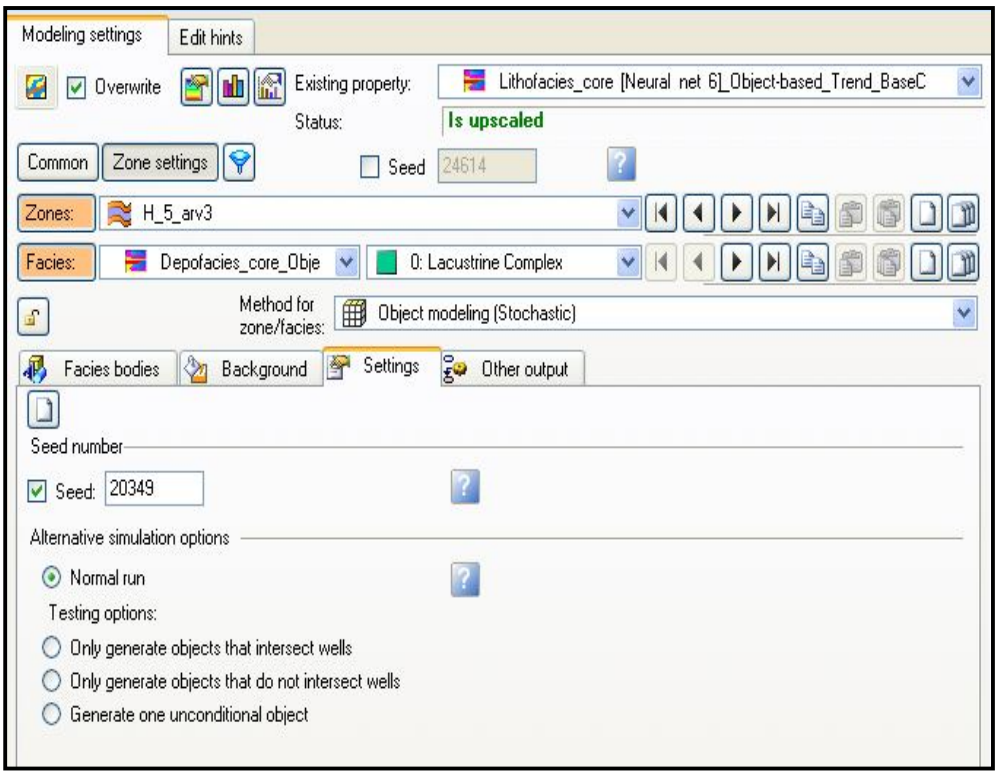

Figure B13: Object-based facies parameters set for reservoir zone lacustrine.

APPENDIX C, SETTING OF RESERVOIR ZONE PANEL

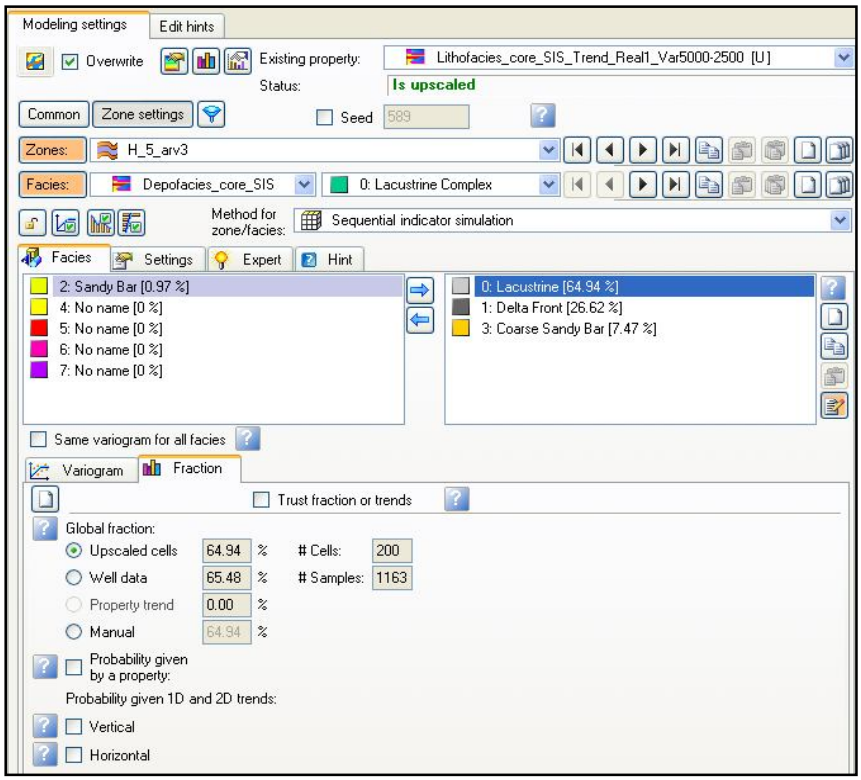

Figure C1: SIS lacustrine deposit facies fraction parameters set for reservoir zone.

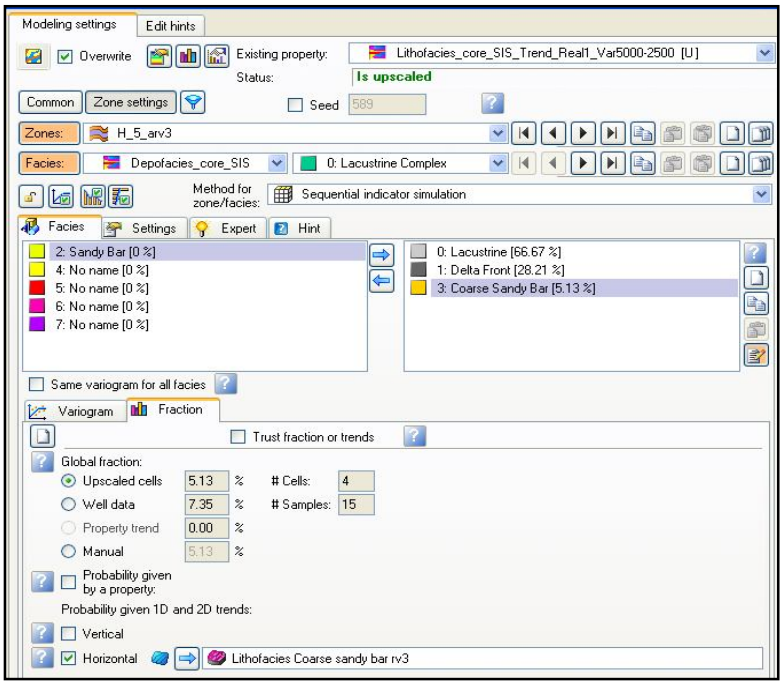

Figure C15: SIS lacustrine deposit, coarse sand facies parameters set for reservoir zone

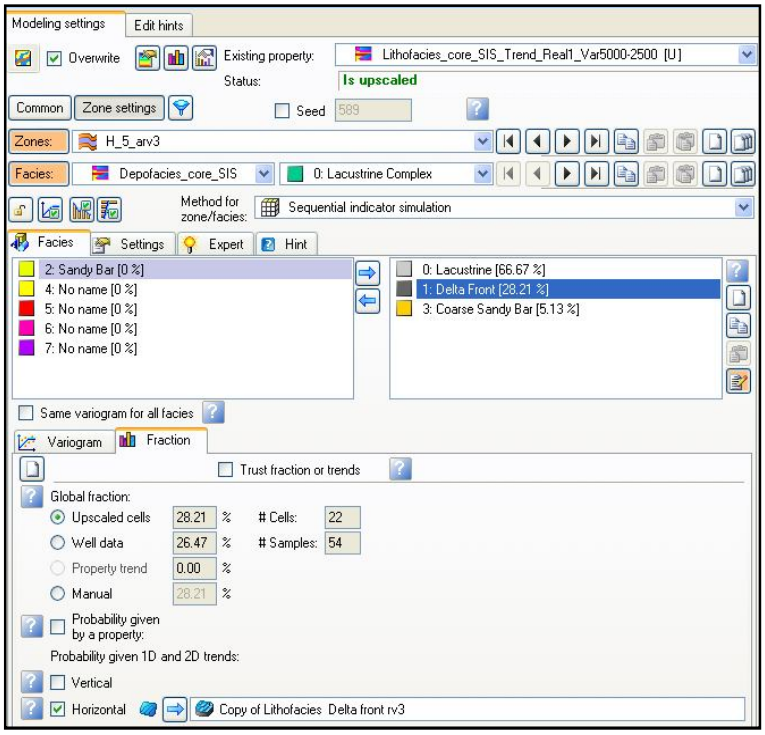

Figure C16: SIS lacustrine deposit, delta facies parameters set for reservoir zone

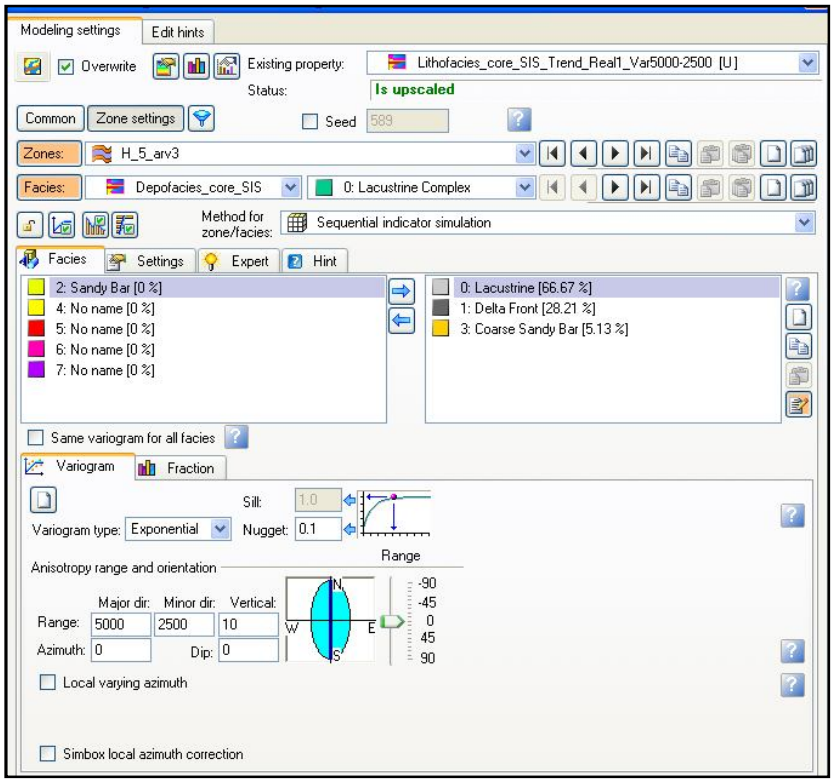

Figure C17: SIS variogram for lacustrine facies parameters set for reservoir zone

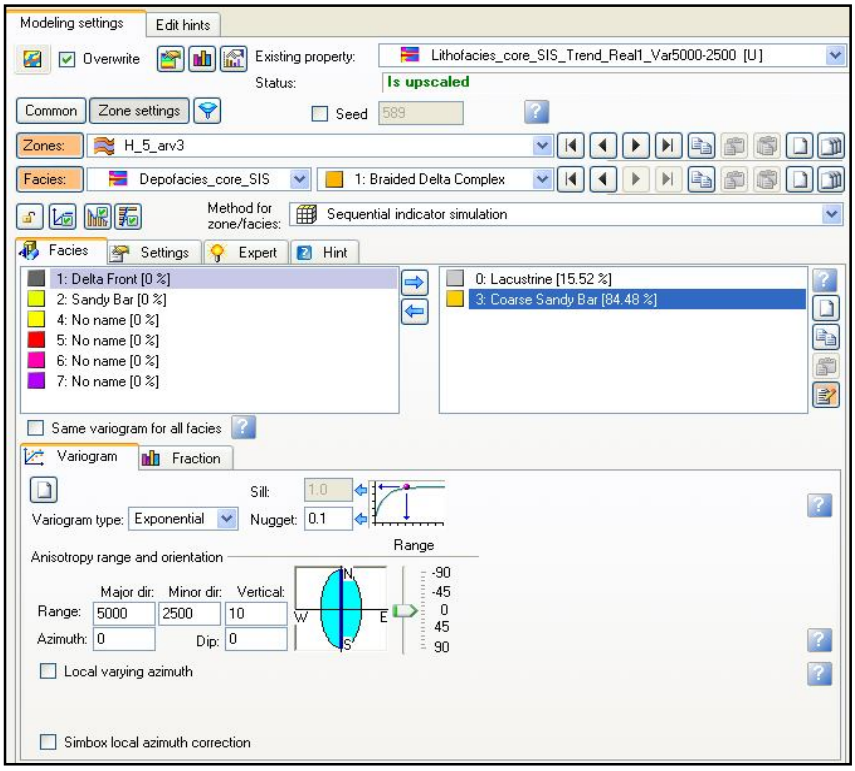

Figure C18: SIS variogram for braided facies parameters set for reservoir zone.

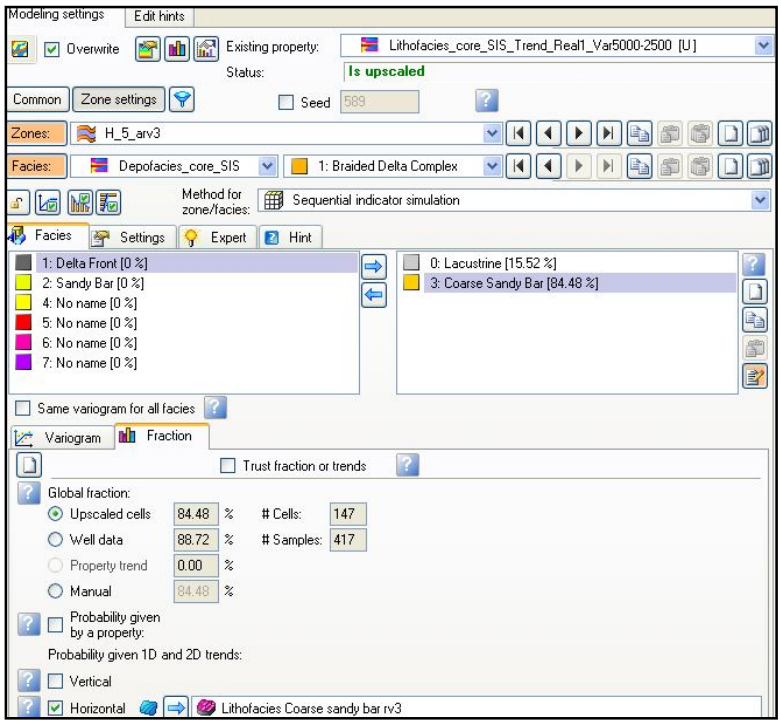

Figure C19: SIS braided deposit coarse sand facies parameters set for reservoir zone.

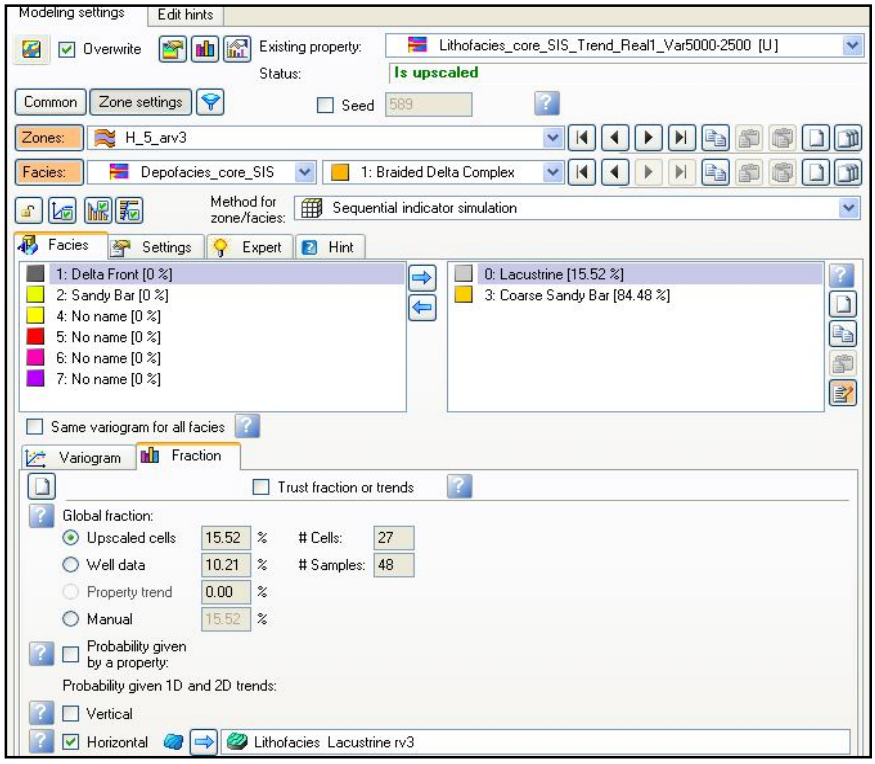

Figure C20: SIS lacustrine facies parameters set for reservoir zone.

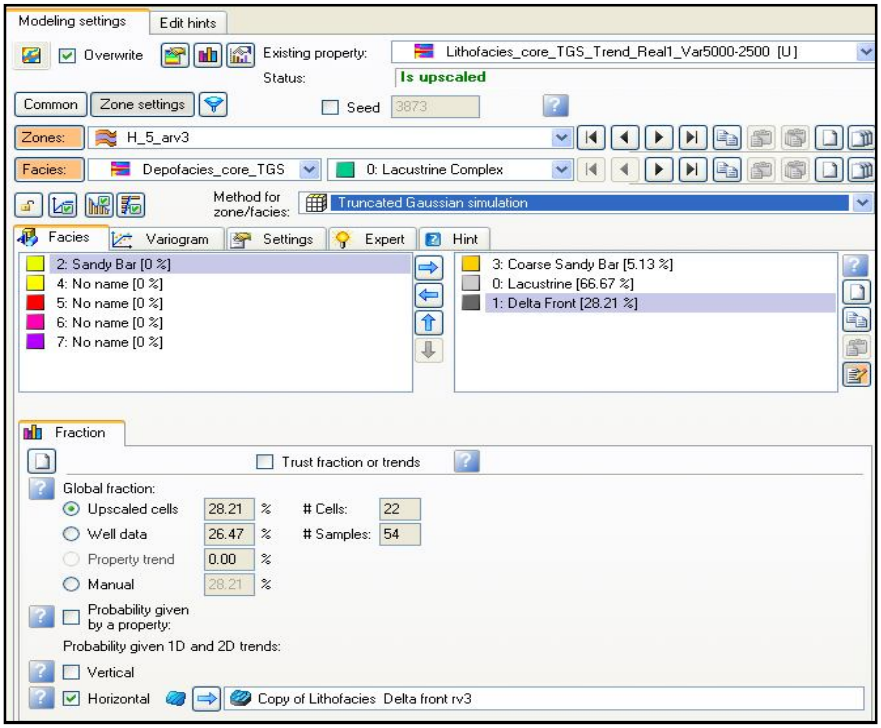

Figure 21 C11: TGS delta facies in lacustrine complex, parameters set for reservoir zone.

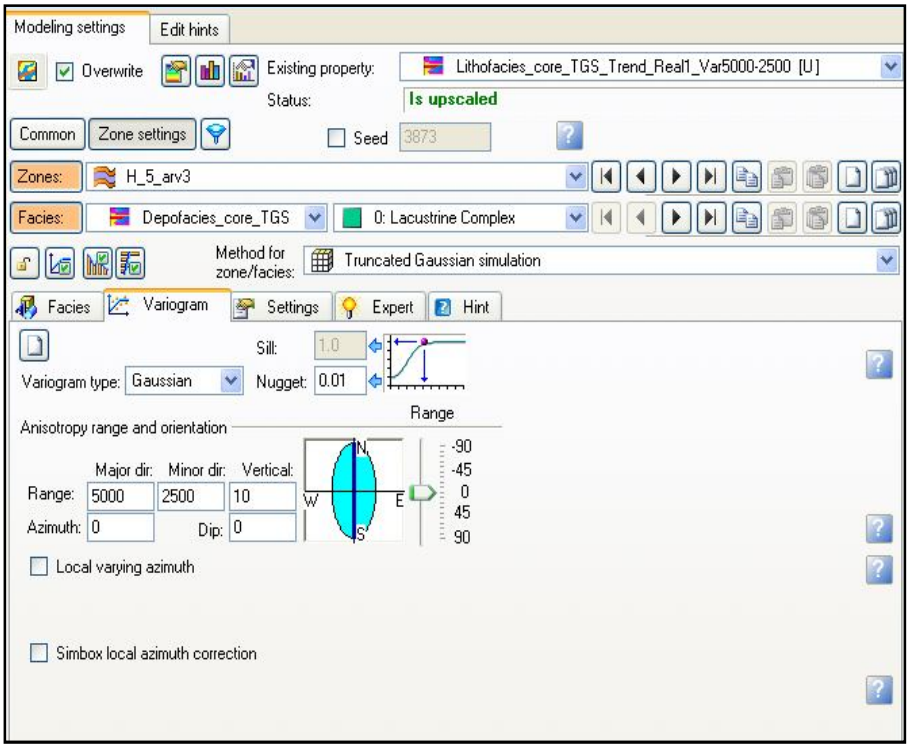

Figure C22: TGS lacustrine complex facies variogram parameters set for reservoir zone.

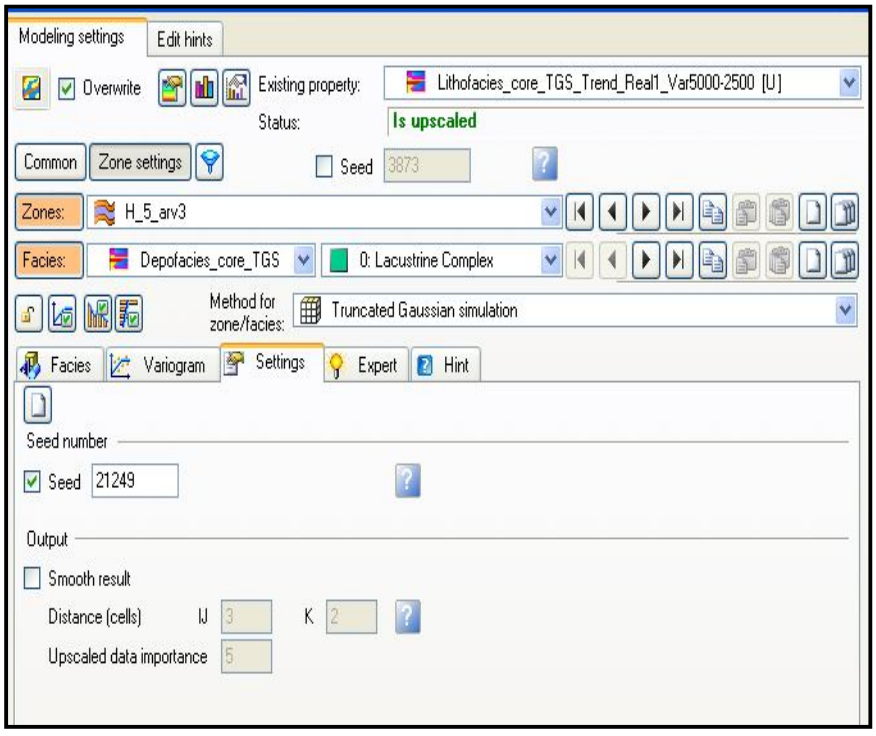

Figure C23: TGS setting seed for lacustrine facies for reservoir zone.

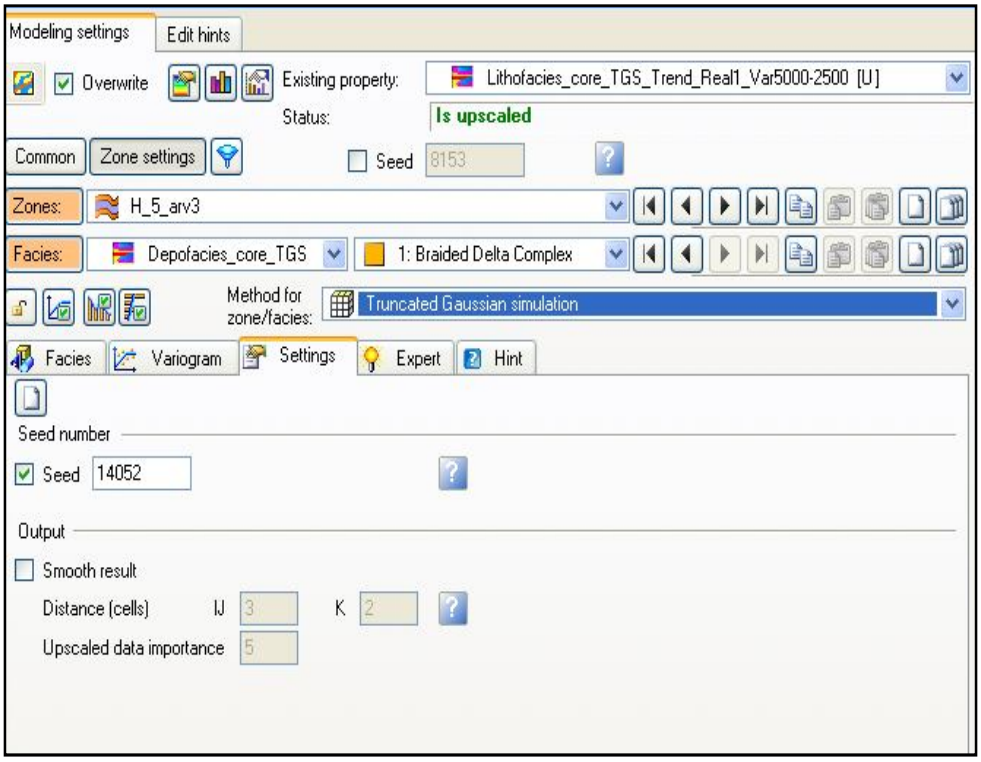

Figure C24: TGS setting seed for braided facies for reservoir zone.

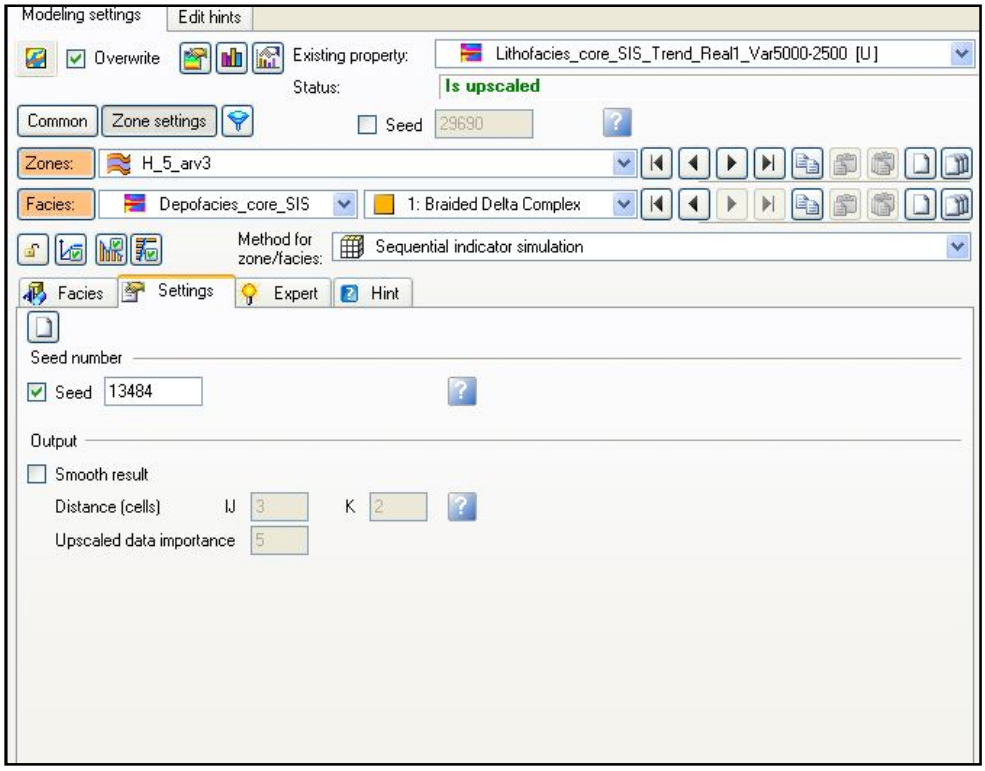

Figure C25: SIS setting seed for braided facies for reservoir zone.

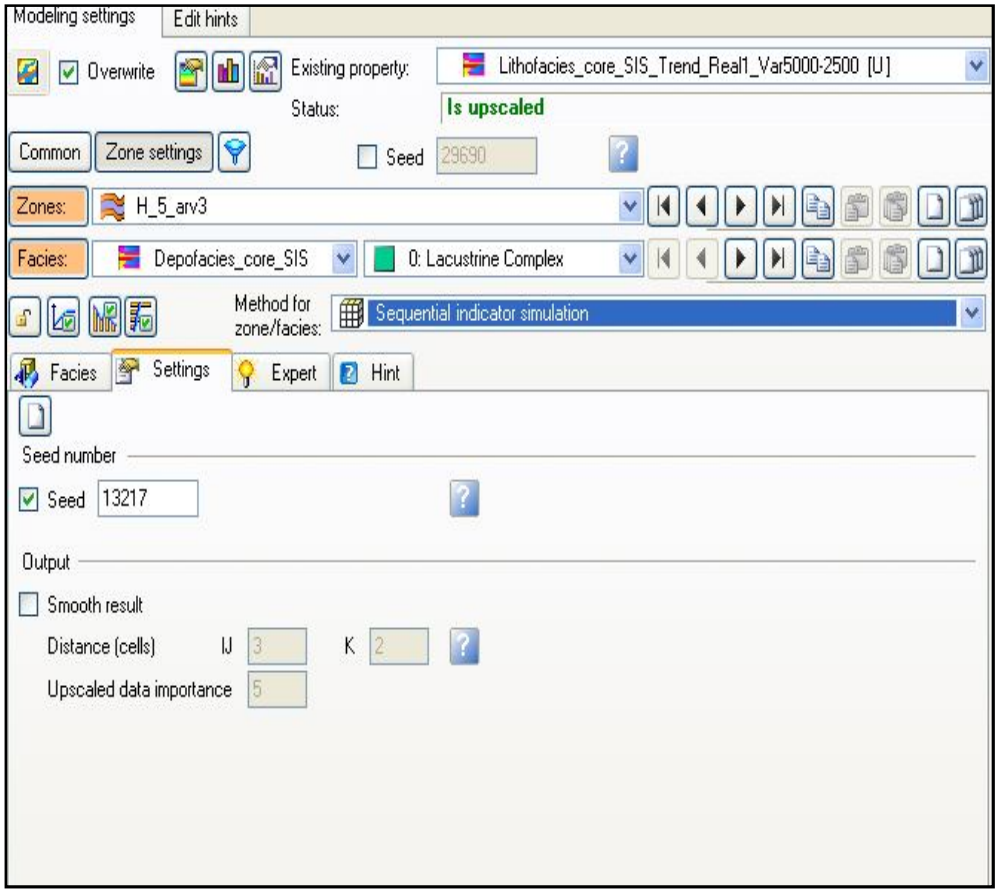

Figure C26: SIS setting seed for lacustrine facies for reservoir zone.

PUBLICATIONS LIST

Journal Papers (1- Under Review):

1. **M. H Hissein,** W. I. Wan Yusoff, 2012, "*3D Object-based Reservoir Facies Modelling of Cretaceous Braided Delta using Core and Wells log Data*", Malaysian Journal of Science *(MJS*), 2013, Malaysia.

Conference Papers (1- Accepted and 2- To be submitted for Review)

1. **M. H Hissein**, W. I. Wan Yusoff and Siti N. M. N, "*Stochastic Lithofacies Modelling of Cretaceous Braided Delta Reservoir using Wells and Core Data*", Second International Conference on Integrated Petroleum Engineering and Geosciences (ICIPEG2012), June 12-14, 2012, Kuala Lumpur, Malaysia.

2. **M. H Hissein** and W. I. Wan Yusoff, "*Reservoir Lithofacies Prediction from Well Logs and Core Data Using Train Estimation*" *Conference on Petroleum Engineering and Geosciences (ICPEG2013*), 2013, Malaysia.